UNIVERSIDAD AUTONOMA DE MADRID

Multi-reference Energy Density Functional calculations for neutrinoless double-beta decay nuclear matrix elements

Tomás R. Rodríguez

ESNT Workshop “Pertinent ingredients for MR-EDF calculations”

Saclay, February, 2017

GOBIERNO DE ESPAÑA
MINISTERIO DE ECONOMÍA Y COMPETITIVIDAD
Investigación
Programa
Ramón y Cajal

Acknowledgments

G. Martínez-Pinedo (TU-Darmstadt)

J. Menéndez (TU-Darmstadt/University of Tokyo)

N. López-Vaquero (UAM-Madrid)

J. L. Egido (UAM-Madrid)

A. Poves (UAM-Madrid)

J. Engel (UNC-Chapel Hill)

N. Hinohara (University of Tsukuba)

Outline

1. Introduction
2. $0\nu\beta\beta$ transition operator
3. Nuclear structure effects
4. Summary and outlook

Neutrinoless double beta decay

Process mediated by the weak interaction which occurs in those even-even nuclei where the single beta decay is energetically forbidden.

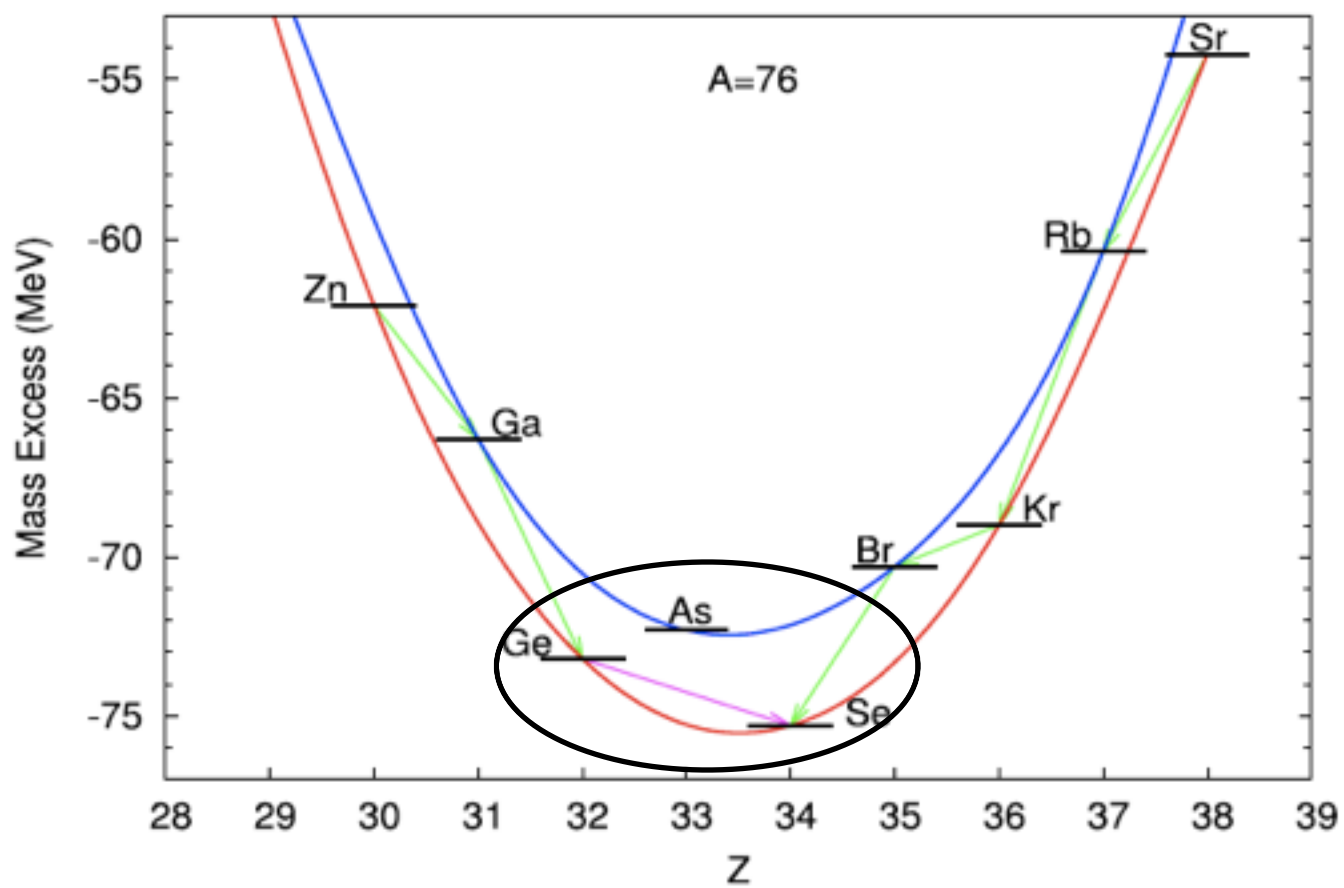

Process mediated by the weak interaction which occurs in those even-even nuclei w decay is energetically forb

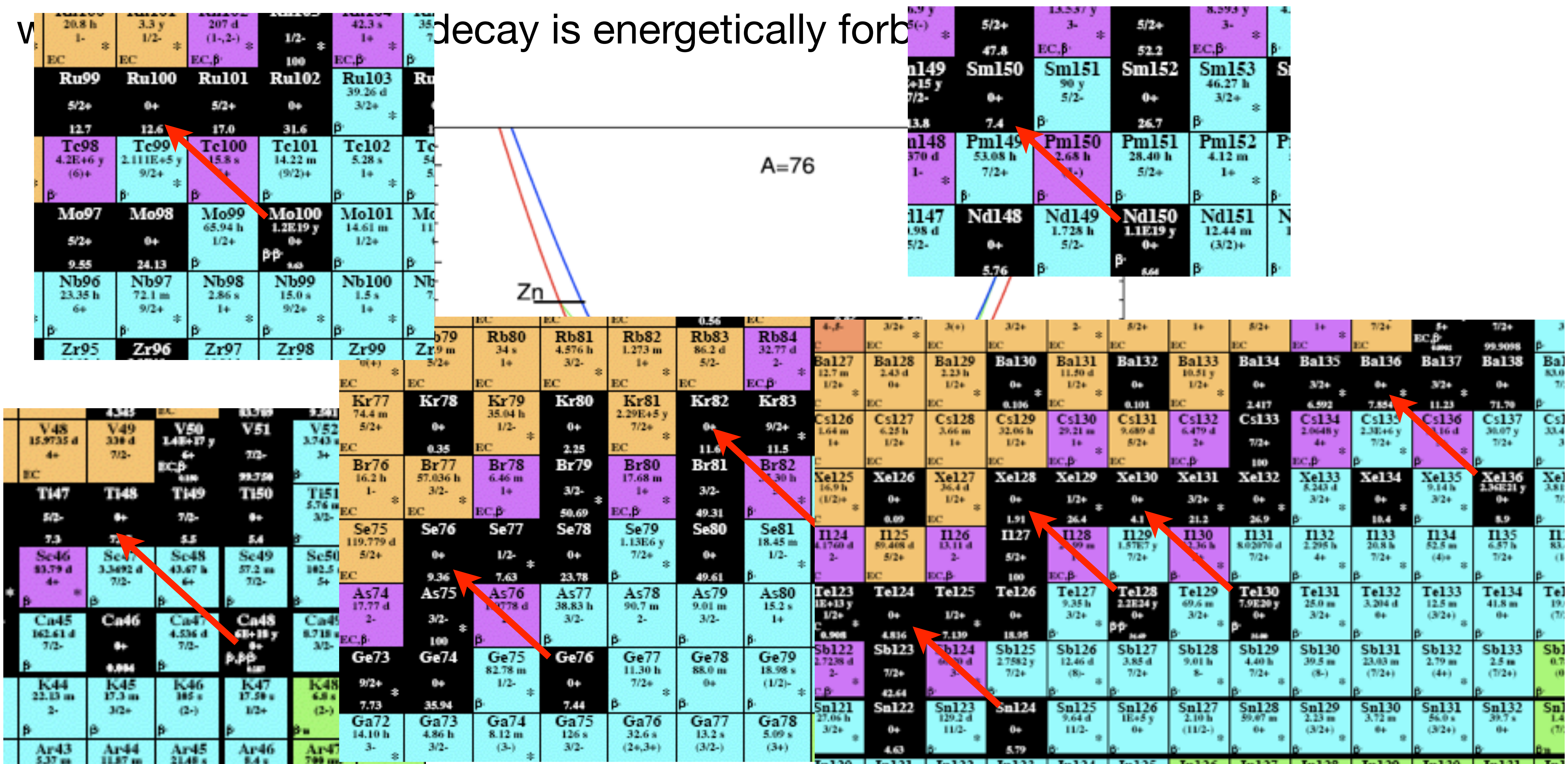

Neutrinoless double beta decay

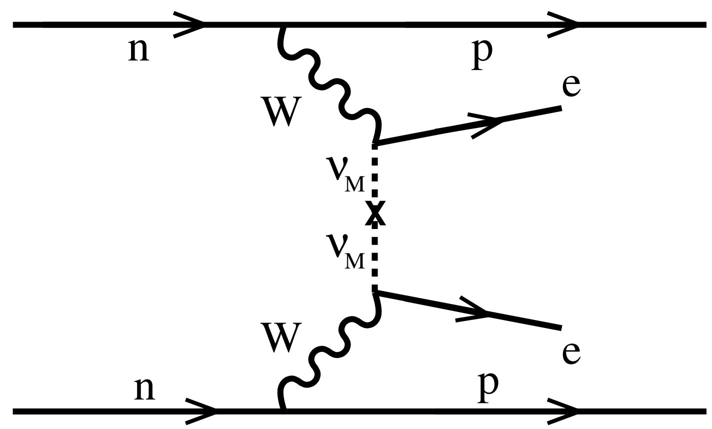

$$ {}^{A}_{Z}X_N \Rightarrow {}^{A}_{Z+2}Y_{N-2} + 2e^- $$

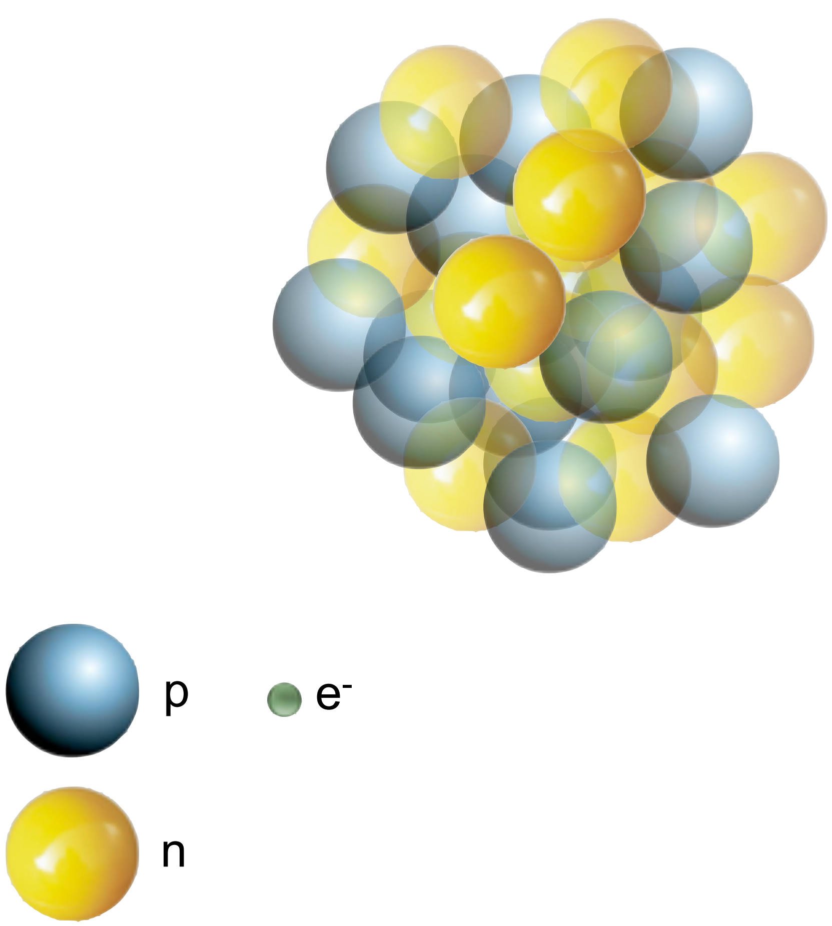

Neutrinoless double beta decay

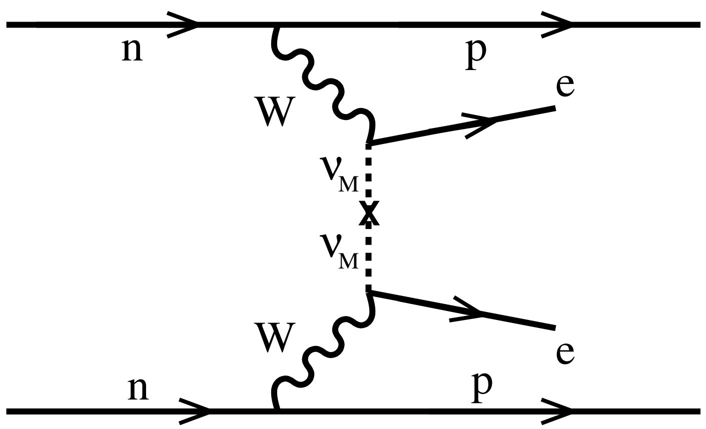

$$ {}^{A}_{Z}X_{N} \Rightarrow {}^{A}_{Z+2}Y_{N-2} + 2e^{-} $$

- Violates the leptonic number conservation
- Neutrinos are massive Majorana particles
- Mass hierarchy of neutrinos
- Experimentally not observed ($T_{1/2} > 10^{25}$ y)
- Beyond the Standard Model
- Most plausible mechanism: exchange of light Majorana neutrinos

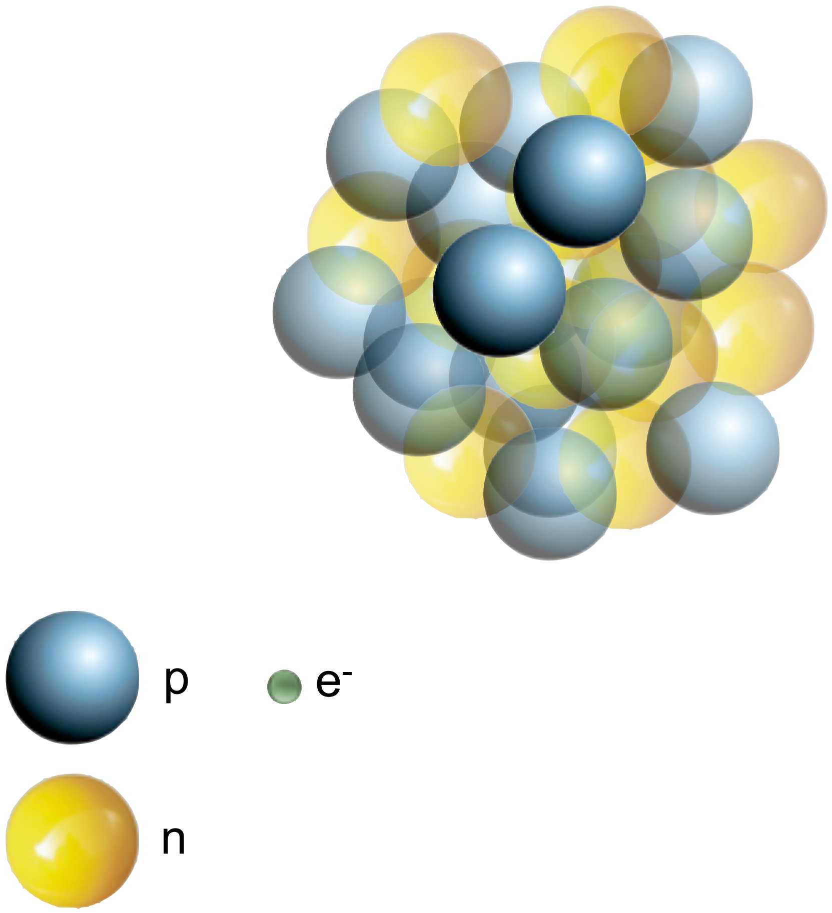

Neutrinoless double beta decay

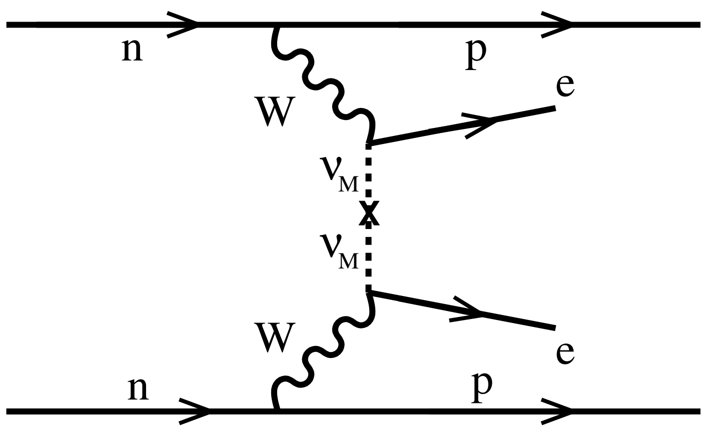

$$^{A}_{Z}X_N \Rightarrow ^{A}_{Z+2}Y_{N-2} + 2e^-$$

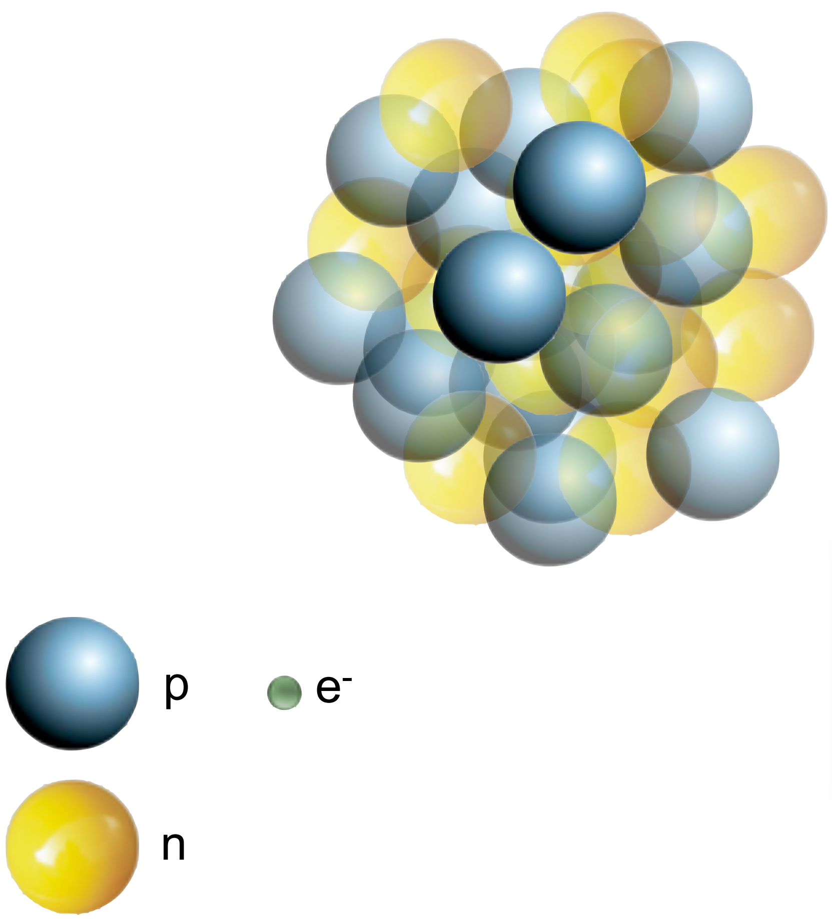

- Violates the leptonic number conservation
- Neutrinos are massive Majorana particles
- Mass hierarchy of neutrinos
- Experimentally not observed ($T_{1/2} > 10^{25}$ y)
- Beyond the Standard Model
- Most plausible mechanism: exchange of light Majorana neutrinos

$$\left(T_{1/2}^{0\nu\beta\beta}(0^+ \rightarrow 0^+)\right)^{-1} = G_{01}\left|M^{0\nu\beta\beta}\right|^2 \left(\frac{\langle m_{\beta\beta}\rangle}{m_e}\right)^2$$

Neutrinoless double beta decay

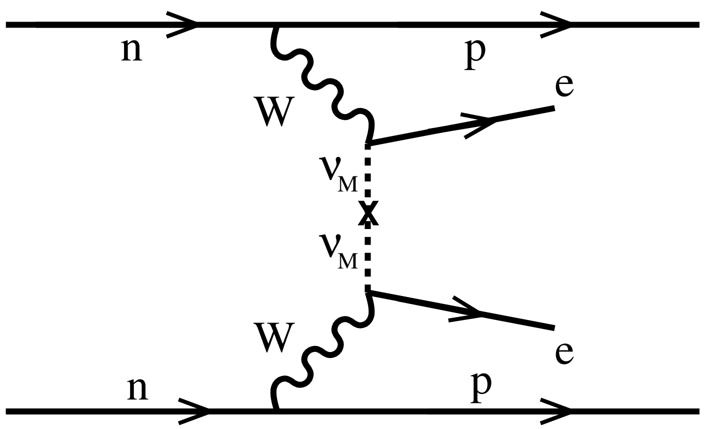

$$^{A}_{Z}X_{N} \Rightarrow ^{A}_{Z+2}Y_{N-2} + 2e^{-}$$

- Violates the leptonic number conservation
- Neutrinos are massive Majorana particles
- Mass hierarchy of neutrinos
- Experimentally not observed ($T_{1/2} > 10^{25}$ y)
- Beyond the Standard Model
- Most plausible mechanism: exchange of light Majorana neutrinos

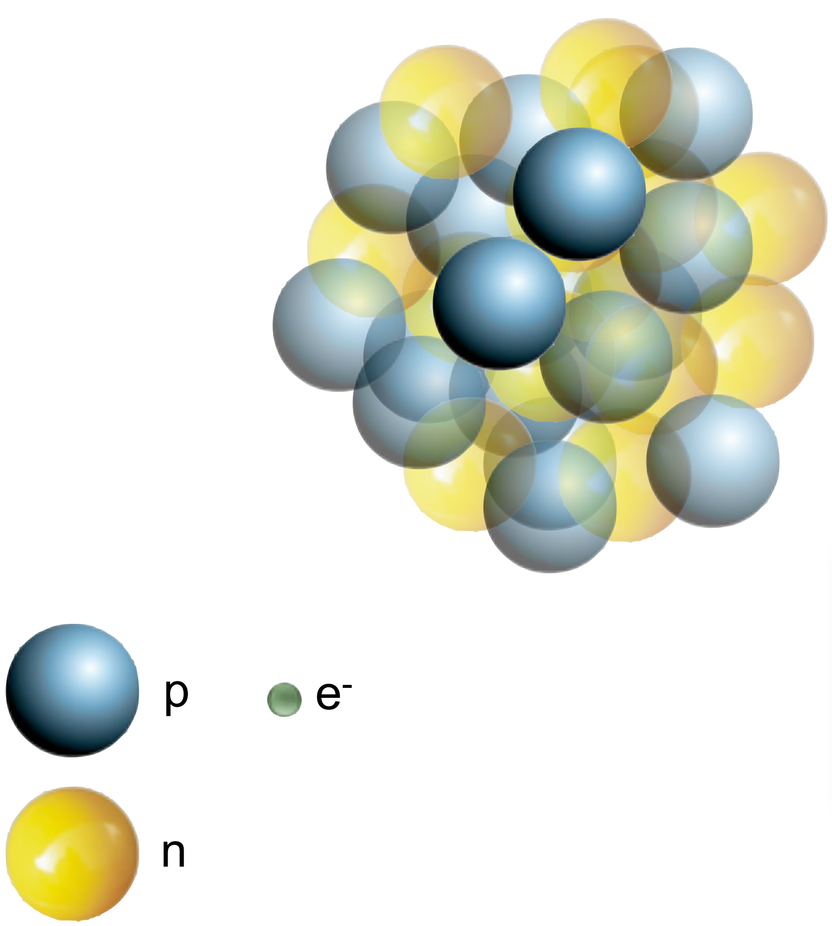

$$\left(T_{1/2}^{0\nu\beta\beta}(0^{+} \rightarrow 0^{+})\right)^{-1} = G_{01}\left|M^{0\nu\beta\beta}\right|^{2}\left(\frac{\langle m_{\beta\beta}\rangle}{m_{e}}\right)^{2}$$

Phys. Rev. C 85, 034316 (2012).

Phys. Rev. C 88, 037303 (2013).

Phase space factor

Neutrinoless double beta decay

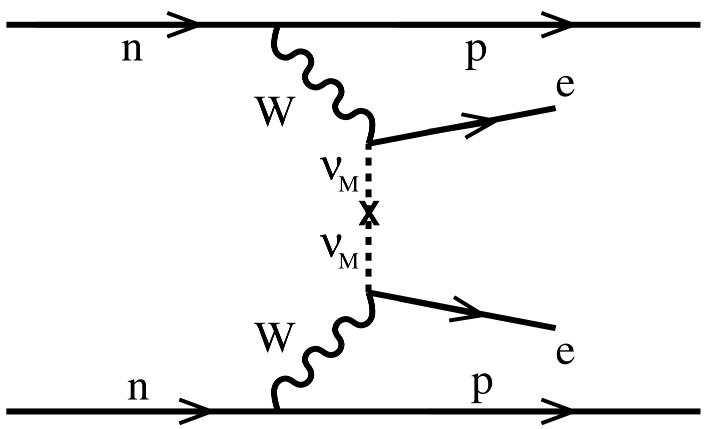

$$^{A}_{Z}X_{N} \Rightarrow ^{A}_{Z+2}Y_{N-2} + 2e^{-}$$

- Violates the leptonic number conservation
- Neutrinos are massive Majorana particles
- Mass hierarchy of neutrinos
- Experimentally not observed ($T_{1/2} > 10^{25}$ y)
- Beyond the Standard Model
- Most plausible mechanism: exchange of light Majorana neutrinos

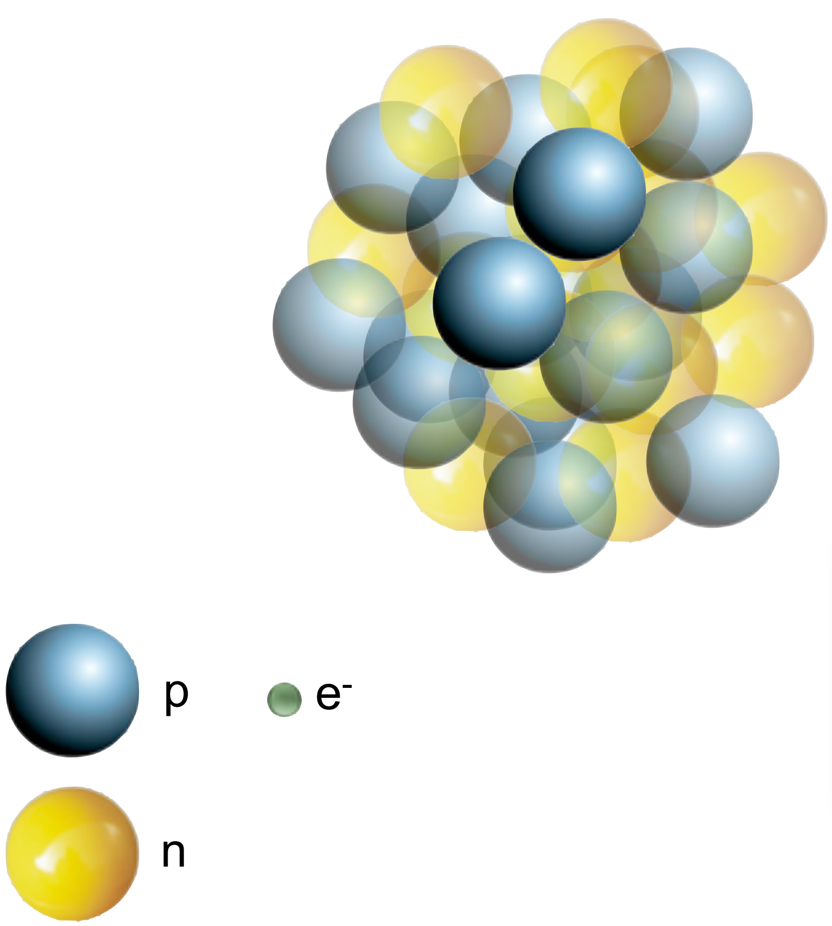

$$\left(T_{1/2}^{0\nu\beta\beta}(0^{+} \rightarrow 0^{+})\right)^{-1} = G_{01}\left|M^{0\nu\beta\beta}\right|^{2}\left(\frac{\langle m_{\beta\beta}\rangle}{m_e}\right)^{2}$$

Nuclear Matrix Element

Experimental status

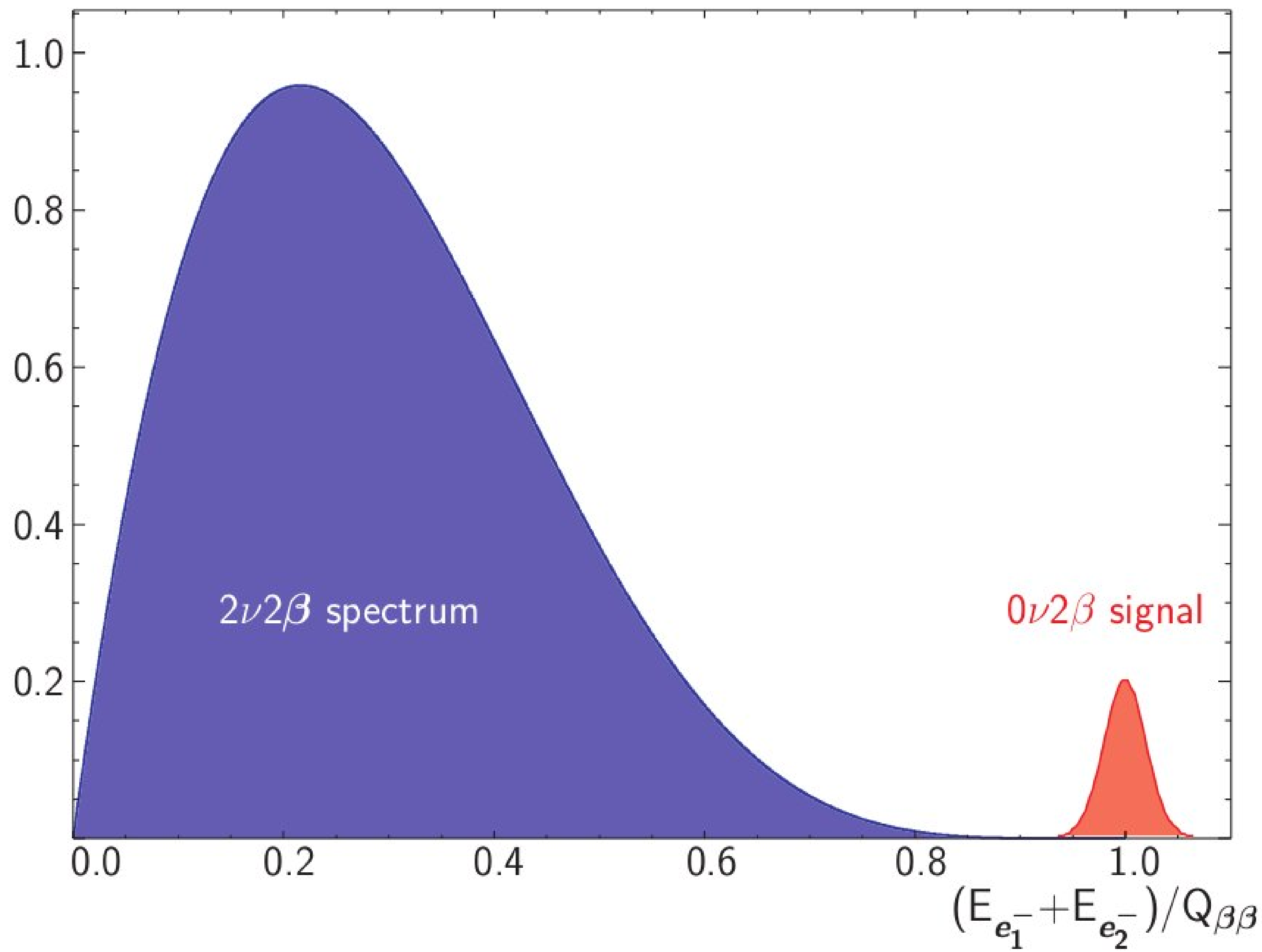

Only lower limits to the half-lives have been measured so far

Experimental status

Experiment	Decay	Present limit $T_{1/2}$	Forecast limit $T_{1/2}$	Ref.
GERDA	^{76}Ge	> 2.1x10^{25} yr	~2x10^{26} yr	PRL. 111, 122503 (2013)
Majorana	^{76}Ge	— —	~4x10^{27} yr	arXiv:nucl-ex/ 0311013
EXO-200	^{136}Xe	> 1.1x10^{25} yr	~1.3x10^{28} yr	Nature 510, 229 (2014)
KamLAND-Zen	^{136}Xe	> 1.9x10^{25} yr	~4x10^{26} yr	PRL 110, 062502 (2013)
NEXT	^{136}Xe	— —	~10^{26} yr	JINST 7, C11007 (2012)
(Super)NEMO3	^{82}Se	> 3.6x10^{23} yr	~1.2x10^{26} yr	PRL 95, 182302 (2005)
CUORICINO (CUORE)	^{130}Te	> 3x10^{24} yr	~2x10^{26} yr	PRC 78, 035502 (2008)
(Super)NEMO3	^{150}Nd	> 1.8x10^{22} yr	~5x10^{25} yr	PRC 80, 032501 (2009)
SNO+	^{150}Nd	— —	> 1.6x10^{25} yr	J. Phys. Conf. Ser. 447, 012065 (2013)

Neutrino mass hierarchy

Neutrino flavor eigenstates are not the same as the mass eigenstates

$$U = \underbrace{\begin{pmatrix} \cos\theta_{12} & \sin\theta_{12} & 0 \\ -\sin\theta_{12} & \cos\theta_{12} & 0 \\ 0 & 0 & 1 \end{pmatrix}}_{\text{solar}} \underbrace{\begin{pmatrix} \cos\theta_{13} & 0 & \sin\theta_{13}e^{-i\delta} \\ 0 & 1 & 0 \\ -\sin\theta_{13}e^{i\delta} & 0 & \cos\theta_{13} \end{pmatrix}}_{\text{reactor}} \underbrace{\begin{pmatrix} 1 & 0 & 0 \\ 0 & \cos\theta_{23} & \sin\theta_{23} \\ 0 & -\sin\theta_{23} & \cos\theta_{23} \end{pmatrix}}_{\text{atmospheric}} \begin{pmatrix} 1 & 0 & 0 \\ 0 & e^{i\alpha_1} & 0 \\ 0 & 0 & e^{i\alpha_1} \end{pmatrix}$$

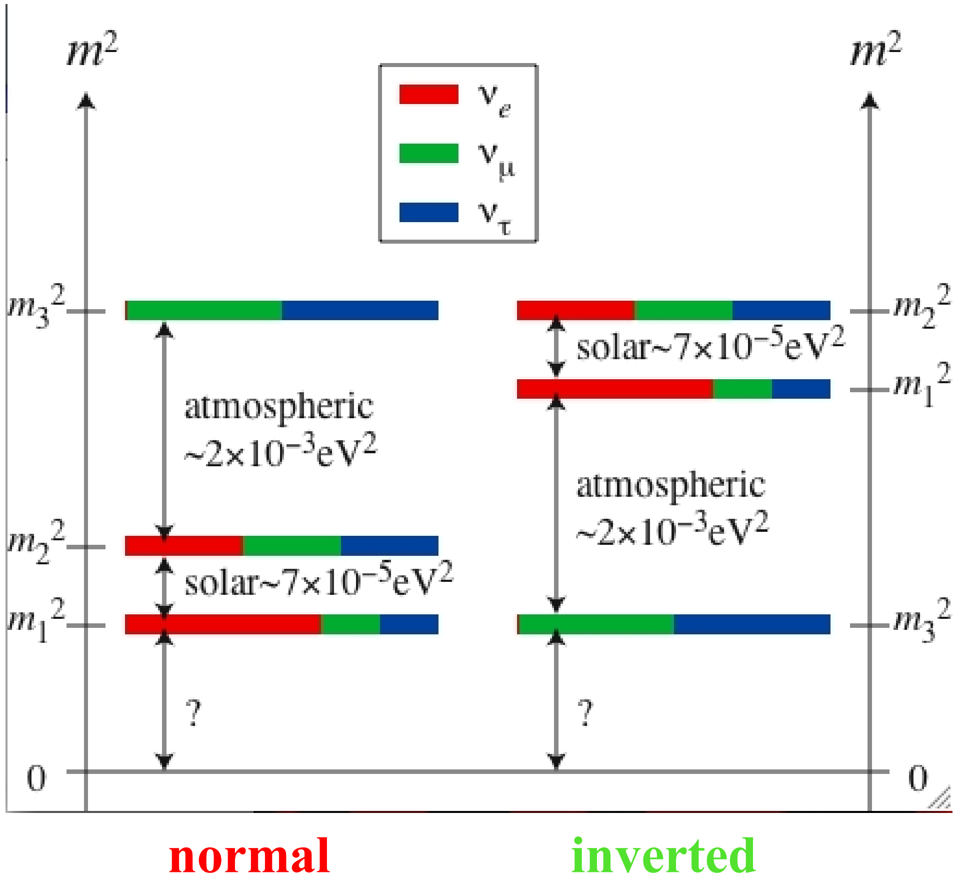

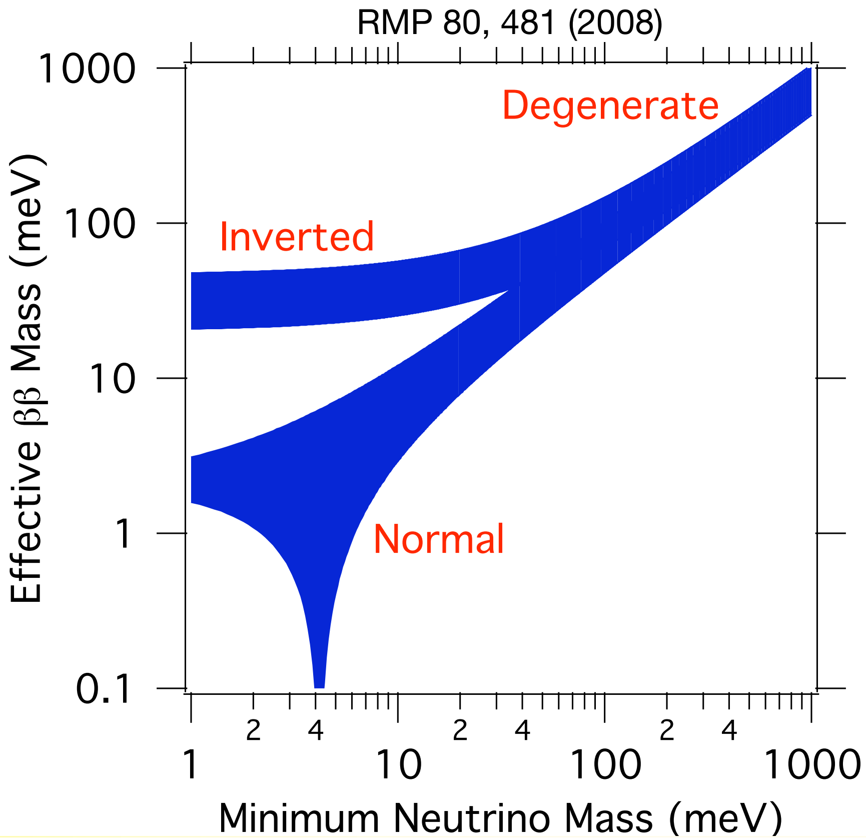

$$\langle m_{\beta\beta}\rangle = \sum_i U_{ei}^2 m_i$$

$$\left(T_{1/2}^{0\nu\beta\beta}(0^+\to 0^+)\right)^{-1} = G_{01}\left|M^{0\nu\beta\beta}\right|^2\left(\frac{\langle m_{\beta\beta}\rangle}{m_e}\right)^2$$

Neutrino mass hierarchy

Neutrino flavor eigenstates are not the same as the mass eigenstates

$$U = \begin{pmatrix} \cos\theta_{12} & \sin\theta_{12} & 0 \\ -\sin\theta_{12} & \cos\theta_{12} & 0 \\ 0 & 0 & 1 \end{pmatrix} \begin{pmatrix} \cos\theta_{13} & 0 & \sin\theta_{13}e^{-i\delta} \\ 0 & 1 & 0 \\ -\sin\theta_{13}e^{i\delta} & 0 & \cos\theta_{13} \end{pmatrix} \begin{pmatrix} 1 & 0 & 0 \\ 0 & \cos\theta_{23} & \sin\theta_{23} \\ 0 & -\sin\theta_{23} & \cos\theta_{23} \end{pmatrix} \begin{pmatrix} 1 & 0 & 0 \\ 0 & e^{i\alpha_1} & 0 \\ 0 & 0 & e^{i\alpha_1} \end{pmatrix}$$

solar reactor atmospheric

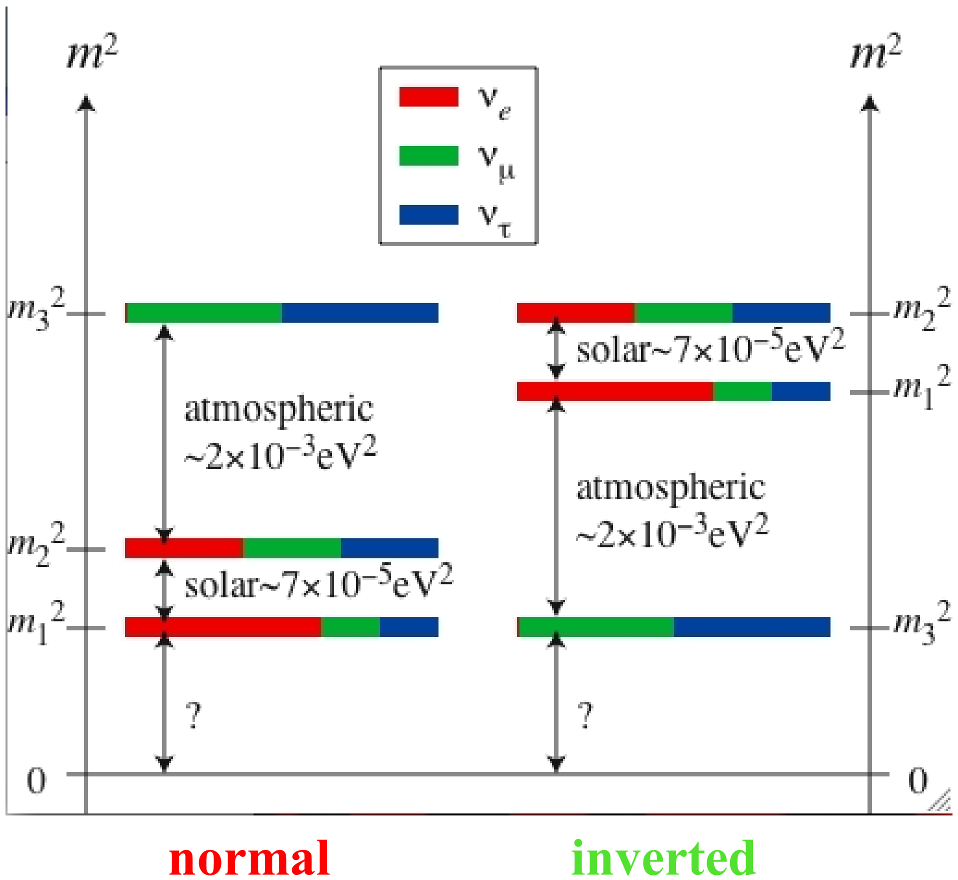

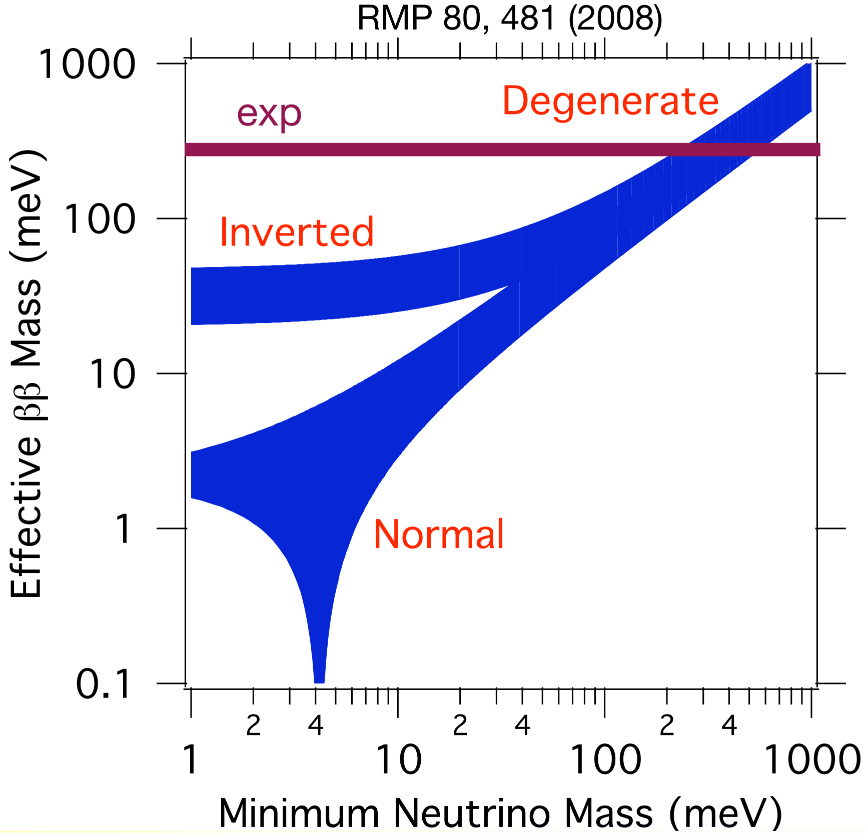

0νββ explores neutrino mass hierarchy and absolute mass scale

$$\langle m_{\beta\beta}\rangle = \sum_i U_{ei}^2 m_i$$

$$\left(T_{1/2}^{0\nu\beta\beta}(0^+\to 0^+)\right)^{-1} = G_{01}\left|M^{0\nu\beta\beta}\right|^2\left(\frac{\langle m_{\beta\beta}\rangle}{m_e}\right)^2$$

Neutrino mass hierarchy

Neutrino flavor eigenstates are not the same as the mass eigenstates

$$U = \underbrace{\begin{pmatrix} \cos\theta_{12} & \sin\theta_{12} & 0 \\ -\sin\theta_{12} & \cos\theta_{12} & 0 \\ 0 & 0 & 1 \end{pmatrix}}_{\text{solar}} \underbrace{\begin{pmatrix} \cos\theta_{13} & 0 & \sin\theta_{13}e^{-i\delta} \\ 0 & 1 & 0 \\ -\sin\theta_{13}e^{i\delta} & 0 & \cos\theta_{13} \end{pmatrix}}_{\text{reactor}} \underbrace{\begin{pmatrix} 1 & 0 & 0 \\ 0 & \cos\theta_{23} & \sin\theta_{23} \\ 0 & -\sin\theta_{23} & \cos\theta_{23} \end{pmatrix}}_{\text{atmospheric}} \begin{pmatrix} 1 & 0 & 0 \\ 0 & e^{i\alpha_1} & 0 \\ 0 & 0 & e^{i\alpha_1} \end{pmatrix}$$

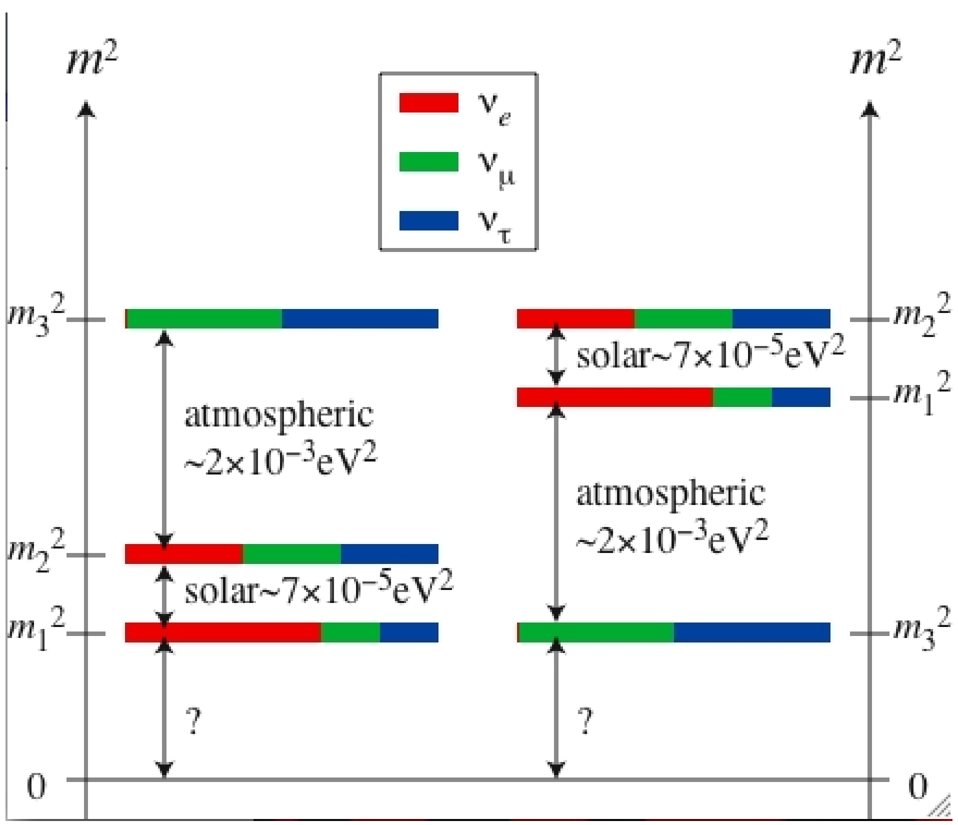

normal **inverted**

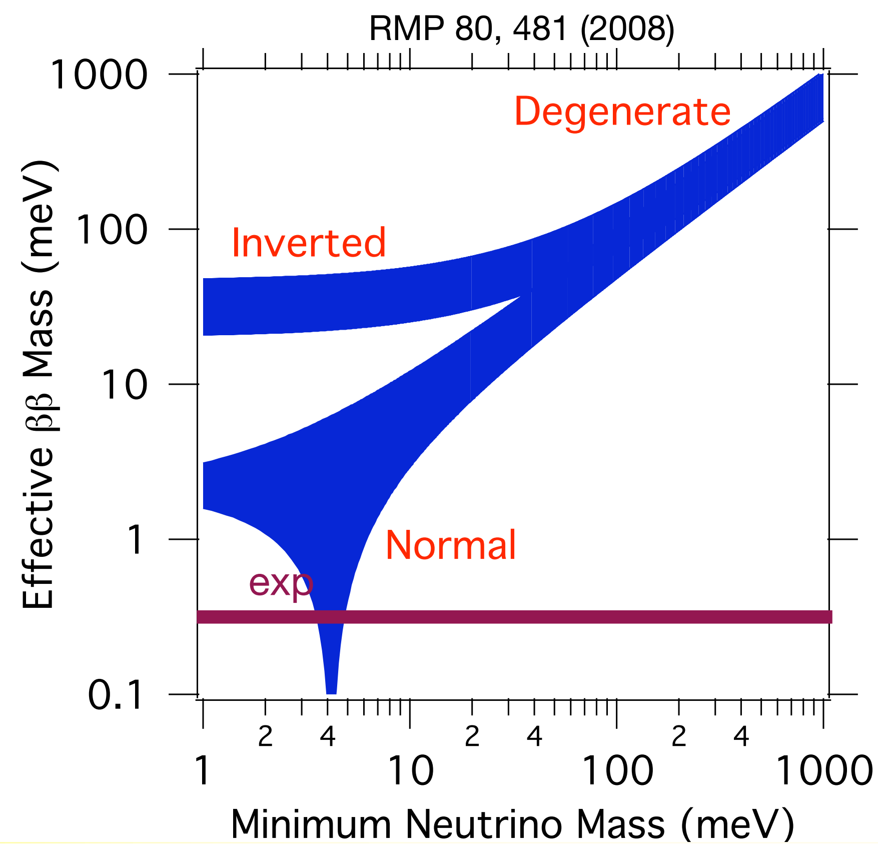

0νββ explores neutrino mass hierarchy and absolute mass scale

$$\langle m_{\beta\beta}\rangle = \sum_i U_{ei}^2 m_i$$

$$\left(T_{1/2}^{0\nu\beta\beta}(0^+\to 0^+)\right)^{-1} = G_{01}\left|M^{0\nu\beta\beta}\right|^2\left(\frac{\langle m_{\beta\beta}\rangle}{m_e}\right)^2$$

NME: Starting points

- Leading lepton number violating process contributing to 0νββ decay
  - **Exchange of light Majorana neutrino.**
  - Exchange of heavy Majorana neutrino.
  - Leptoquarks.
  - Supersymmetric particles.
  - …
- Transition operator connecting initial and final states
  - Relativistic/Non-relativistic.
  - Nucleon size effects.
  - Two-body weak currents.
  - Form factors.
  - Short-range correlations.
  - Closure approximation.
  - …
- Nuclear structure method (fully consistent or not with the operator) for calculating these NME.
  - Correlations.
  - Symmetry conservation.
  - Valence space.
  - …

Nuclear structure methods

Method	Recent references
Interacting Shell Model (ISM)	- Phys. Rev. Lett. 100, 052503 (2008). - Nucl. Phys. A 818, 139 (2009). - Phys. Rev. C 87, 014320 (2013). - Phys. Rev. Lett. 113, 262501 (2014).
pnQRPA	- Phys. Rev. C 77, 045503 (2008). - Phys Rev. C 87, 045501 (2013). - J. Phys. G 39, 124005 (2012).
Interacting Boson Model (IBM)	- Phys. Rev. C 79, 044301 (2009). - Phys Rev. C 87, 014315 (2013).
Generator Coordinate Method (GCM-EDF)	- Phys. Rev. Lett. 105, 252503 (2010). - Phys. Rev. Lett 111, 142501 (2013). - Phys. Rev. C 90, 031031(R) (2014). - Phys. Rev. C 90, 054309 (2014). - Phys. Rev. C 91, 024316 (2015).

Current theoretical status

Different methods give different values of NME's with a factor ~3 difference

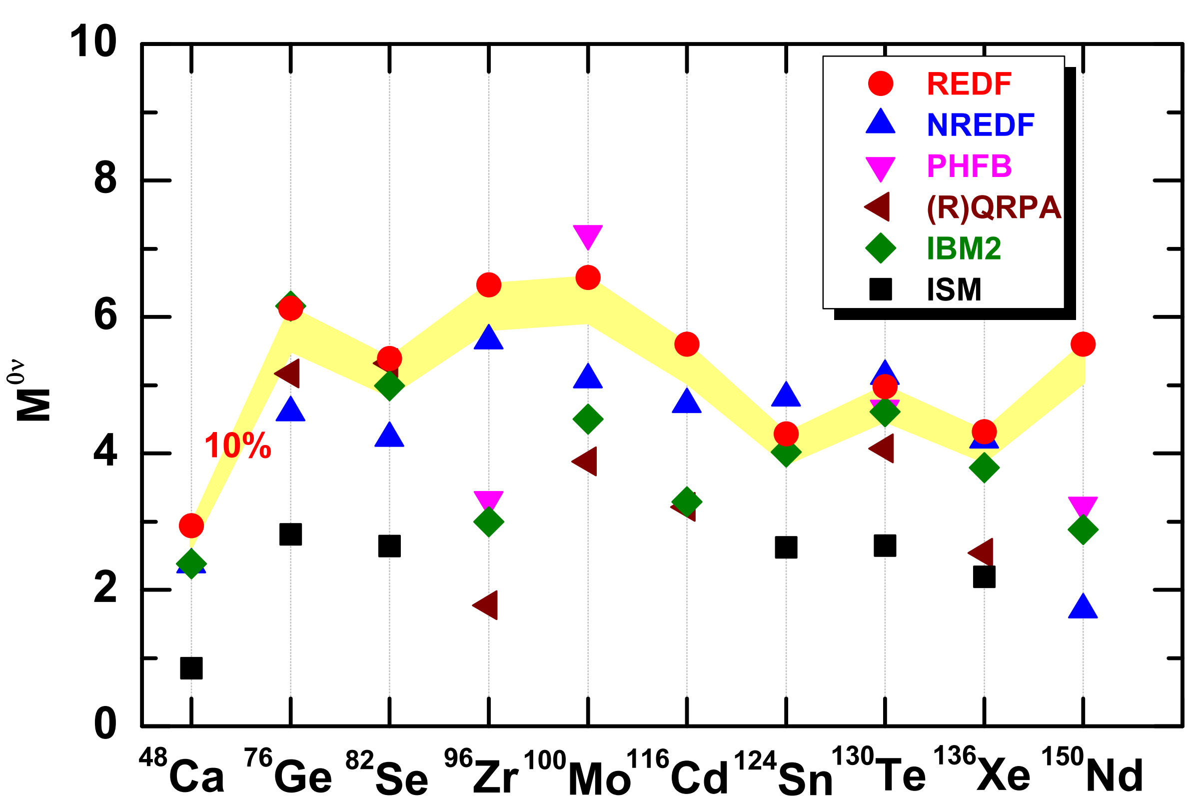

J. M. Yao et al.,Phys. Rev. C 91, 024316 (2015)

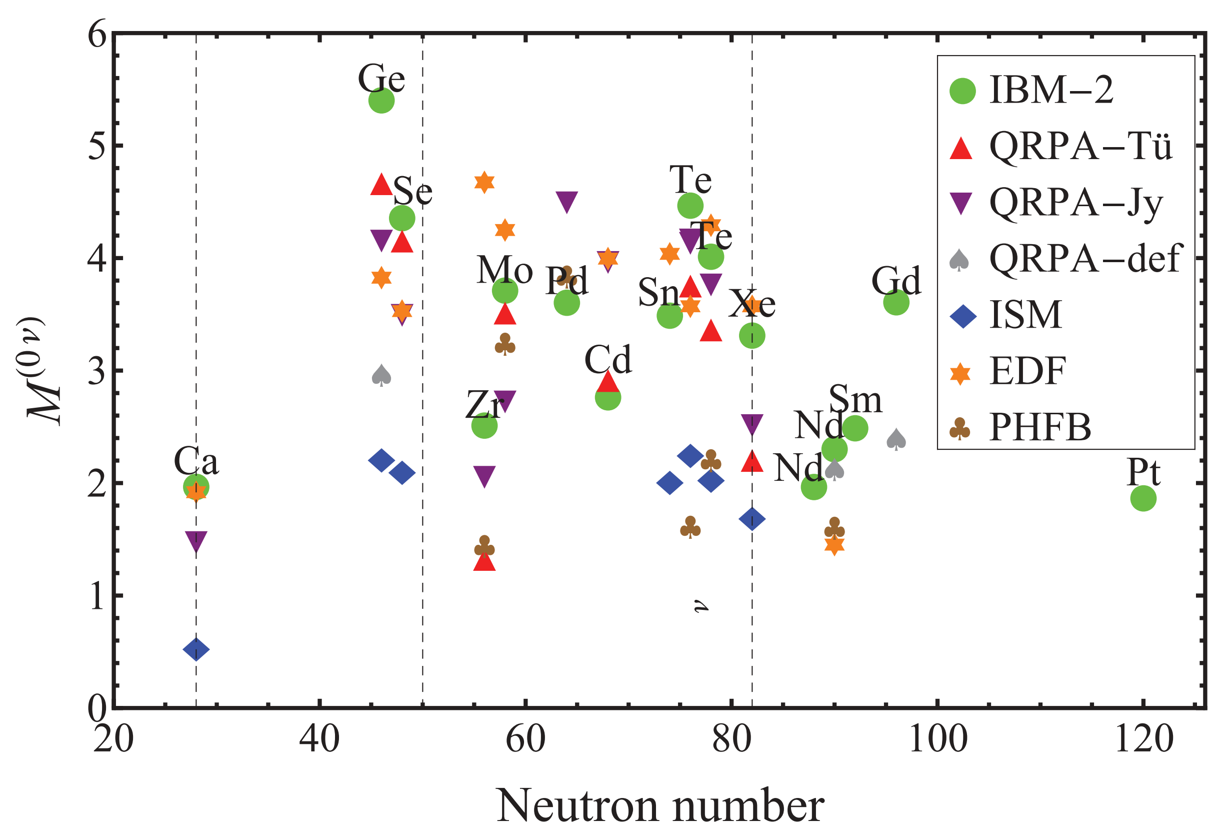

J. Barea, J. Kotila and F. Iachello, Phys. Rev. C 87, 014315 (2013)

Current theoretical status

Different methods give different values of NME's with a factor ~3 difference

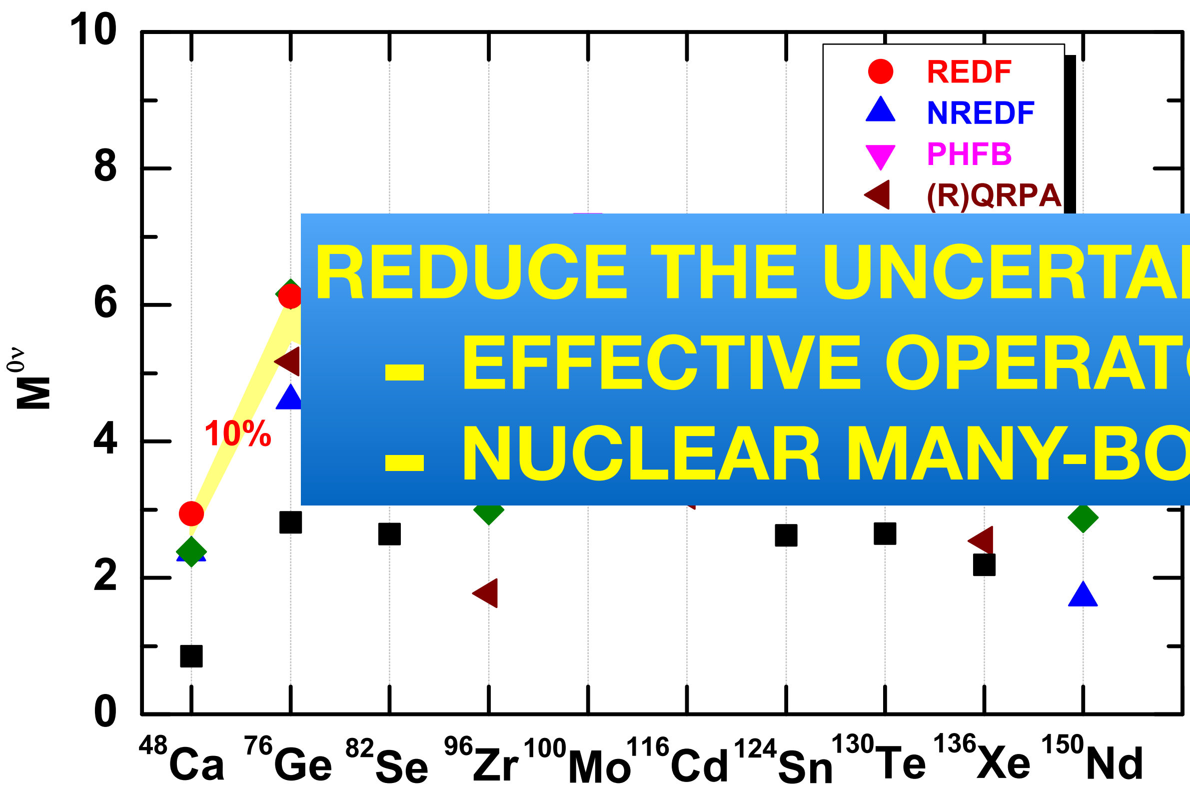

J. M. Yao et al.,Phys. Rev. C 91, 024316 (2015)

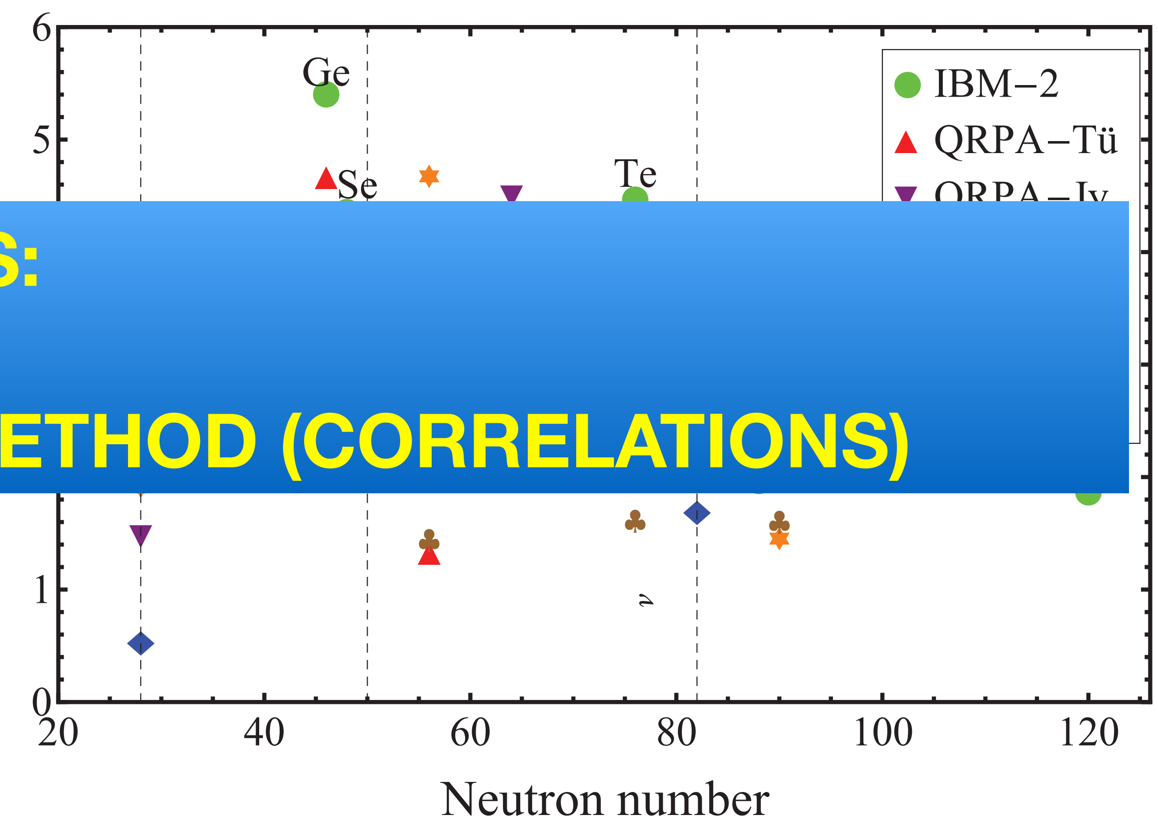

J. Barea, J. Kotila and F. Iachello, Phys. Rev. C 87, 014315 (2013)

REDUCE THE UNCERTAINTIES:

- **EFFECTIVE OPERATOR**
- **NUCLEAR MANY-BODY METHOD (CORRELATIONS)**

Transition operator

- Relativistic form

$$\mathcal{H}_{\text{weak}}(x) = \frac{G_F \cos\theta_C}{\sqrt{2}} j^\mu(x) \mathcal{J}_\mu^\dagger(x) + \text{h.c.},$$

$$j^\mu(x) = \bar{e}(x)\gamma^\mu(1-\gamma_5)\nu_e(x).$$

$$\begin{aligned}\mathcal{J}_\mu^\dagger(x) &= \bar{\psi}(x)\Big[g_V(q^2)\gamma_\mu + \mathrm{i} g_M(q^2)\frac{\sigma_{\mu\nu}}{2m_p}q^\nu \\ &- g_A(q^2)\gamma_\mu\gamma_5 - g_P(q^2)q_\mu\gamma_5\Big]\tau_-\psi(x),\end{aligned}$$

$$M^{0\nu}(0_I^+ \to 0_F^+) \equiv \langle 0_F^+|\hat{\mathcal{O}}^{0\nu}|0_I^+\rangle,$$

$$\hat{\mathcal{O}}^{0\nu} = \sum_i \hat{\mathcal{O}}_i^{0\nu}, \quad (i = VV, AA, AP, PP, MM)$$

$$\hat{\mathcal{O}}_i^{0\nu} = \frac{4\pi R}{g_A^2}\int d^3x_1 d^3x_2 \int \frac{d^3q}{(2\pi)^3}\frac{\mathrm{e}^{\mathrm{i}\boldsymbol{q}\cdot(\boldsymbol{x}_1-\boldsymbol{x}_2)}}{q(q+E_d)}\left[\mathcal{J}_\mu^\dagger \mathcal{J}^{\mu\dagger}\right]_i$$

$$\begin{aligned}
&g_V^2(\boldsymbol{q}^2)\left(\bar{\psi}\gamma_\mu\tau_-\psi\right)^{(1)}\left(\bar{\psi}\gamma^\mu\tau_-\psi\right)^{(2)},\\
&g_A^2(\boldsymbol{q}^2)\left(\bar{\psi}\gamma_\mu\gamma_5\tau_-\psi\right)^{(1)}\left(\bar{\psi}\gamma^\mu\gamma_5\tau_-\psi\right)^{(2)},\\
&2g_A(\boldsymbol{q}^2)g_P(\boldsymbol{q}^2)\left(\bar{\psi}\boldsymbol{\gamma}\gamma_5\tau_-\psi\right)^{(1)}\left(\bar{\psi}\boldsymbol{q}\gamma_5\tau_-\psi\right)^{(2)},\\
&g_P^2(\boldsymbol{q}^2)\left(\bar{\psi}\boldsymbol{q}\gamma_5\tau_-\psi\right)^{(1)}\left(\bar{\psi}\boldsymbol{q}\gamma_5\tau_-\psi\right)^{(2)},\\
&g_M^2(\boldsymbol{q}^2)\left(\bar{\psi}\frac{\sigma_{\mu i}}{2m_p}q^i\tau_-\psi\right)^{(1)}\left(\bar{\psi}\frac{\sigma^{\mu j}}{2m_p}q_j\tau_-\psi\right)^{(2)}.
\end{aligned}$$

L. S. Song et al., Phys. Rev. C 90, 054309 (2014).

Transition operator

- Relativistic form

$$\mathcal{H}_{\text{weak}}(x) = \frac{G_F \cos\theta_C}{\sqrt{2}} j^\mu(x)\mathcal{J}^\dagger_\mu(x) + \text{h.c.},$$

$$\hat{\mathcal{O}}^{0\nu} = \sum_i \hat{\mathcal{O}}^{0\nu}_i, \quad (i = VV, AA, AP, PP, MM)$$

$$j^\mu(x) = \bar{e}(x)\gamma^\mu(1 -$$

$$\frac{d^3q}{(2\pi)^3}\frac{e^{i\boldsymbol{q}\cdot(\boldsymbol{x}_1-\boldsymbol{x}_2)}}{q(q+E_d)}\left[\mathcal{J}^\dagger_\mu \mathcal{J}^{\mu\dagger}\right]_i$$

$$\mathcal{J}^\dagger_\mu(x) = \bar{\psi}(x)\Big[g_V(q^2)$$

$$- \; g_A(q^2)\gamma_\mu\gamma_5 - g_P(q^2)q_\mu\gamma_5\Big]\tau_-\psi(x),$$

$$\bar{\psi}\gamma^\mu\tau_-\psi)^{(2)},$$

$$g_A^2(\boldsymbol{q}^2)\left(\bar{\psi}\gamma_\mu\gamma_5\tau_-\psi\right)^{(1)}\left(\bar{\psi}\gamma^\mu\gamma_5\tau_-\psi\right)^{(2)},$$

$$2g_A(\boldsymbol{q}^2)g_P(\boldsymbol{q}^2)\left(\bar{\psi}\boldsymbol{\gamma}\gamma_5\tau_-\psi\right)^{(1)}\left(\bar{\psi}\boldsymbol{q}\gamma_5\tau_-\psi\right)^{(2)},$$

$$g_P^2(\boldsymbol{q}^2)\left(\bar{\psi}\boldsymbol{q}\gamma_5\tau_-\psi\right)^{(1)}\left(\bar{\psi}\boldsymbol{q}\gamma_5\tau_-\psi\right)^{(2)},$$

$$g_M^2(\boldsymbol{q}^2)\left(\bar{\psi}\frac{\sigma_{\mu i}}{2m_p}q^i\tau_-\psi\right)^{(1)}\left(\bar{\psi}\frac{\sigma^{\mu j}}{2m_p}q_j\tau_-\psi\right)^{(2)}.$$

$$M^{0\nu}(0^+_I \to 0^+_F) \equiv \langle 0^+_F|\hat{\mathcal{O}}^{0\nu}|0^+_I\rangle,$$

Fully relativistic treatment:

L. S. Song et al., arXiv:1407.1368
J. M. Yao et al., arXiv:1410.6326

L. S. Song et al., Phys. Rev. C 90, 054309 (2014).

- Non-relativistic reduction

$$M^{0\nu}(0_I^+ \to 0_F^+) \equiv \langle 0_F^+|\hat{\mathcal{O}}^{0\nu}|0_I^+\rangle,$$

$$\hat{\mathcal{O}}^{0\nu} = \sum_i \hat{\mathcal{O}}_i^{0\nu}, \quad (i = VV, AA, AP, PP, MM)$$

$$\hat{\mathcal{O}}_i^{0\nu} = \frac{4\pi R}{g_A^2}\int d^3x_1 d^3x_2 \int \frac{d^3q}{(2\pi)^3}\frac{e^{i\boldsymbol{q}\cdot(\boldsymbol{x}_1-\boldsymbol{x}_2)}}{q(q+E_d)}\left[\mathcal{J}_\mu^\dagger \mathcal{J}^{\mu\dagger}\right]_i$$

The non-relativistic "two-current" operator $[\mathcal{J}_\mu^\dagger \mathcal{J}^{\mu\dagger}]_{\rm NR}$ can be decomposed, as in other non-relativistic calculations, into the Fermi, the Gamow-Teller, and the tensor parts:

$$\left[-h_{\rm F}(\boldsymbol{q}^2) + h_{\rm GT}(\boldsymbol{q}^2)\sigma_{12} + h_{\rm T}(\boldsymbol{q}^2)S_{12}^q\right]\tau_-^{(1)}\tau_-^{(2)}, \quad (34)$$

with the tensor operator $S_{12}^q = 3(\boldsymbol{\sigma}^{(1)}\cdot\hat{\boldsymbol{q}})(\boldsymbol{\sigma}^{(2)}\cdot\hat{\boldsymbol{q}}) - \sigma_{12}$ and $\sigma_{12} = \boldsymbol{\sigma}^{(1)}\cdot\boldsymbol{\sigma}^{(2)}$. Each channel ($K$: F, GT, T) of Eq. (34) can be labeled by the terms of the hadronic current from which it originates, as

$$h_K(\boldsymbol{q}^2) = \sum_i h_{K-i}(\boldsymbol{q}^2), \quad (i = VV, AA, AP, PP, MM)$$

with

$$\begin{aligned}
h_{\rm F-\it VV}(\boldsymbol{q}^2) &= -g_V^2(\boldsymbol{q}^2), && (35a)\\
h_{\rm GT-\it AA}(\boldsymbol{q}^2) &= -g_A^2(\boldsymbol{q}^2), && (35b)\\
h_{\rm GT-\it AP}(\boldsymbol{q}^2) &= \frac{2}{3}g_A(\boldsymbol{q}^2)g_P(\boldsymbol{q}^2)\frac{\boldsymbol{q}^2}{2m_p}, && (35c)\\
h_{\rm GT-\it PP}(\boldsymbol{q}^2) &= -\frac{1}{3}g_P^2(\boldsymbol{q}^2)\frac{\boldsymbol{q}^4}{4m_p^2}, && (35d)\\
h_{\rm GT-\it MM}(\boldsymbol{q}^2) &= -\frac{2}{3}g_M^2(\boldsymbol{q}^2)\frac{\boldsymbol{q}^2}{4m_p^2}, && (35e)\\
h_{\rm T-\it AP}(\boldsymbol{q}^2) &= h_{GT-AP}(\boldsymbol{q}^2), && (35f)\\
h_{\rm T-\it PP}(\boldsymbol{q}^2) &= h_{GT-PP}(\boldsymbol{q}^2), && (35g)\\
h_{\rm T-\it MM}(\boldsymbol{q}^2) &= -\frac{1}{2}h_{GT-MM}(\boldsymbol{q}^2). && (35h)
\end{aligned}$$

F. Simkovic et. al, PRC 60, 055502 (1999)

L. S. Song et al., Phys. Rev. C 90, 054309 (2014).

Transition operator

- Non-relativisti

$$M^{0\nu}(0^+_I \to 0^+_F$$

$$\hat{\mathcal{O}}^{0\nu} = \sum_i \hat{\mathcal{O}}^{0\nu}_i, \quad (i$$

$$\hat{\mathcal{O}}^{0\nu}_i = \frac{4\pi R}{g_A^2}\int d^3x_1 d^3$$

ator $[\mathcal{J}^\dagger_\mu \mathcal{J}^{\mu\dagger}]_{\rm NR}$ ativistic calcula- , and the tensor

$] \tau^{(1)}_- \tau^{(2)}_-$, (34)

$\hat{q})(\sigma^{(2)}\cdot\hat{q}) - \sigma_{12}$ (K: F, GT, T) of the hadronic

$, AP, PP, MM)$

(35a)

(35b)

$q^2)\frac{q^2}{2m_p}$, (35c)

(35d)

(35e)

(35f)

(35g)

$h_{T-MM}(q^2) = -\frac{1}{2}h_{GT-MM}(q^2)$. (35h)

Table 1: The normalized NME $\tilde{M}^{0\nu}$ for the $0\nu\beta\beta$-decay obtained with the particle number projected spherical mean-field configuration ($\beta_I = \beta_F = 0$) by the PC-PK1 force using both the relativistic and non-relativistic reduced (first-order of q/m_p in the one-body current) transition operators. The ratio of the AA term to the total NME, $R_{AA} \equiv \tilde{M}^{0\nu}_{AA}/\tilde{M}^{0\nu}$, the relativistic effect $\Delta_{\rm Rel.} \equiv (\tilde{M}^{0\nu} - \tilde{M}^{0\nu}_{\rm NR})/\tilde{M}^{0\nu}$ and the ratio of the tensor part to the total NME, $R_T \equiv \tilde{M}^{0\nu}_{\rm NR,T}/\tilde{M}^{0\nu}_{\rm NR}$, are also presented.

Sph+PNP (PC-PK1)	$\tilde{M}^{0\nu}$	R_{AA}	$\tilde{M}^{0\nu}_{\rm NR}$	$\Delta_{\rm Rel.}$	R_T
^{48}Ca $\to ^{48}$Ti	3.66	81%	3.74	−2.1%	−2.4%
^{76}Ge $\to ^{76}$Se	7.59	94%	7.71	−1.6%	3.5%
^{82}Se $\to ^{82}$Kr	7.58	93%	7.68	−1.4%	2.9%
^{96}Zr $\to ^{96}$Mo	5.64	95%	5.63	0.2%	3.6%
^{100}Mo $\to ^{100}$Ru	10.92	95%	10.91	0.1%	3.5%
^{116}Cd $\to ^{116}$Sn	6.18	94%	6.13	0.7%	1.9%
^{124}Sn $\to ^{124}$Te	6.66	94%	6.78	−1.8%	4.9%
^{130}Te $\to ^{130}$Xe	9.50	94%	9.64	−1.4%	4.3%
^{136}Xe $\to ^{136}$Ba	6.59	94%	6.70	−1.7%	4.1%
^{150}Nd $\to ^{150}$Sm	13.25	95%	13.08	1.3%	2.5%

J. M. Yao et al., Phys. Rev. C 90, 054309 (2014)

F. Simkovic et. al, PRC 60, 055502 (1999)

L. S. Song et al., Phys. Rev. C 90, 054309 (2014).

Transition operator

- Non-relativistic reduction

- Neglect the tensor term.
- Closure approximation
(10% error at most, from QRPA and ISM calculations)

$$M^{0\nu\beta\beta} = -\left(\frac{g_V(0)}{g_A(0)}\right)^2 M_F^{0\nu\beta\beta} + M_{GT}^{0\nu\beta\beta} - \cancel{M_T^{0\nu\beta\beta}}$$

$$\begin{aligned} M_F^{0\nu\beta\beta} &= \left(\frac{g_A(0)}{g_V(0)}\right)^2 \langle 0_f^+ | \hat{V}_F(1,2)\hat{\tau}_-^{(1)}\hat{\tau}_-^{(2)} | 0_i^+ \rangle \\ M_{GT}^{0\nu\beta\beta} &= \langle 0_f^+ | \hat{V}_{GT}(1,2)\hat{\tau}_-^{(1)}\hat{\tau}_-^{(2)} | 0_i^+ \rangle \end{aligned}$$

$$\begin{aligned} \langle \vec{r}_1\vec{r}_2 | \hat{V}_F(1,2) | \vec{r}'_1\vec{r}'_2 \rangle &= v_F(|\vec{r}_1 - \vec{r}_2|)\delta(\vec{r}_1 - \vec{r}'_1)\delta(\vec{r}_2 - \vec{r}'_2) \\ \langle \vec{r}_1\vec{r}_2 | \hat{V}_{GT}(1,2) | \vec{r}'_1\vec{r}'_2 \rangle &= v_{GT}(|\vec{r}_1 - \vec{r}_2|)\delta(\vec{r}_1 - \vec{r}'_1)\delta(\vec{r}_2 - \vec{r}'_2)\hat{\vec{\sigma}}^{(1)} \cdot \hat{\vec{\sigma}}^{(2)} \end{aligned}$$

Transition operator

- Non-relativistic reduction

- Neglect the tensor term.
- Closure approximation
(10% error at most, from QRPA and ISM calculations)

$$M^{0\nu\beta\beta} = -\left(\frac{g_V(0)}{g_A(0)}\right)^2 M_F^{0\nu\beta\beta} + M_{GT}^{0\nu\beta\beta} - \cancel{M_T^{0\nu\beta\beta}}$$

$$\begin{aligned} M_F^{0\nu\beta\beta} &= \left(\frac{g_A(0)}{g_V(0)}\right)^2 \langle 0_f^+|\hat{V}_F(1,2)\hat{\tau}_-^{(1)}\hat{\tau}_-^{(2)}|0_i^+\rangle \\ M_{GT}^{0\nu\beta\beta} &= \langle 0_f^+|\hat{V}_{GT}(1,2)\hat{\tau}_-^{(1)}\hat{\tau}_-^{(2)}|0_i^+\rangle \end{aligned}$$

$$\begin{aligned} \langle \vec{r}_1\vec{r}_2|\hat{V}_F(1,2)|\vec{r}\,'_1\vec{r}\,'_2\rangle &= v_F(|\vec{r}_1-\vec{r}_2|)\delta(\vec{r}_1-\vec{r}\,'_1)\delta(\vec{r}_2-\vec{r}\,'_2) \\ \langle \vec{r}_1\vec{r}_2|\hat{V}_{GT}(1,2)|\vec{r}\,'_1\vec{r}\,'_2\rangle &= v_{GT}(|\vec{r}_1-\vec{r}_2|)\delta(\vec{r}_1-\vec{r}\,'_1)\delta(\vec{r}_2-\vec{r}\,'_2)\hat{\vec{\sigma}}^{(1)}\cdot\hat{\vec{\sigma}}^{(2)} \end{aligned}$$

Neutrino potentials

Neutrino potentials

Starting from the weak Lagrangian that describes the process some approximations are made:

1. Non-relativistic approach in the hadronic part.
2. Closure approximation in the virtual intermediate state
3. Nucleon form factors taken in the dipolar approximation.
4. Tensor contribution is neglected.
5. High order currents are included (HOC).
6. Short range correlations are included with an UCOM correlator.

- Find the initial and final 0^+ (and, in the no closure approximation, the intermediate) states
- Evaluate the transition operators between these states

- The 'bare' operator should be transformed into an 'effective' operator defined in the valence space

MBPT

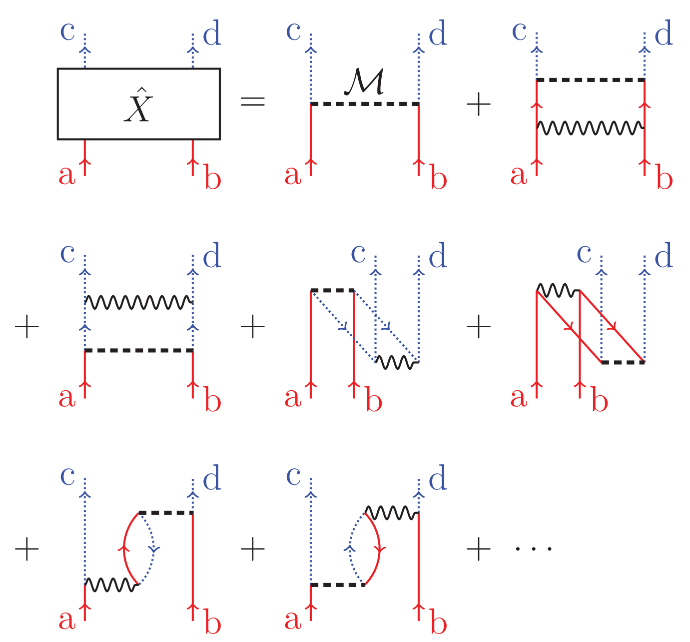

FIG. 2. (Color online) The $\hat{X}$ box to first order in $V_{\mathrm{low}\,k}$. Solid (red online) up- or down-going lines indicate neutrons and dotted (blue online) lines indicate protons. The wavy horizontal lines, as in Fig. 1, represent $V_{\mathrm{low}\,k}$, and the dashed horizontal lines represent the $0\nu\beta\beta$-decay operator in Eq. (1).

J.D. Holt, J. Engel, Phys. Rev. C 87, 064315 (2013)

Transition operator

- The 'bare' operator should be transformed into an 'effective' operator defined in the valence space

MBPT

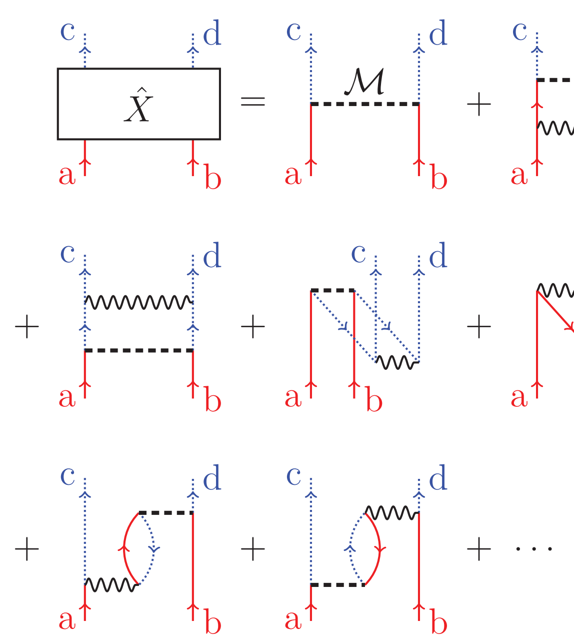

In-medium SRG could also do the job!

FIG. 2. (Color online) The $\hat{X}$ box to first order in $V_{\mathrm{low}\,k}$. Solid (red online) up- or down-going lines indicate neutrons and dotted (blue online) lines indicate protons. The wavy horizontal lines, as in Fig. 1, represent $V_{\mathrm{low}\,k}$, and the dashed horizontal lines represent the $0\nu\beta\beta$-decay operator in Eq. (1).

J.D. Holt, J. Engel, Phys. Rev. C 87, 064315 (2013)

Transition operator

- The ‘bare’ operator should be transformed into an ‘effective’ operator defined in the valence space

MBPT

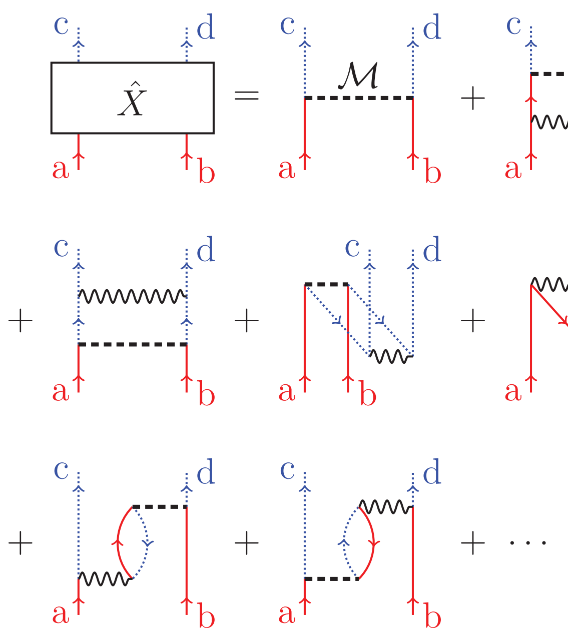

In-medium SRG could also do the job!

FIG. 2. (Color online) The $\hat{X}$ box to first order in $V_{\text{low}\,k}$. Solid (red online) up- or down-going lines indicate neutrons and dotted (blue online) lines indicate protons. The wavy horizontal lines, as in Fig. 1, represent $V_{\text{low}\,k}$, and the dashed horizontal lines represent the $0\nu\beta\beta$-decay operator in Eq. (1).

J.D. Holt, J. Engel, Phys. Rev. C 87, 064315 (2013)

- Two-body weak currents could play a relevant role

ISM

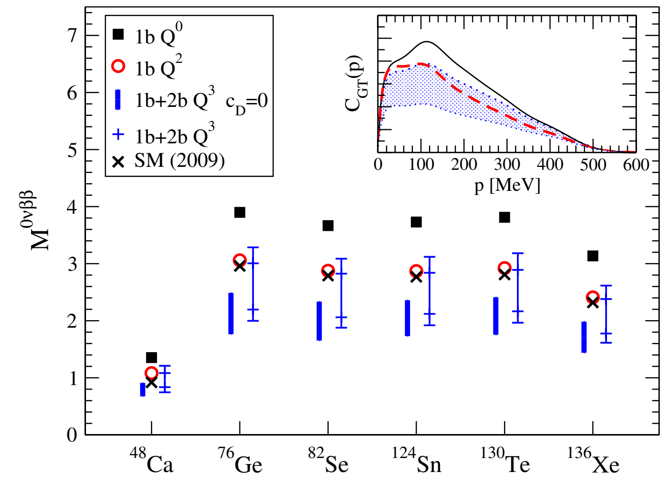

FIG. 2 (color online). Nuclear matrix elements $M^{0\nu\beta\beta}$ for $0\nu\beta\beta$ decay. At order Q^0, the NMEs include only the leading $p=0$ axial and vector $1b$ currents. At the next order, all Q^2 $1b$-current contributions not suppressed by parity are taken into account. At order Q^3, the thick bars are predicted from the long-range parts of $2b$ currents ($c_D = 0$). The thin bars estimate the theoretical uncertainty from the short-range coupling c_D by taking an extreme range for the quenching (see text). For comparison, we show the SM results of Ref. [12] based on phenomenological $1b$ currents only. The inset (representative for ^{136}Xe) shows that the GT part, $M_{\text{GT}}^{0\nu\beta\beta} = \int dp C_{\text{GT}}(p)$, is dominated by $p \sim 100$ MeV.

J. Menéndez, D. Gazit, A. Schwenk, Phys. Rev. Lett. 107, 062501 (2011)

pnQRPA

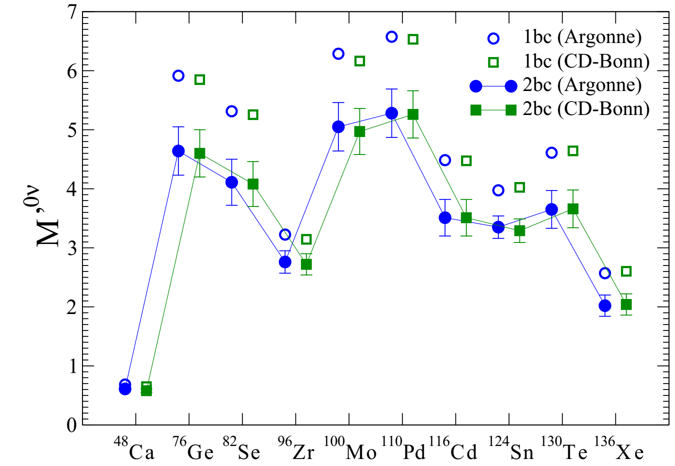

FIG. 1. (Color online) Nuclear matrix elements $M'^{0\nu}$ for all the nuclei considered here. The empty circles and squares represent the results with the one-body current only, and the solid circles and squares the average of the results with two-body currents included. The error bars represent the dispersion in those values (see text).

J. Engel, F. Simkovic, P. Vogel, Phys. Rev. C 89, 064308 (2014)

Transition operator

- The ‘bare’ operator should be transformed into an ‘effective’ operator defined in the valence space

MBPT

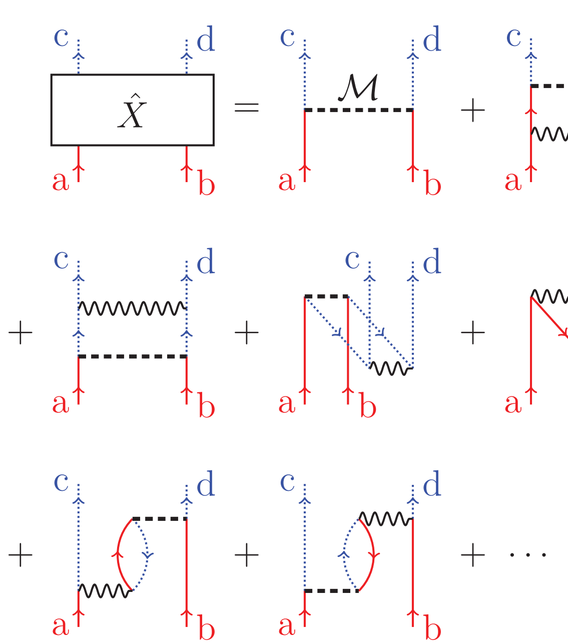

In-medium SRG could also do the job!

FIG. 2. (Color online) The $\hat{X}$ box to first order in $V_{\mathrm{low}\,k}$. Solid (red online) up- or down-going lines indicate neutrons and dotted (blue online) lines indicate protons. The wavy horizontal lines, as in Fig. 1, represent $V_{\mathrm{low}\,k}$, and the dashed horizontal lines represent the $0\nu\beta\beta$-decay operator in Eq. (1).

J.D. Holt, J. Engel, Phys. Rev. C 87, 064315 (2013)

- Two-body weak currents could play a relevant role

ISM

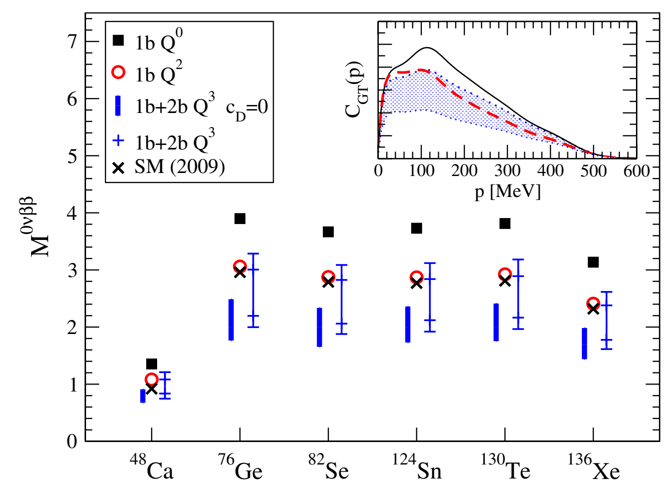

FIG. 2 (color online). Nuclear matrix elements $M^{0\nu\beta\beta}$ for $0\nu\beta\beta$ decay. At order Q^0, the NMEs include only the leading $p=0$ axial and vector $1b$ currents. At the next order, all Q^2 $1b$-current contributions not suppressed by parity are taken into account. At order Q^3, the thick bars are predicted from the long-range parts of $2b$ currents ($c_D=0$). The thin bars estimate the theoretical uncertainty from the short-range coupling c_D by taking an extreme range for the quenching (see text). For comparison, we show the SM results of Ref. [12] based on phenomenological $1b$ currents only. The inset (representative for ^{136}Xe) shows that the GT part, $M^{0\nu\beta\beta}_{\mathrm{GT}} = \int dp C_{\mathrm{GT}}(p)$, is dominated by $p \sim 100$ MeV.

J. Menéndez, D. Gazit, A. Schwenk, Phys. Rev. Lett. 107, 062501 (2011)

pnQRPA

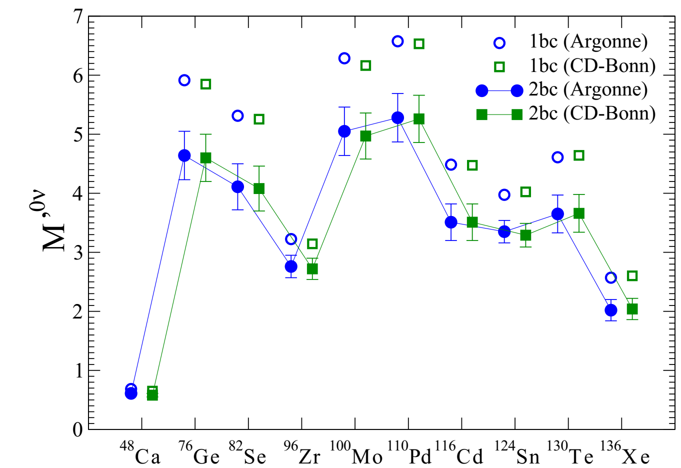

FIG. 1. (Color online) Nuclear matrix elements $M'^{0\nu}$ for all the nuclei considered here. The empty circles and squares represent the results with the one-body current only, and the solid circles and squares the average of the results with two-body currents included. The error bars represent the dispersion in those values (see text).

J. Engel, F. Simkovic, P. Vogel, Phys. Rev. C 89, 064308 (2014)

➥ these are problems closely related to the quenching of Gamow-Teller strength

NME: Nuclear structure aspects

We want to study the role of

- Deformation and shape mixing.
- Pairing pp/nn/pn correlations.
- Shell effects.
- Isospin conservation.
- Pair breaking (seniority).
- Occupation numbers.
- Size of the valence space.

in the nuclear matrix elements using a standard prescription for the transition operator.

Particle number projection

Determination of initial and final states (I)

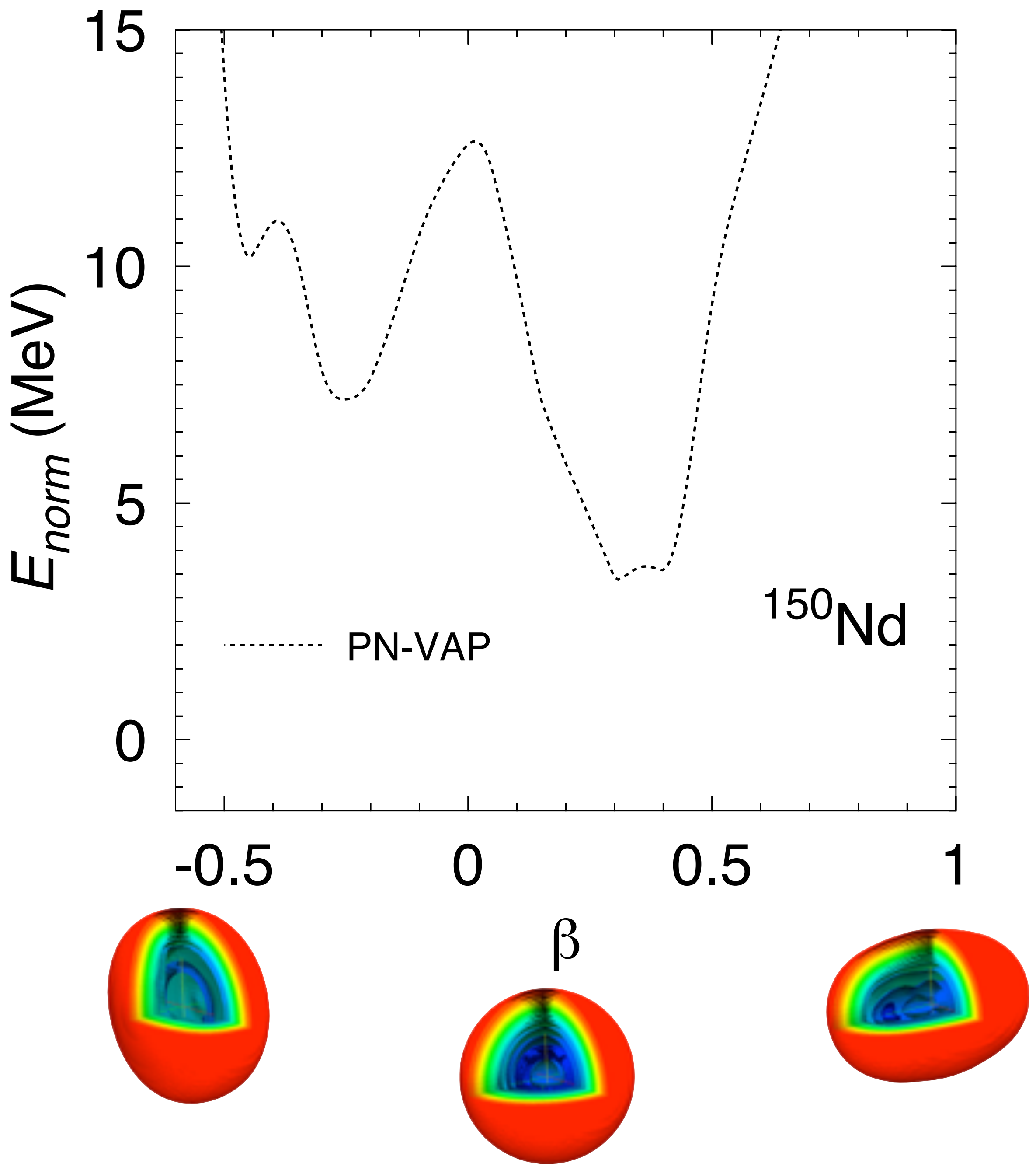

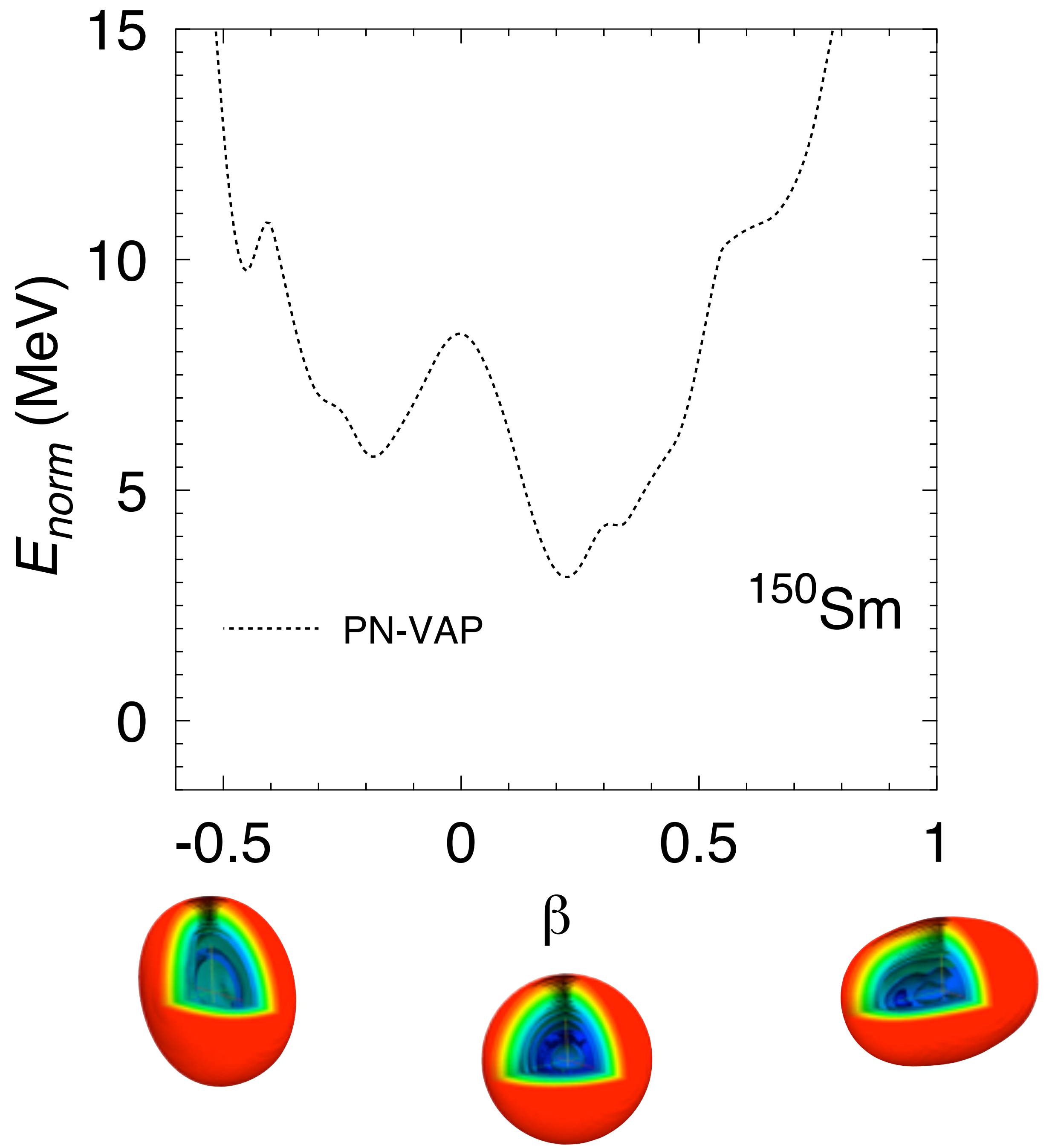

Particle number and angular momentum projection

Determination of initial and final states (II)

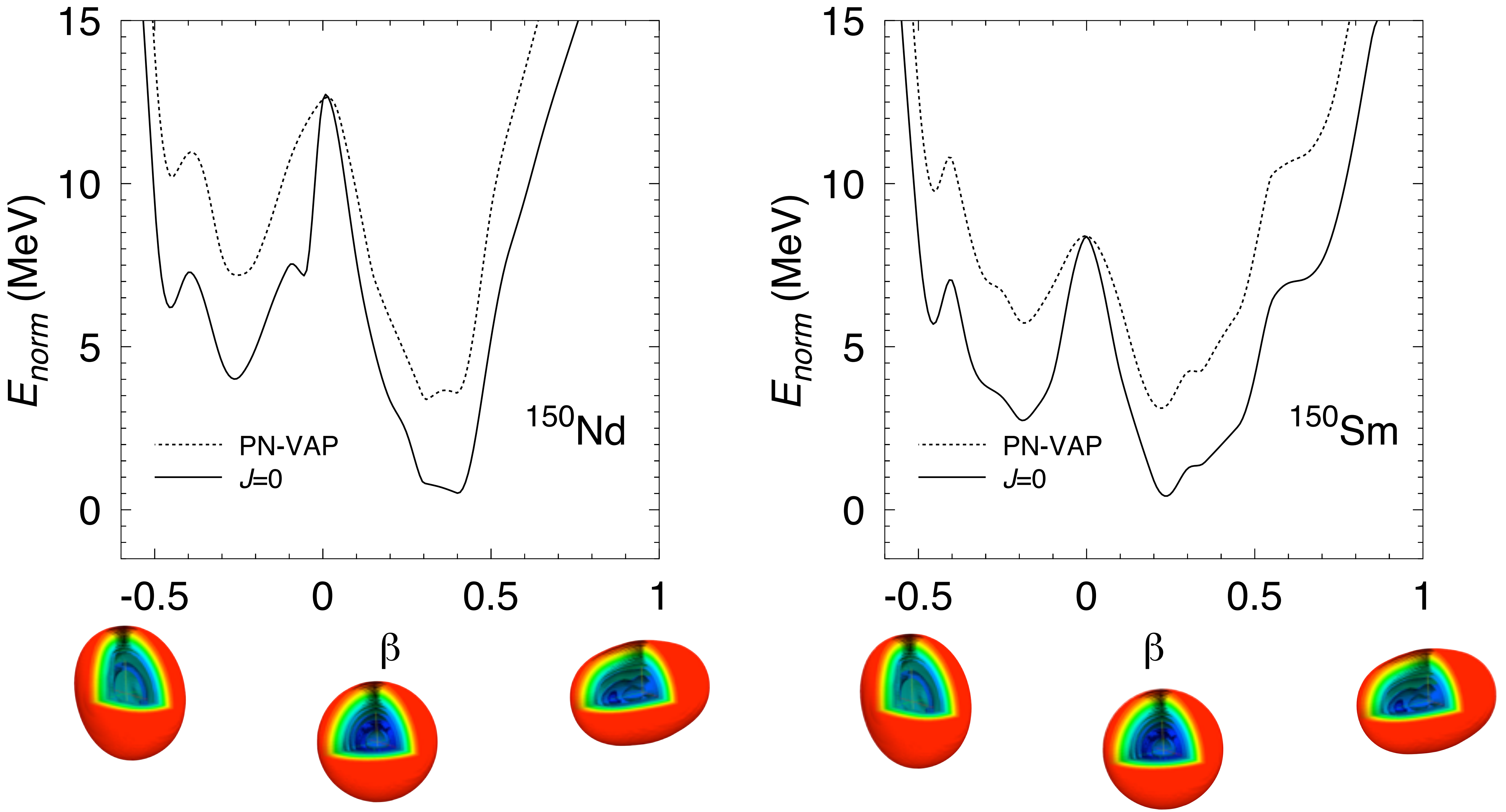

Configuration (shape) mixing

Determination of initial and final states (& III)

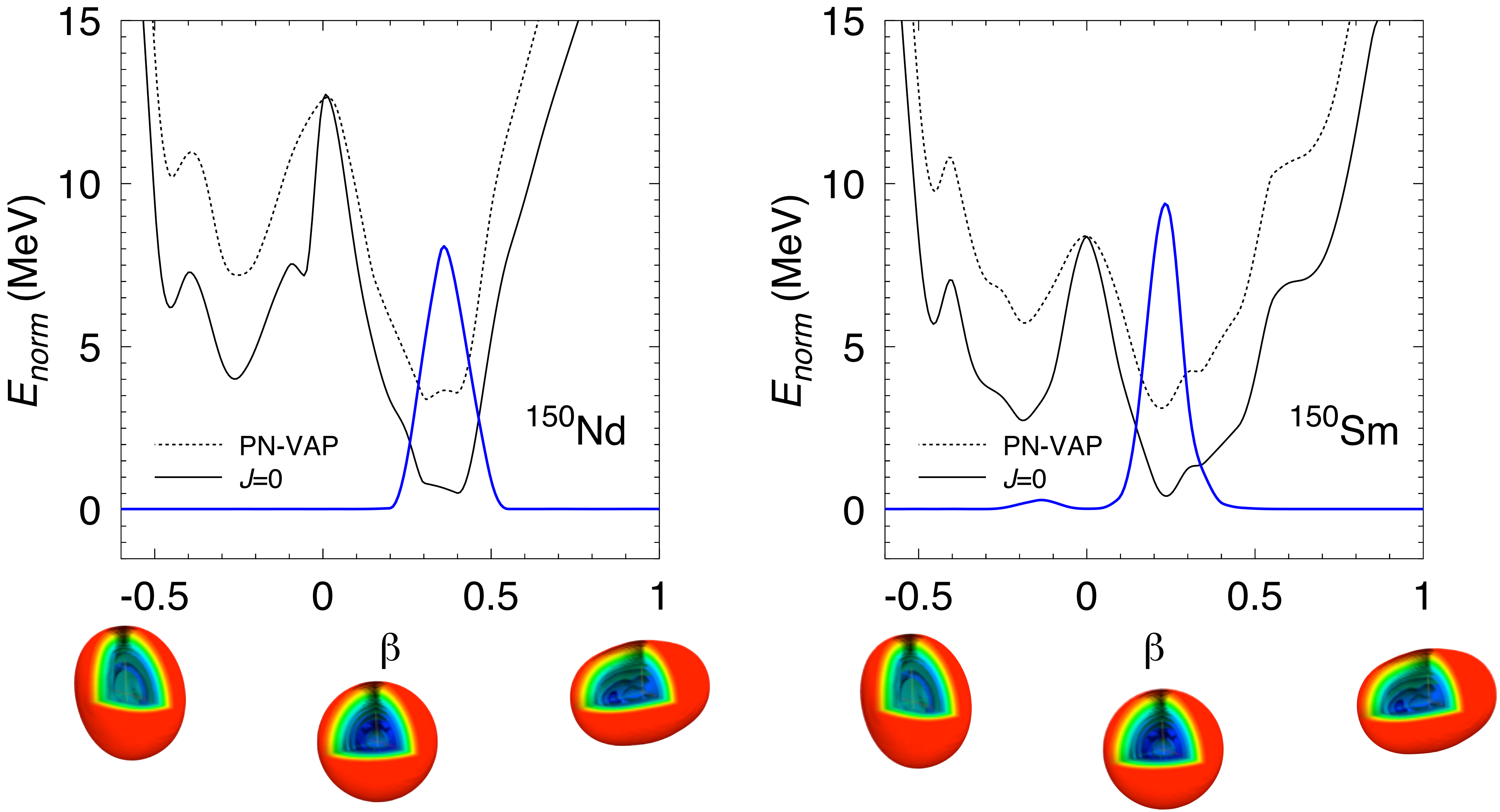

Transitions

1. Axial states $K=0$
2. Angular momentum $I=0$
3. Quadrupole deformations $q=q_{20}$
4. Quadrupole and pairing pp/nn correlations $q=(q_{20},\delta)$
5. Quadrupole and pn correlations $q=(q_{20},p_0)$
6. Quadrupole and octupole deformations $q=(q_{20},q_{30})$

$\longrightarrow$

$$|0;N_iZ_i;\sigma\rangle = \sum_{\Lambda_i} G^{0;N_iZ_i;\sigma}_{\Lambda_i}|\Lambda_i^{0;N_iZ_i}\rangle$$

$$|0;N_fZ_f;\sigma\rangle = \sum_{\Lambda_f} G^{0;N_fZ_f;\sigma}_{\Lambda_f}|\Lambda_f^{0;N_fZ_f}\rangle$$

Transitions

1. Axial states $K=0$
2. Angular momentum $I=0$
3. Quadrupole deformations $q=q_{20}$
4. Quadrupole and pairing pp/nn correlations $q=(q_{20},\delta)$
5. Quadrupole and pn correlations $q=(q_{20},p_0)$
6. Quadrupole and octupole deformations $q=(q_{20},q_{30})$

$\longrightarrow$

$$|0;N_iZ_i;\sigma\rangle = \sum_{\Lambda_i} G_{\Lambda_i}^{0;N_iZ_i;\sigma}|\Lambda_i^{0;N_iZ_i}\rangle$$

$$|0;N_fZ_f;\sigma\rangle = \sum_{\Lambda_f} G_{\Lambda_f}^{0;N_fZ_f;\sigma}|\Lambda_f^{0;N_fZ_f}\rangle$$

TRANSITIONS:

$$M_\xi^{0\nu\beta\beta} = \langle 0_f^+|\hat{O}_\xi^{0\nu\beta\beta}|0_i^+\rangle = \langle 0;N_fZ_f|\hat{O}_\xi^{0\nu\beta\beta}|0;N_iZ_i\rangle =$$

$$\sum_{\Lambda_f\Lambda_i}\left(G_{\Lambda_f}^{0;N_fZ_f}\right)^*\langle\Lambda_f^{0;N_fZ_f}|\hat{O}_\xi^{0\nu\beta\beta}|\Lambda_i^{0;N_iZ_i}\rangle G_{\Lambda_i}^{0;N_iZ_i} = \sum_{q_iq_f;\Lambda_f\Lambda_i}$$

$$\left(\frac{u_{q_f,\Lambda_f}^{0;N_fZ_f}}{\sqrt{n_{\Lambda_f}^{0;N_fZ_f}}}\right)^*\left(G_{\Lambda_f}^{0;N_fZ_f}\right)^*\langle 0;N_fZ_f;q_f|\hat{O}_\xi^{0\nu\beta\beta}|0;N_iZ_i;q_i\rangle\left(G_{\Lambda_i}^{0;N_iZ_i}\right)\left(\frac{u_{q_i,\Lambda_i}^{0;N_iZ_i}}{\sqrt{n_{\Lambda_i}^{0;N_iZ_i}}}\right)$$

Transitions

1. Axial states $K=0$
2. Angular momentum $I=0$
3. Quadrupole deformations $q=q_{20}$
4. Quadrupole and pairing pp/nn correlations $q=(q_{20},\delta)$
5. Quadrupole and pn correlations $q=(q_{20},p_0)$
6. Quadrupole and octupole deformations $q=(q_{20},q_{30})$

$\longrightarrow$

$$|0;N_iZ_i;\sigma\rangle = \sum_{\Lambda_i} G^{0;N_iZ_i;\sigma}_{\Lambda_i}|\Lambda^{0;N_iZ_i}_i\rangle$$

$$|0;N_fZ_f;\sigma\rangle = \sum_{\Lambda_f} G^{0;N_fZ_f;\sigma}_{\Lambda_f}|\Lambda^{0;N_fZ_f}_f\rangle$$

TRANSITIONS:

$$M^{0\nu\beta\beta}_{\xi} = \langle 0^+_f|\hat{O}^{0\nu\beta\beta}_{\xi}|0^+_i\rangle = \langle 0;N_fZ_f|\hat{O}^{0\nu\beta\beta}_{\xi}|0;N_iZ_i\rangle =$$

$$\sum_{\Lambda_f\Lambda_i}\left(G^{0;N_fZ_f}_{\Lambda_f}\right)^*\langle\Lambda^{0;N_fZ_f}_f|\hat{O}^{0\nu\beta\beta}_{\xi}|\Lambda^{0;N_iZ_i}_i\rangle G^{0;N_iZ_i}_{\Lambda_i} = \sum_{q_iq_f;\Lambda_f\Lambda_i}$$

$$\left(\frac{u^{0;N_fZ_f}_{q_f,\Lambda_f}}{\sqrt{n^{0;N_fZ_f}_{\Lambda_f}}}\right)^*\left(G^{0;N_fZ_f}_{\Lambda_f}\right)^*\langle 0;N_fZ_f;q_f|\hat{O}^{0\nu\beta\beta}_{\xi}|0;N_iZ_i;q_i\rangle\left(G^{0;N_iZ_i}_{\Lambda_i}\right)\left(\frac{u^{0;N_iZ_i}_{q_i,\Lambda_i}}{\sqrt{n^{0;N_iZ_i}_{\Lambda_i}}}\right)$$

Matrix elements of the double beta transition operators between particle number and angular momentum projected states

NME: deformation and mixing

$$\frac{\langle 0; N_f Z_f; q_f | \hat{O}_{\xi}^{0\nu\beta\beta} | 0; N_i Z_i; q_i \rangle}{\sqrt{\langle 0; N_f Z_f; q_f | 0; N_f Z_f; q_f \rangle \langle 0; N_i Z_i; q_i | 0; N_i Z_i; q_i \rangle}}$$

A=150

T.R.R., Martínez-Pinedo, PRL 105, 252503 (2010)

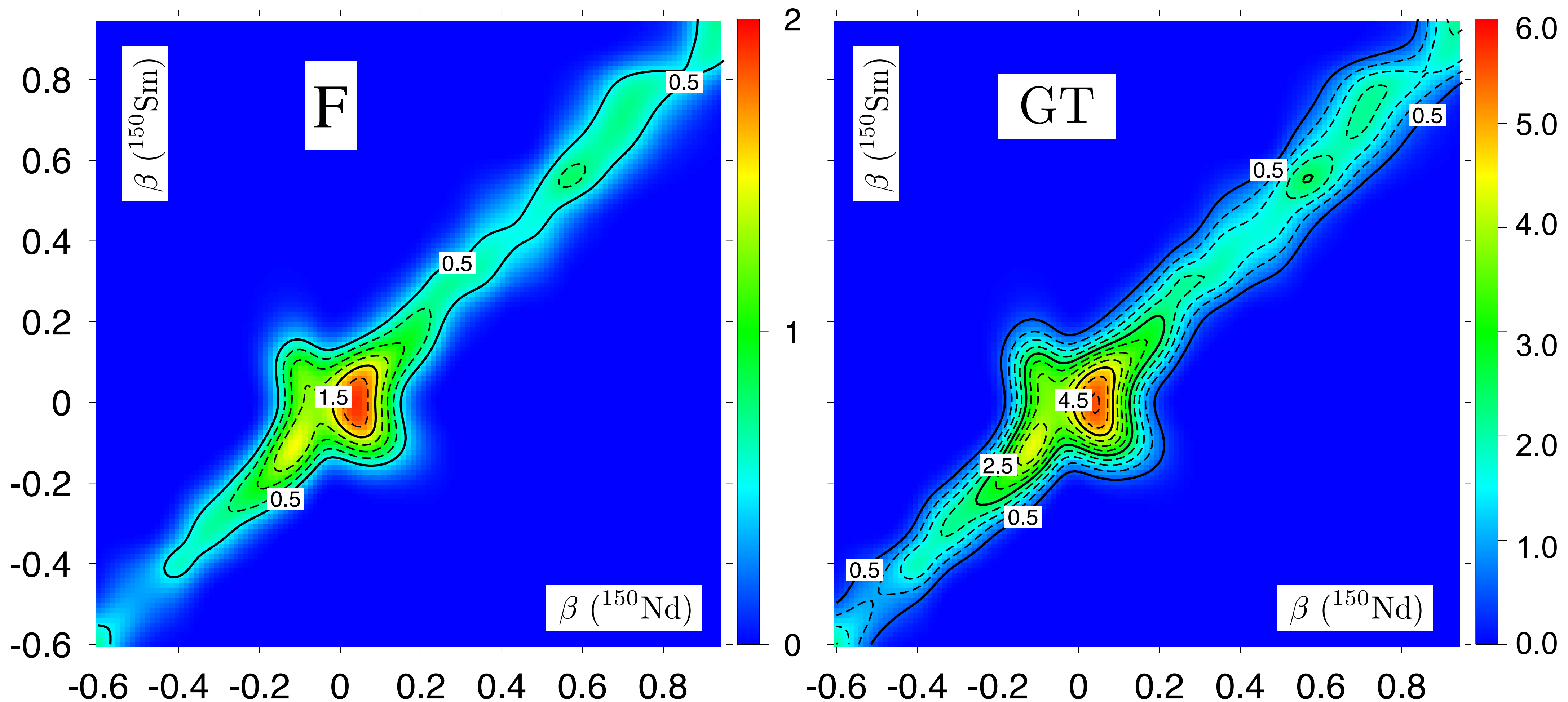

- GT strength greater than Fermi.
- Similar deformation between mother and granddaughter is favored by the transition operators
- Maxima are found close to sphericity although some other local maxima are found

NME: deformation and mixing

T.R.R., Martínez-Pinedo, PRL 105, 252503 (2010)

$$\frac{\langle 0; N_f Z_f; q_f|\hat{O}^{0\nu\beta\beta}_{\xi}|0; N_i Z_i; q_i\rangle}{\sqrt{\langle 0; N_f Z_f; q_f|0; N_f Z_f; q_f\rangle\langle 0; N_i Z_i; q_i|0; N_i Z_i; q_i\rangle}}$$

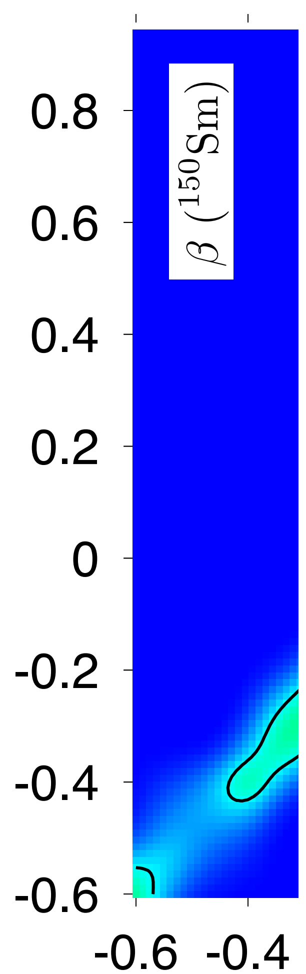

A=150

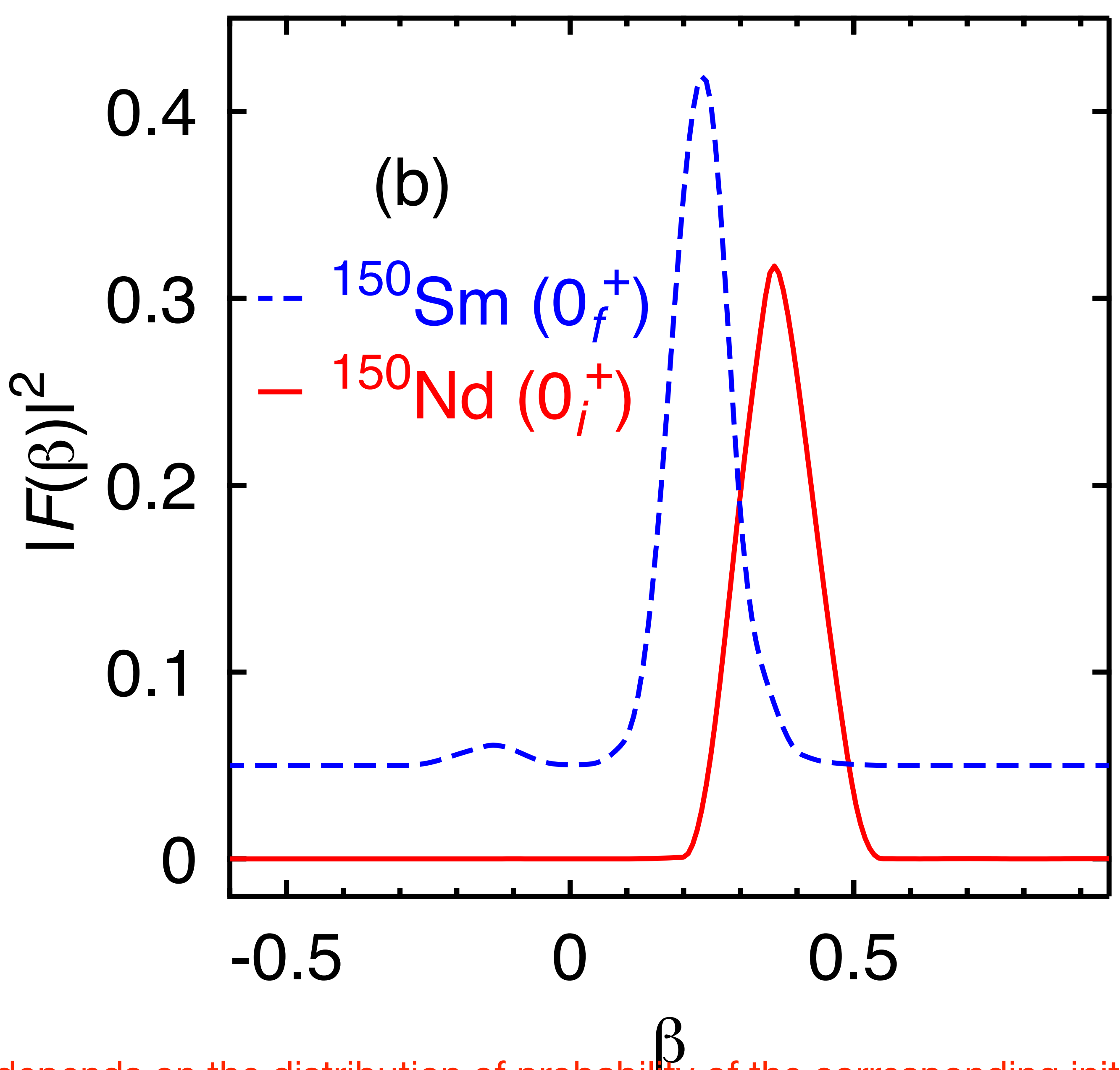

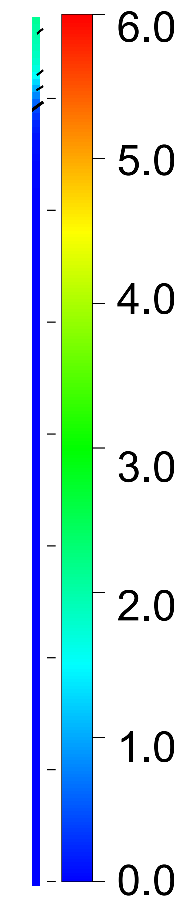

- GT streng
- Similar de
- Maxima a
- Final result depends on the distribution of probability of the corresponding initial and final collective states within this plot

NME: deformation and mixing

$$\frac{\langle 0; N_f Z_f; q_f | \hat{O}_{\xi}^{0\nu\beta\beta} | 0; N_i Z_i; q_i \rangle}{\sqrt{\langle 0; N_f Z_f; q_f | 0; N_f Z_f; q_f \rangle \langle 0; N_i Z_i; q_i | 0; N_i Z_i; q_i \rangle}}$$

A=150

T.R.R., Martínez-Pinedo, PRL 105, 252503 (2010)

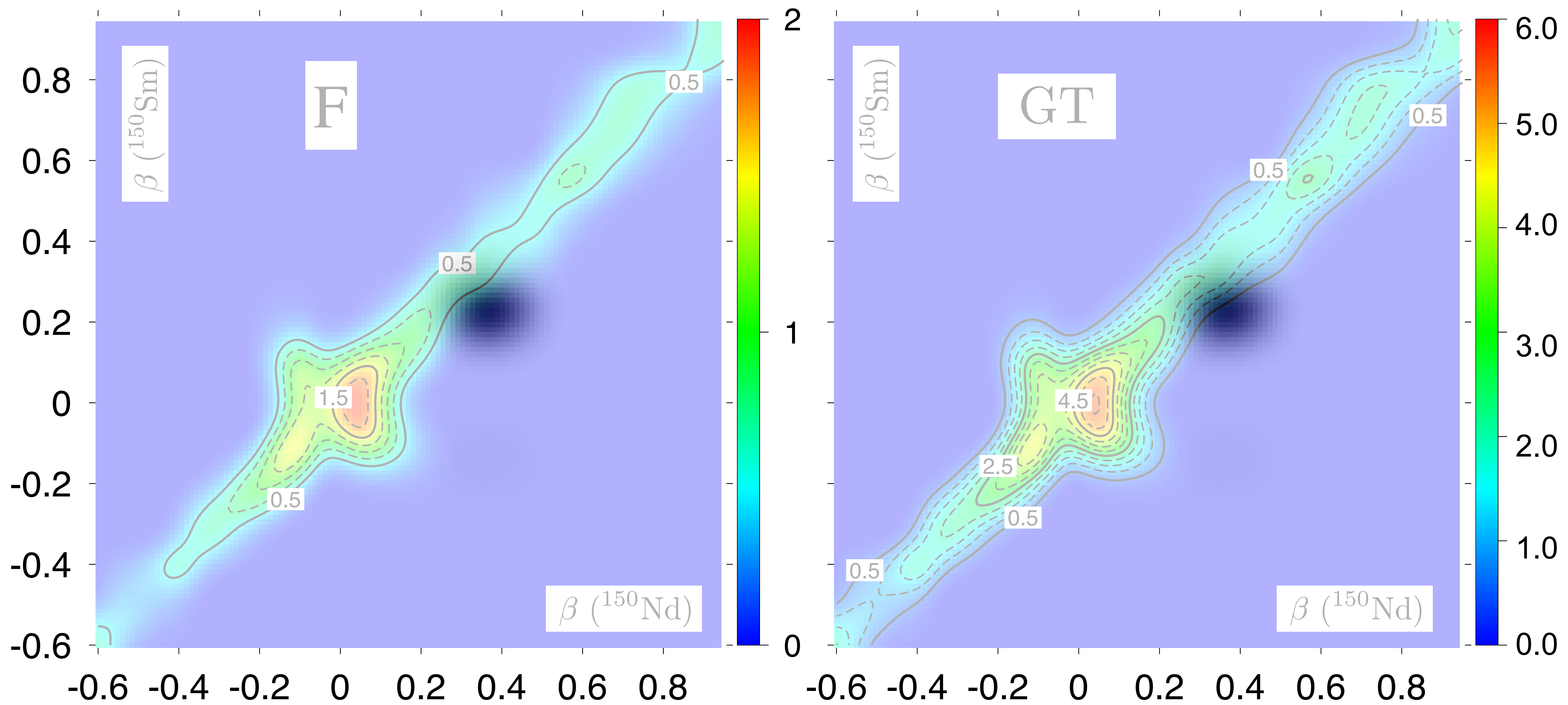

- GT strength greater than Fermi.
- Similar deformation between mother and granddaughter is favored by the transition operators
- Maxima are found close to sphericity although some other local maxima are found
- Final result depends on the distribution of probability of the corresponding initial and final collective states within this plot

NME: deformation and mixing

$$\frac{\langle 0; N_f Z_f; q_f | \hat{O}_{\xi}^{0\nu\beta\beta} | 0; N_i Z_i; q_i \rangle}{\sqrt{\langle 0; N_f Z_f; q_f | 0; N_f Z_f; q_f \rangle \langle 0; N_i Z_i; q_i | 0; N_i Z_i; q_i \rangle}}$$

A=150

T.R.R., Martínez-Pinedo, PRL 105, 252503 (2010)

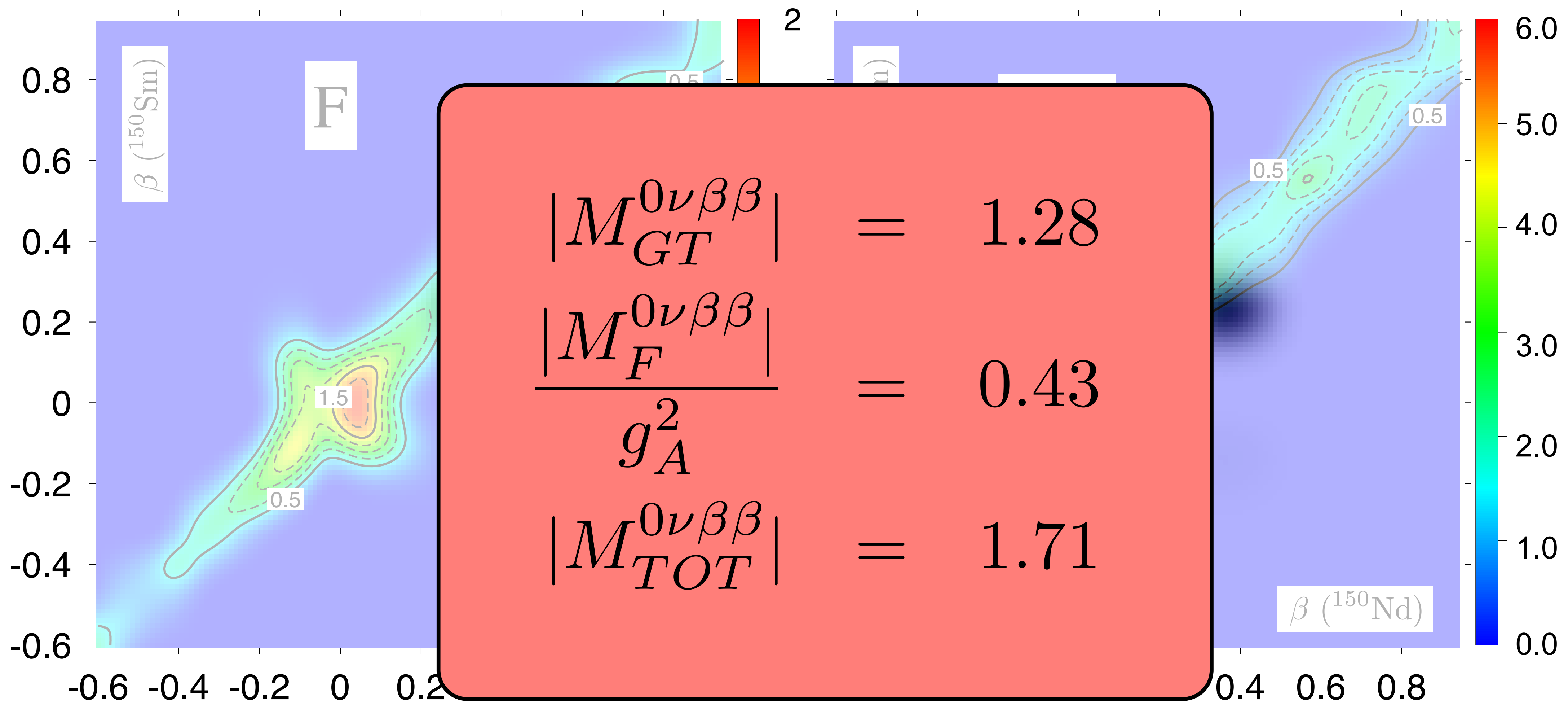

$$|M_{GT}^{0\nu\beta\beta}| = 1.28$$

$$\frac{|M_{F}^{0\nu\beta\beta}|}{g_A^2} = 0.43$$

$$|M_{TOT}^{0\nu\beta\beta}| = 1.71$$

- GT strength greater than Fermi.
- Similar deformation between mother and granddaughter is favored by the transition operators
- Maxima are found close to sphericity although some other local maxima are found
- Final result depends on the distribution of probability of the corresponding initial and final collective states within this plot

NME: deformation and mixing

J. M. Yao and J. Engel, arXiv 1604.06297 (2016)

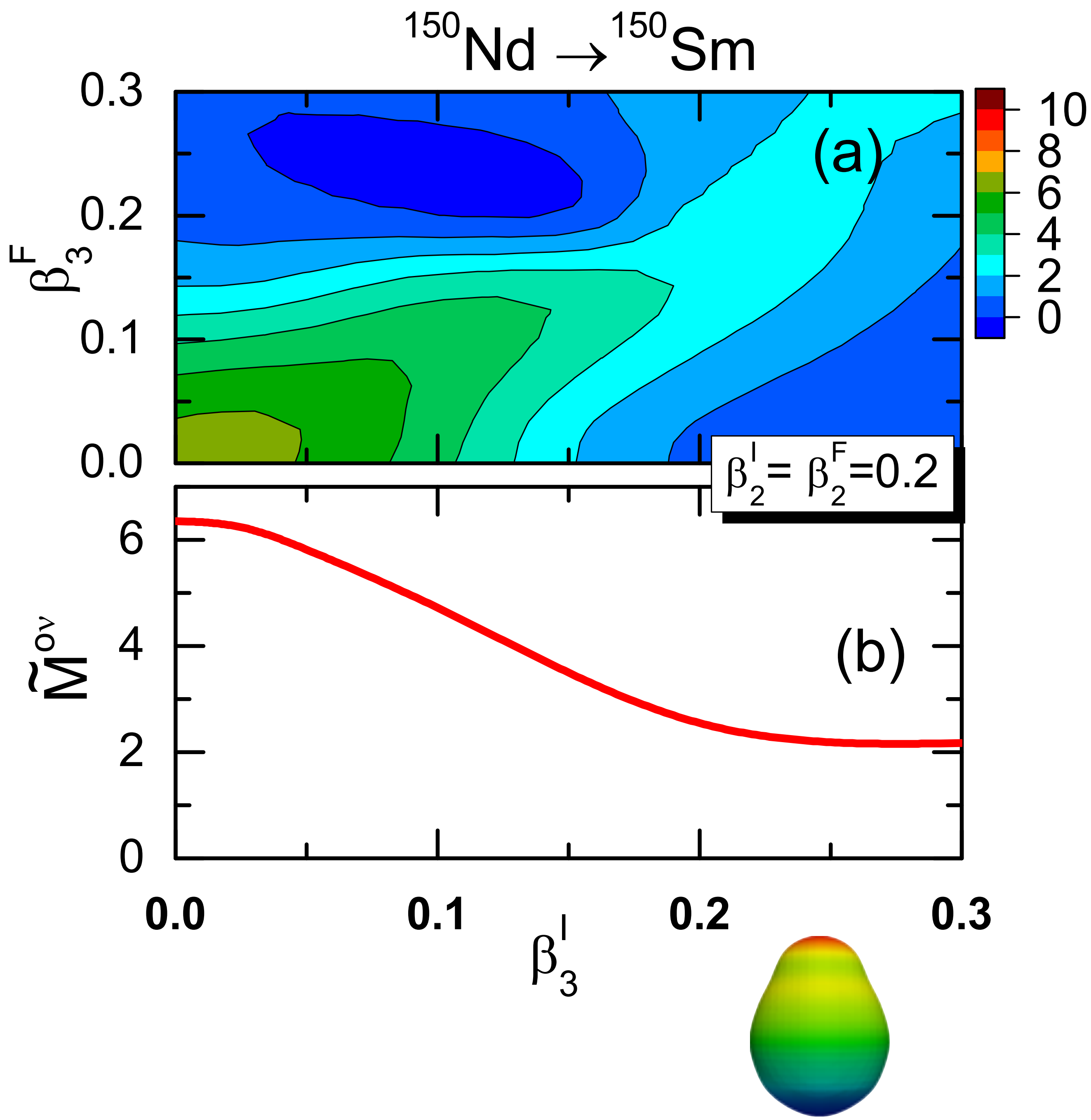

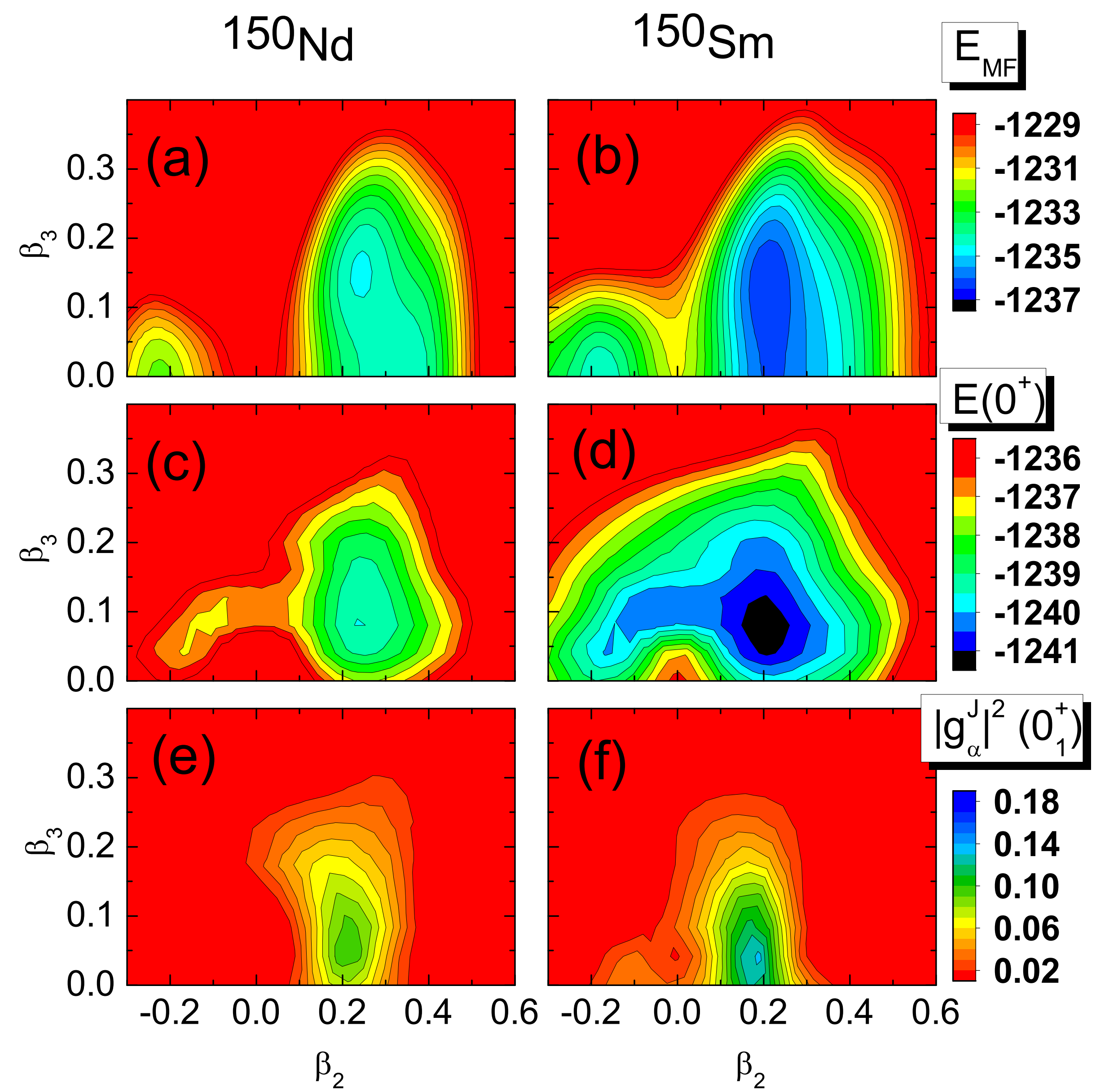

NME: deformation and mixing

J. M. Yao and J. Engel, arXiv 1604.06297 (2016)

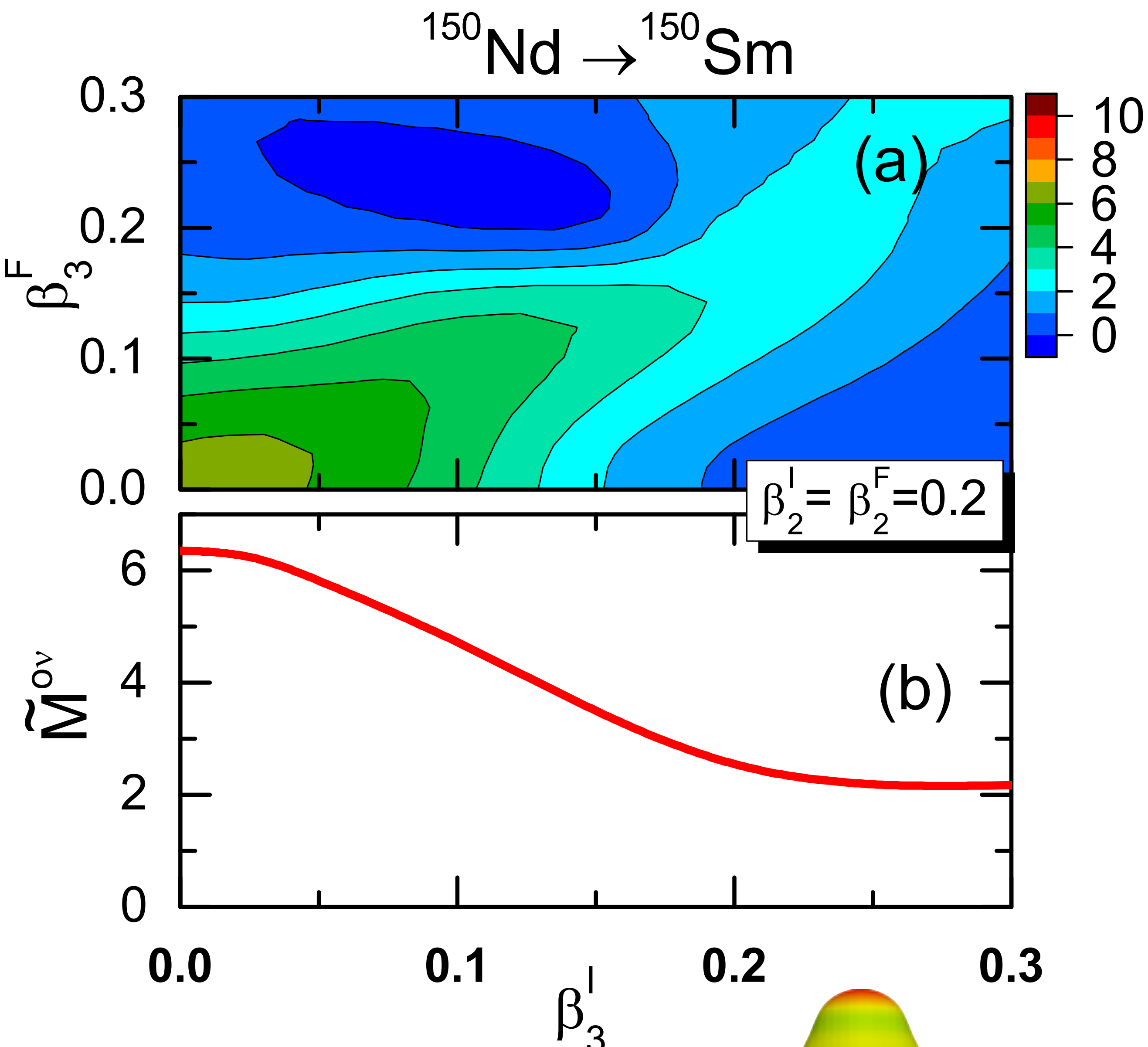

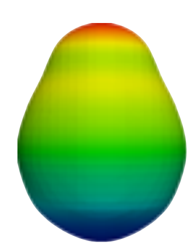

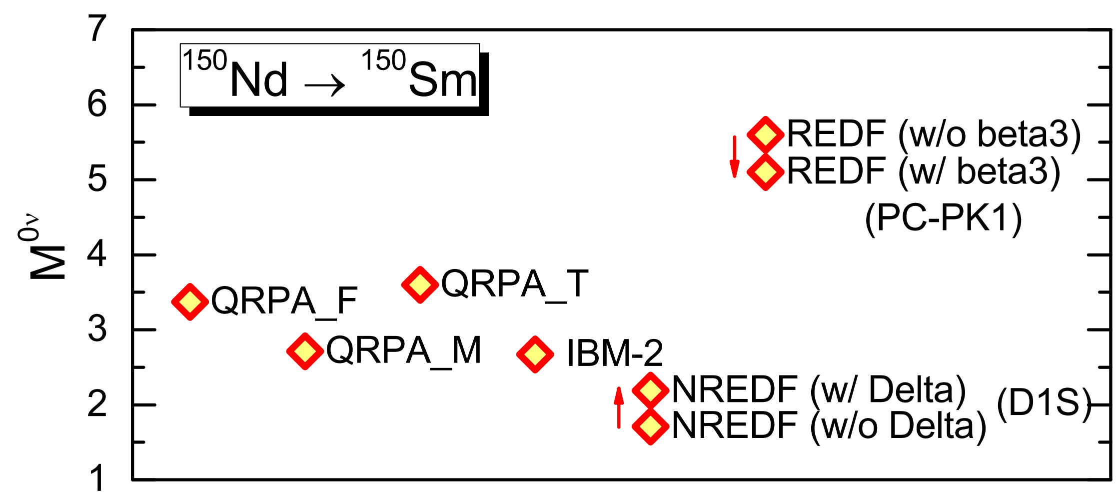

FIG. 5: (Color online) The final matrix element $M^{0\nu}$ from the GCM calculation with and without [46] octupole shape fluctuations (REDF) and those of the QRPA ("QRPA_F" [66], "QRPA_M" [45], "QRPA_T" [47]), the IMB-2 [67], and the non-relativistic GCM, based on the Gogny D1S interaction, with [68] and without [44] pairing fluctuations.

NME: deformation and mixing

UNIVERSIDAD AUTONOMA DE MADRID

A=76

T. R. R., J. Phys. G 44, 034002 (2017)

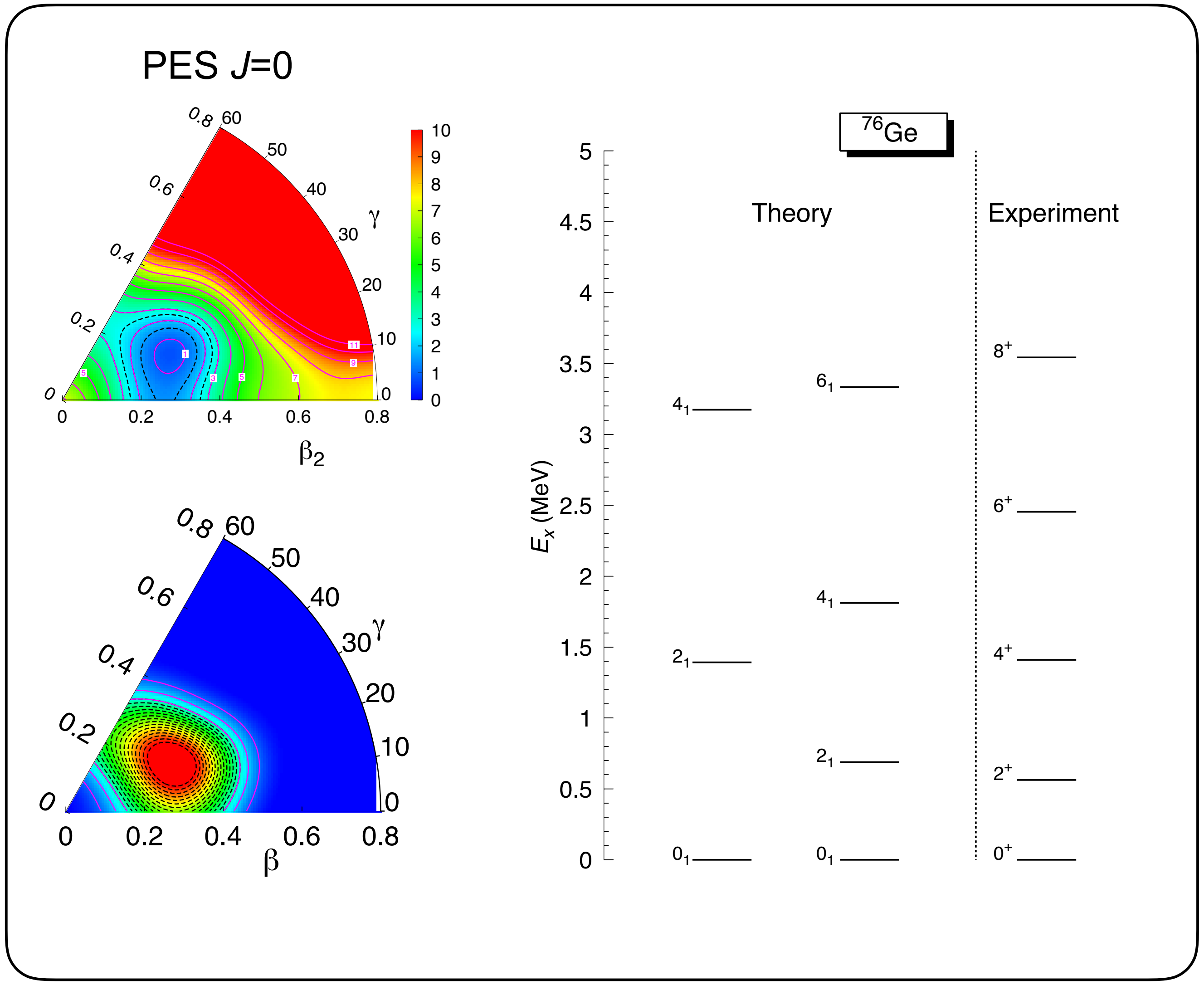

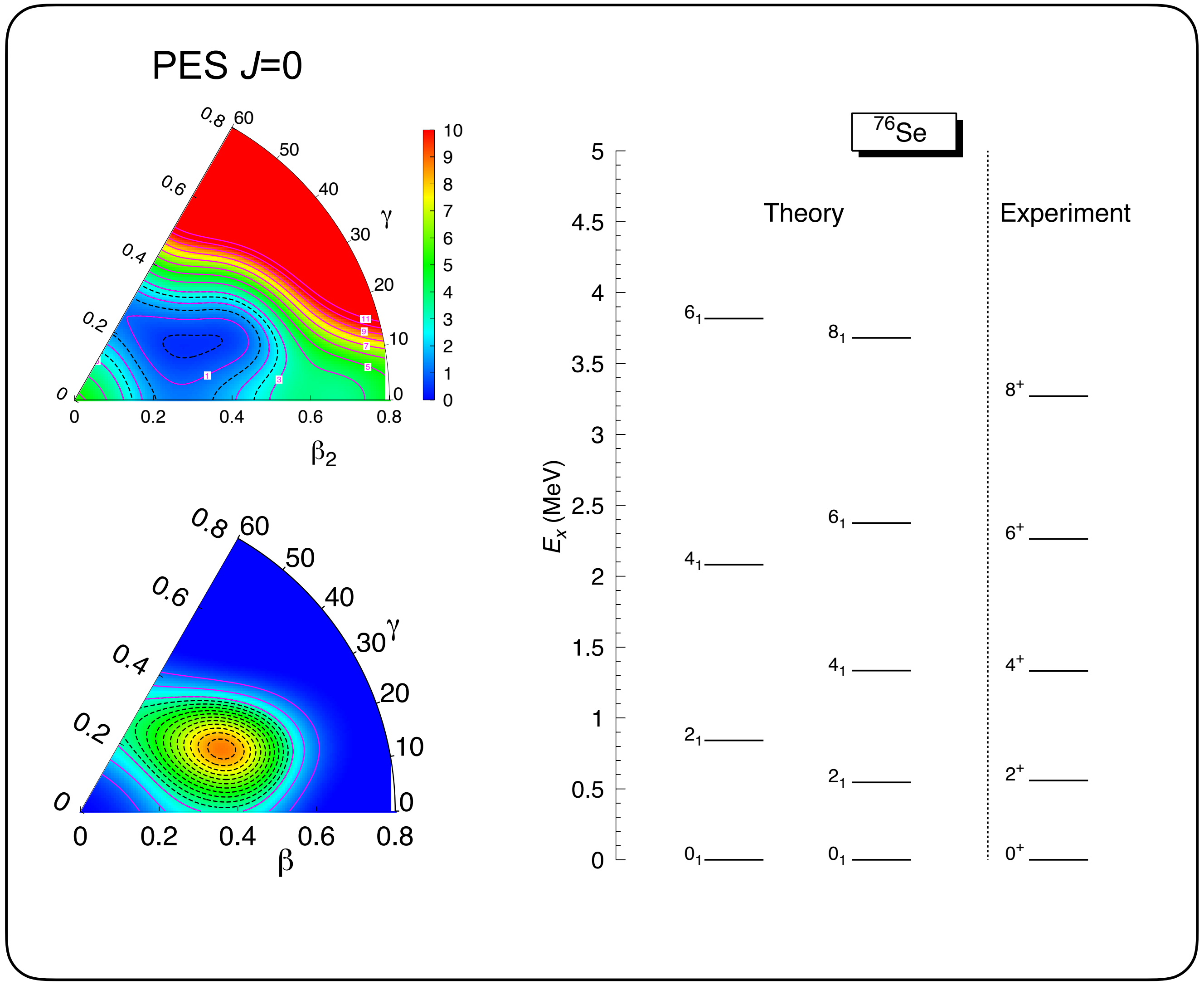

NME: deformation and mixing

A=76

T. R. R., J. Phys. G 44, 034002 (2017)

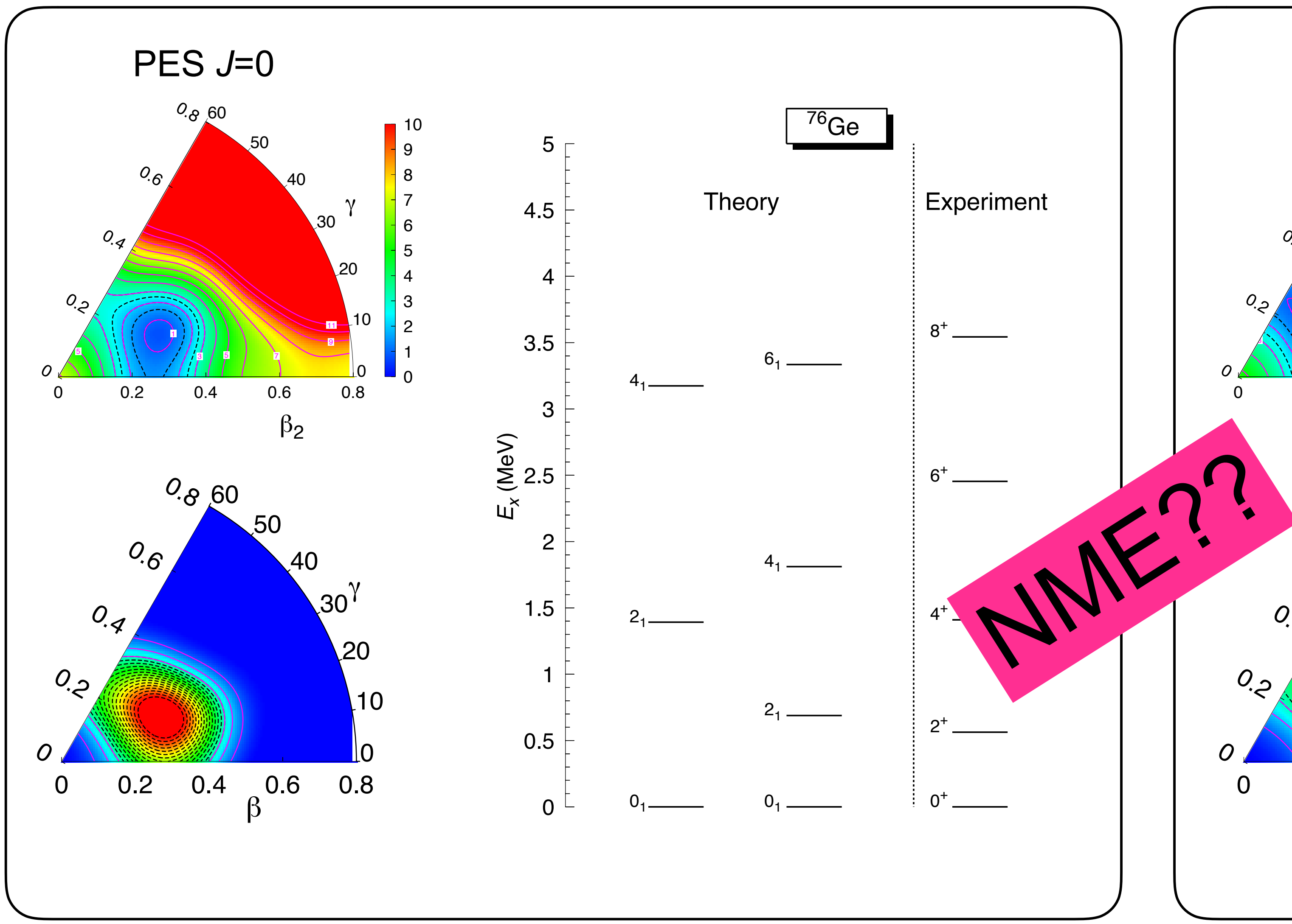

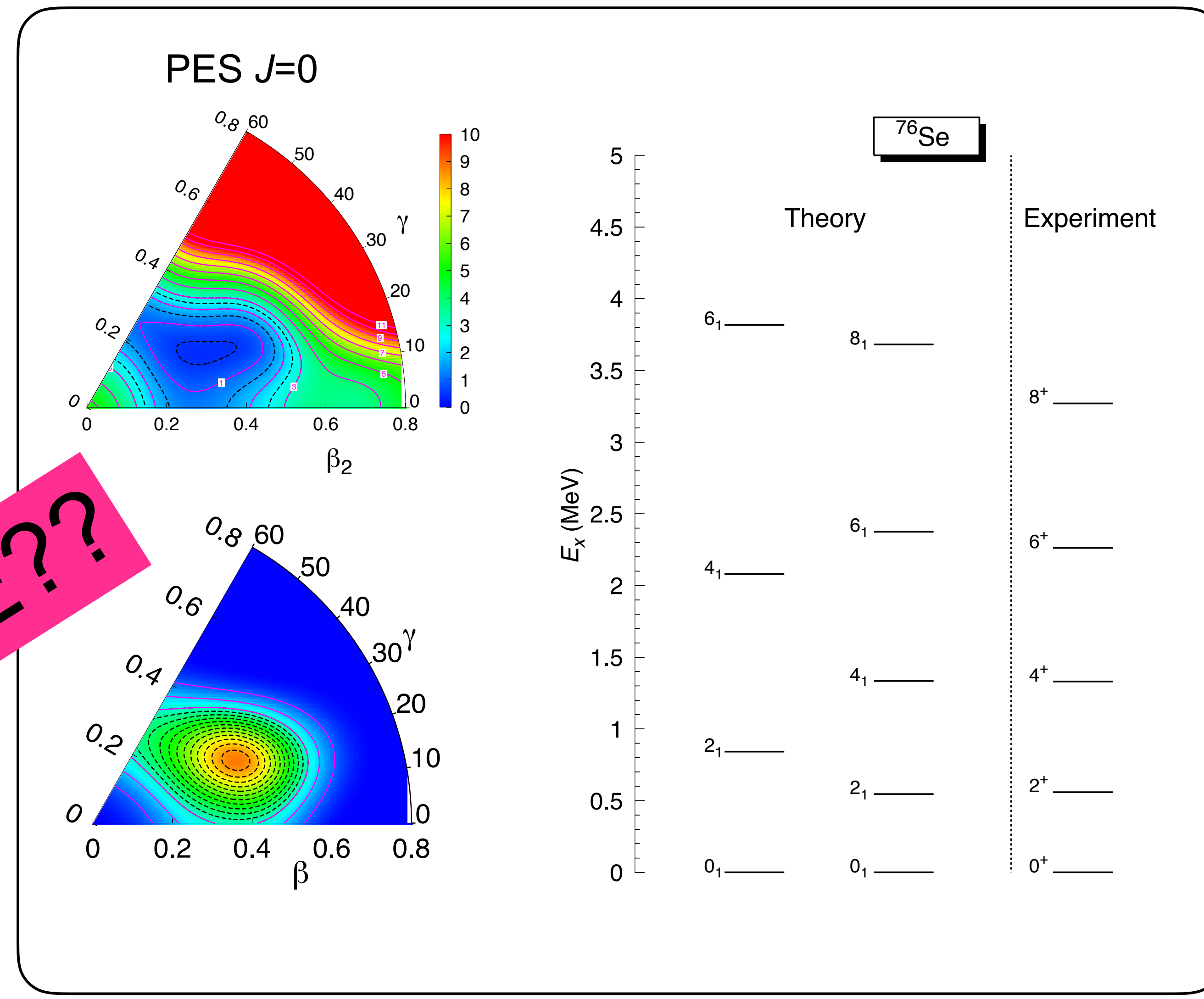

NME: deformation and mixing

HFB-PES

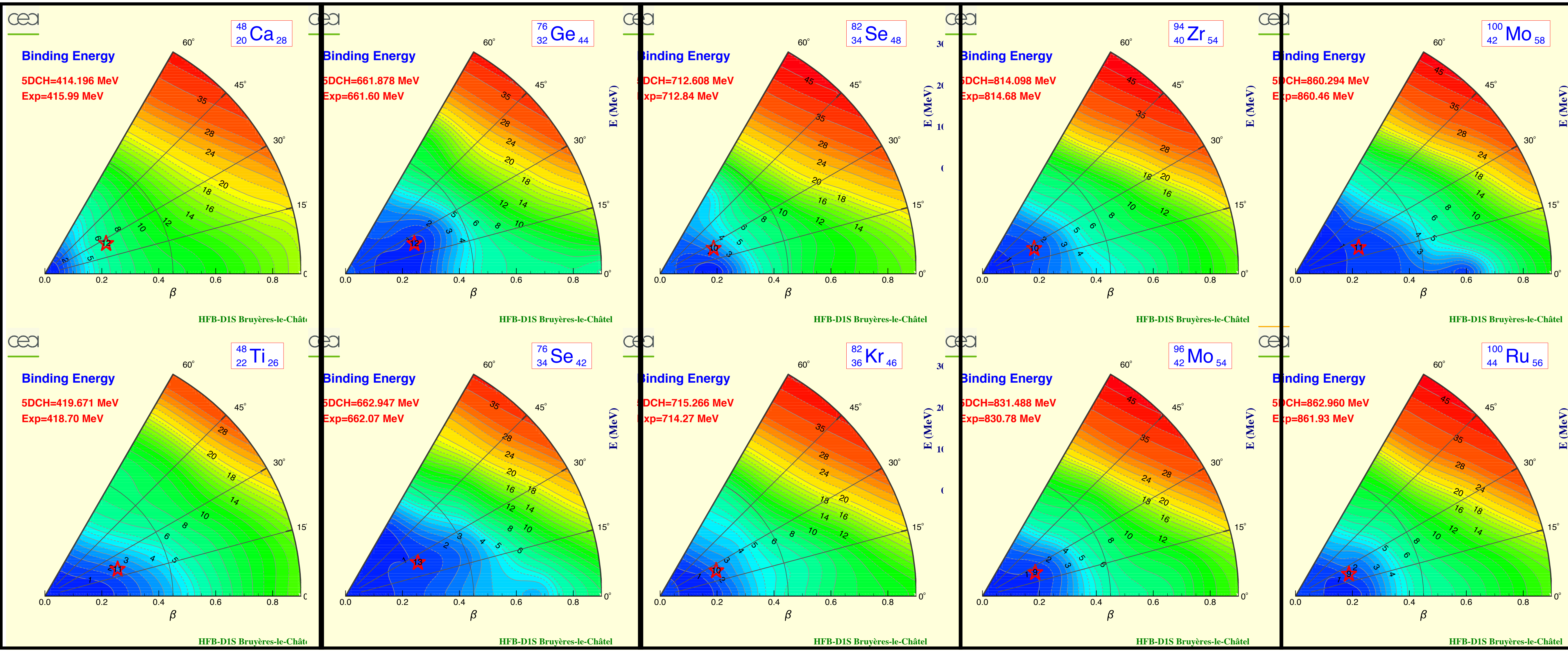

CEA-Bruyeres-le-Chatel data base

HFB-PES

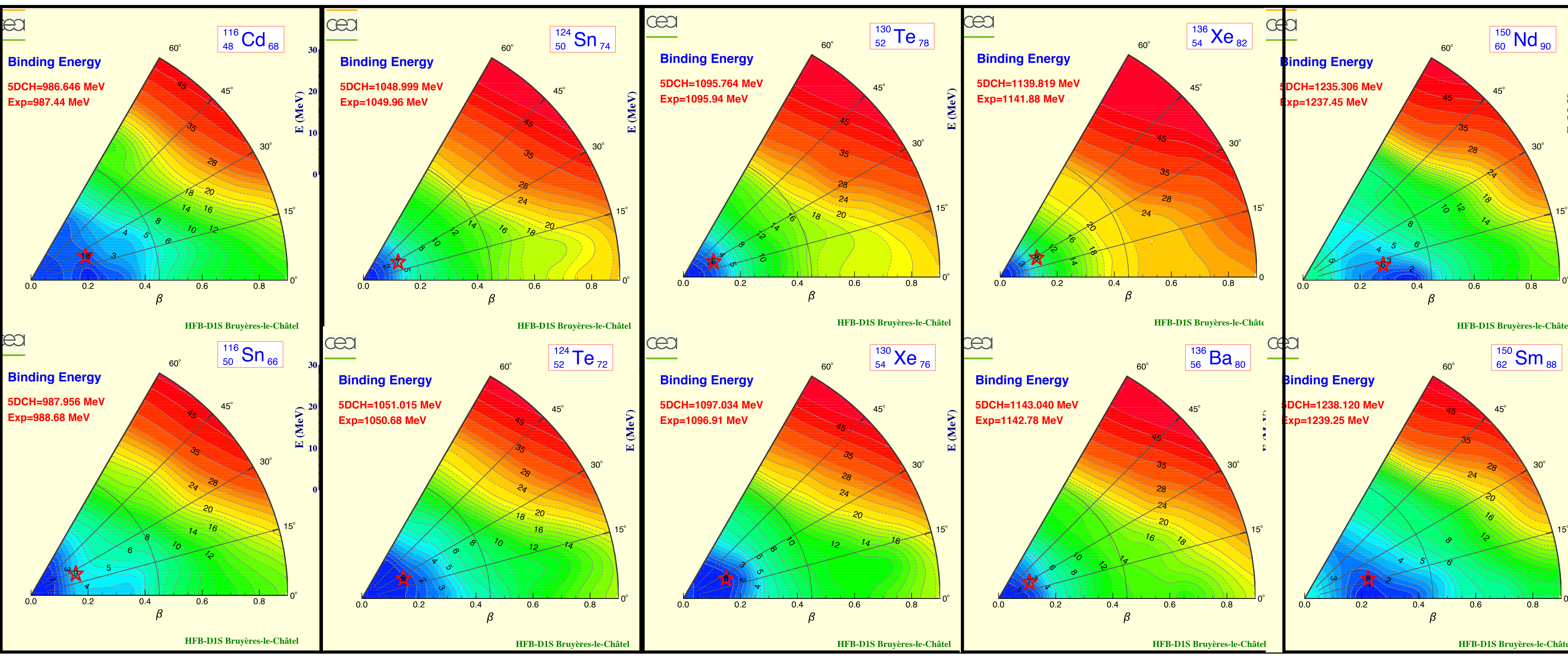

CEA-Bruyeres-le-Chatel data base

Shape and pp/nn pairing fluctuations

Angular momentum projected potential energy surfaces

Collective ground state wave functions

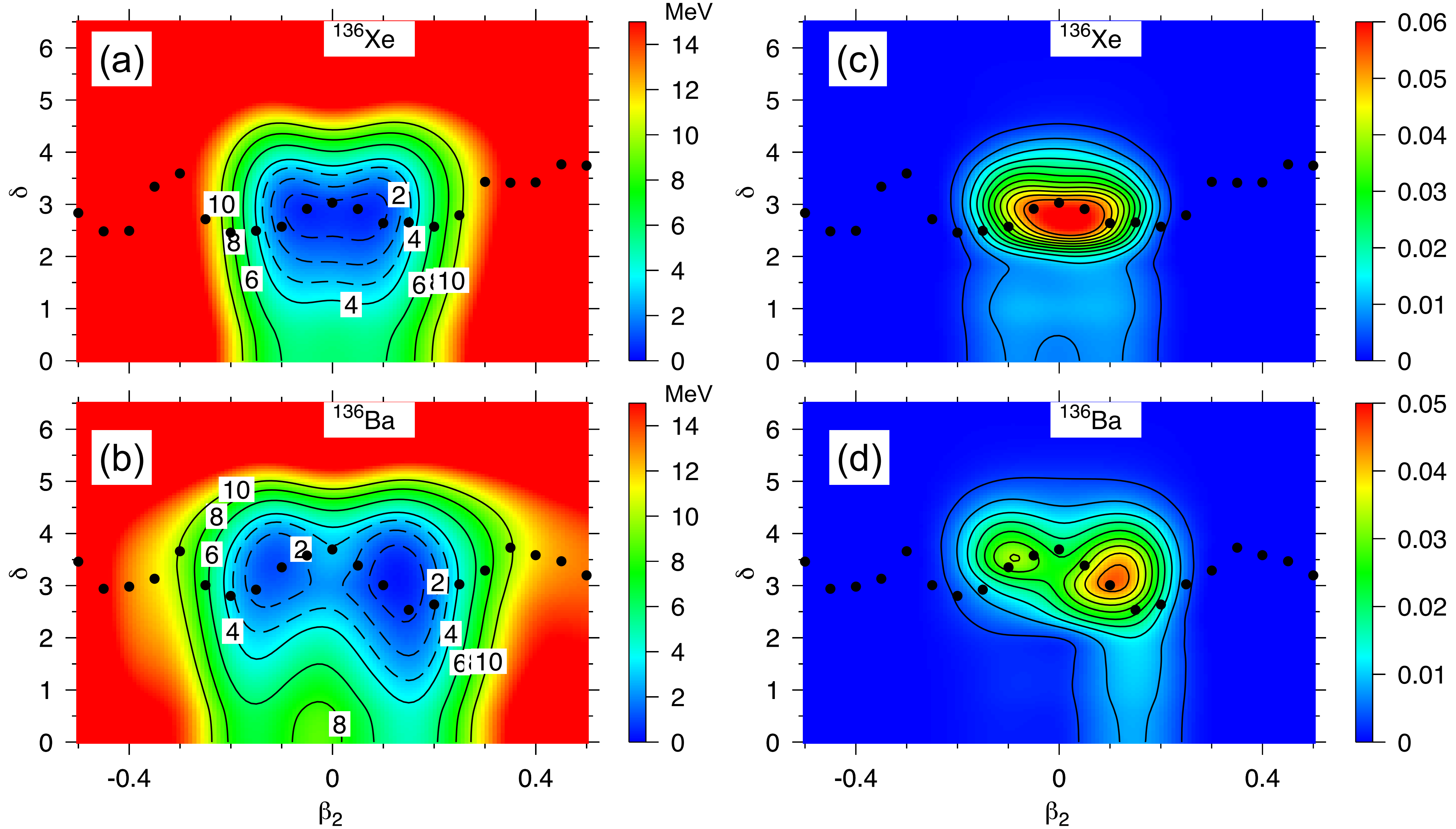

N. López-Vaquero, T.R.R., J.L. Egido, PRL 111, 142501 (2013)

Shape and pp/nn pairing fluctuations

UNIVERSIDAD AUTONOMA DE MADRID

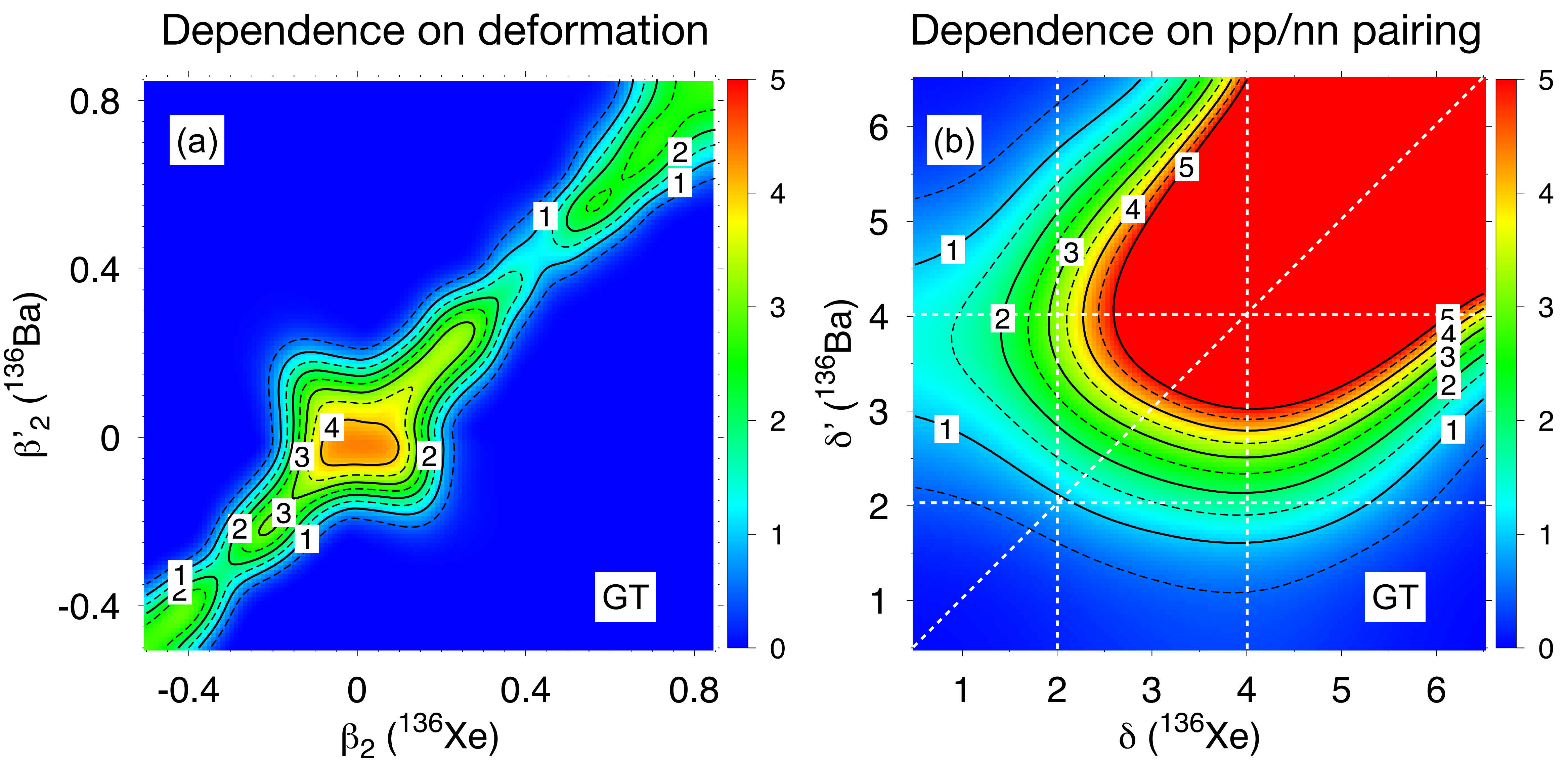

N. López-Vaquero, T.R.R., J.L. Egido, PRL 111, 142501 (2013)

Shape and pp/nn pairing fluctuations

Isotope	$\Delta Q(\beta_2)$	$\Delta Q(\beta_2,\delta)$	$M^{0\nu}(\beta_2)$	$M^{0\nu}(\beta_2,\delta)$	Var (%)	$\frac{T_{1/2}(\beta_2,\delta)}{T_{1/2}(\beta_2)}$
^{48}Ca	0.265	0.131	$2.370^{1.914}_{0.456}$	$2.229^{1.797}_{0.431}$	-6	1.13
^{76}Ge	0.271	0.190	$4.601^{3.715}_{0.886}$	$5.551^{4.470}_{1.082}$	21	0.69
^{82}Se	-0.366	-0.246	$4.218^{3.381}_{0.837}$	$4.674^{3.743}_{0.931}$	11	0.81
^{96}Zr	2.580	2.628	$5.650^{4.618}_{1.032}$	$6.498^{5.296}_{1.202}$	15	0.76
^{100}Mo	1.879	1.757	$5.084^{4.149}_{0.935}$	$6.588^{5.361}_{1.227}$	30	0.60
^{116}Cd	1.365	1.337	$4.795^{3.931}_{0.864}$	$5.348^{4.372}_{0.976}$	12	0.80
^{124}Sn	-0.830	-0.687	$4.808^{3.893}_{0.916}$	$5.787^{4.680}_{1.107}$	20	0.69
^{128}Te	-0.564	-0.594	$4.107^{3.079}_{1.027}$	$5.687^{4.255}_{1.432}$	38	0.52
^{130}Te	-0.348	-0.628	$5.130^{4.141}_{0.989}$	$6.405^{5.161}_{1.244}$	25	0.64
^{136}Xe	-1.027	-0.787	$4.199^{3.673}_{0.526}$	$4.773^{4.170}_{0.604}$	14	0.77
^{150}Nd	-0.380	-0.282	$1.707^{1.278}_{0.429}$	$2.190^{1.639}_{0.551}$	29	0.61

N. López-Vaquero, T.R.R., J.L. Egido, PRL 111, 142501 (2013)

Shape and pn pairing fluctuations

$$H = h_0 - \sum_{\mu=-1}^{1} g_\mu^{T=1}\, S_\mu^\dagger S_\mu - \frac{\chi}{2}\sum_{K=-2}^{2} Q_{2K}^\dagger Q_{2K}$$
$$- g^{T=0}\sum_{\nu=-1}^{1} P_\nu^\dagger P_\nu + g_{ph}\sum_{\mu,\nu=-1}^{1} F_\nu^{\mu\dagger} F_\nu^\mu\,, \qquad (2)$$

where h_0 contains spherical single particle energies, Q_{2K} are the components of a quadrupole operator defined in Ref. [15], and

$$S_\mu^\dagger = \frac{1}{\sqrt{2}}\sum_l \hat{l}[c_l^\dagger c_l^\dagger]^{001}_{00\mu}\,, \quad P_\mu^\dagger = \frac{1}{\sqrt{2}}\sum_l \hat{l}[c_l^\dagger c_l^\dagger]^{010}_{0\mu 0}\,,$$
$$F_\nu^\mu = \frac{1}{2}\sum_i \sigma_i^\mu \tau_i^\nu = \sum_l \hat{l}[c_l^\dagger \bar{c}_l]^{011}_{0\mu\nu}\,. \qquad (3)$$

$$H' = H - \lambda_Z N_Z - \lambda_N N_N - \lambda_Q Q_{20} - \frac{\lambda_P}{2}\left(P_0 + P_0^\dagger\right)\,, \quad (6)$$

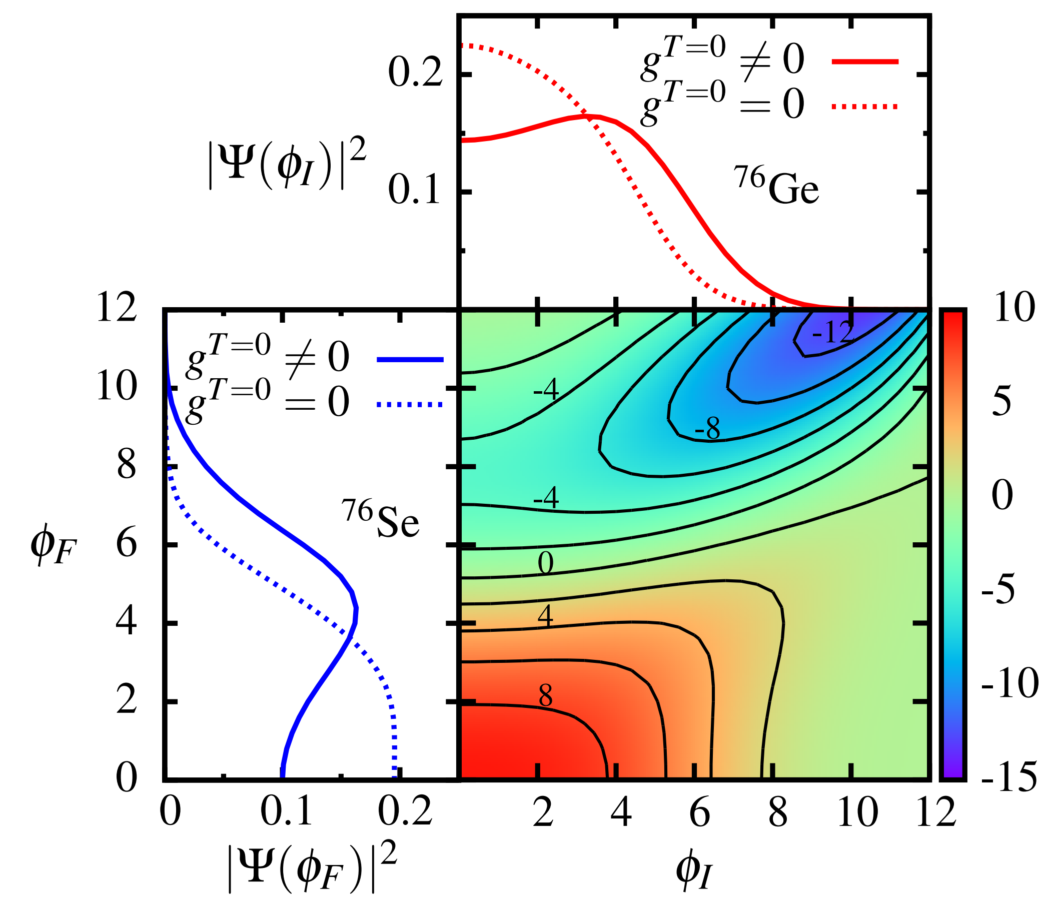

FIG. 3. (Color online.) **Bottom right:** $\mathcal{N}_{\phi_I}\mathcal{N}_{\phi_F}\langle\phi_F|\mathcal{P}_F\hat{M}_{0\nu}\mathcal{P}_I|\phi_I\rangle$ for projected quasiparticle vacua with different values of the initial and final isoscalar pairing amplitudes ϕ_I and ϕ_F, from the SkO′-based interaction (see text). **Top and bottom left:** Square of collective wave functions in ^{76}Ge and ^{76}Se.

N. Hinohara and J. Engel, PRC 031031(R) (2014)

Shape and pn pairing fluctuations

$$H = h_0 - \sum_{\mu=-1}^{1} g_\mu^{T=1}\, S_\mu^\dagger S_\mu - \frac{\chi}{2}\sum_{K=-2}^{2} Q_{2K}^\dagger Q_{2K}$$

$$- g^{T=0}\sum_{\nu=-1}^{1} P_\nu^\dagger P_\nu + \ldots$$

where h_0 contains spherical ... are the components of a qu... Ref. [15], and

$$S_\mu^\dagger = \frac{1}{\sqrt{2}}\sum_l \hat{l}[c_l^\dagger c_l^\dagger]^{001}_{00\mu}\,, \ldots$$

$$F_\nu^\mu = \frac{1}{2}\sum_i \sigma_i^\mu \tau_i^\nu = \sum_l \hat{l}[c_l^\dagger \bar{c}_l]^{011}_{0\mu\nu}\,. \qquad (3)$$

$$H' = H - \lambda_Z N_Z - \lambda_N N_N - \lambda_Q Q_{20} - \frac{\lambda_P}{2}\left(P_0 + P_0^\dagger\right)\,, \quad (6)$$

Exploring explicitly pp/nn and pn pairing could produce cancellations

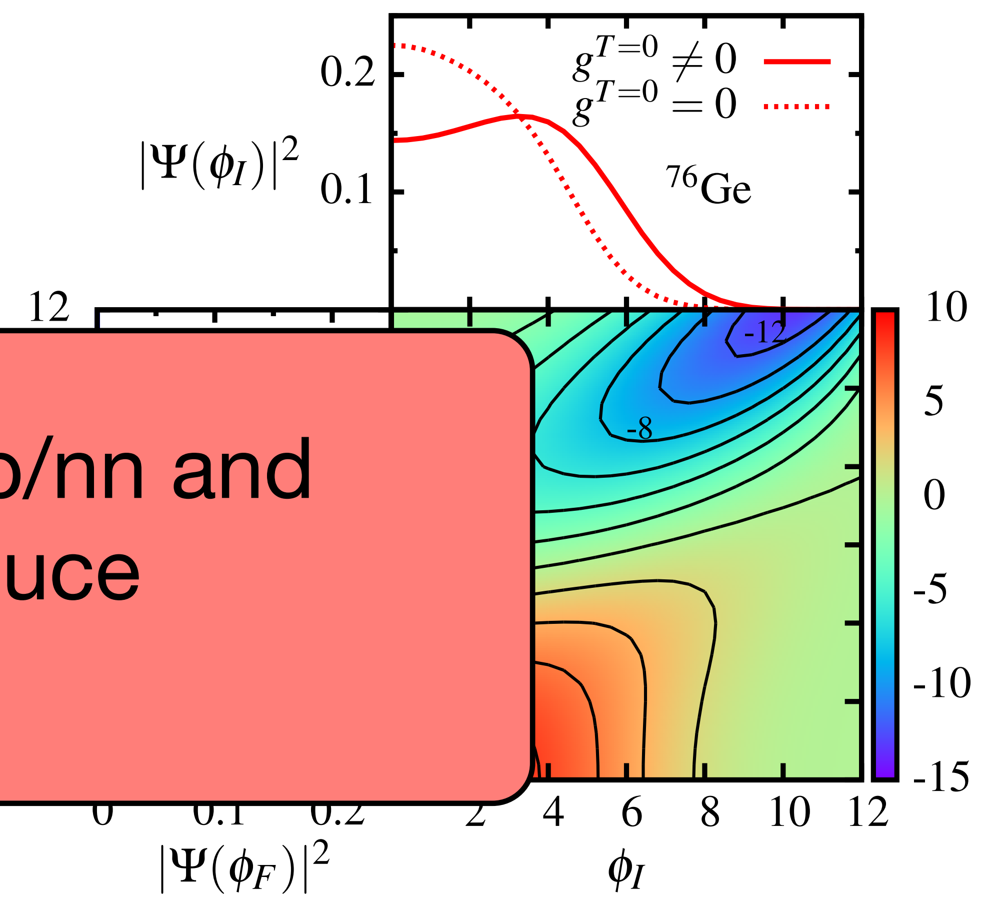

FIG. 3. (Color online.) **Bottom right:** $\mathcal{N}_{\phi_I}\mathcal{N}_{\phi_F}\langle\phi_F|\mathcal{P}_F\hat{M}_{0\nu}\mathcal{P}_I|\phi_I\rangle$ for projected quasiparticle vacua with different values of the initial and final isoscalar pairing amplitudes ϕ_I and ϕ_F, from the SkO′-based interaction (see text). **Top and bottom left:** Square of collective wave functions in ^{76}Ge and ^{76}Se.

N. Hinohara and J. Engel, PRC 031031(R) (2014)

NME: ^{116}Cd→^{116}Sn

A=116 (possible candidate for detection)

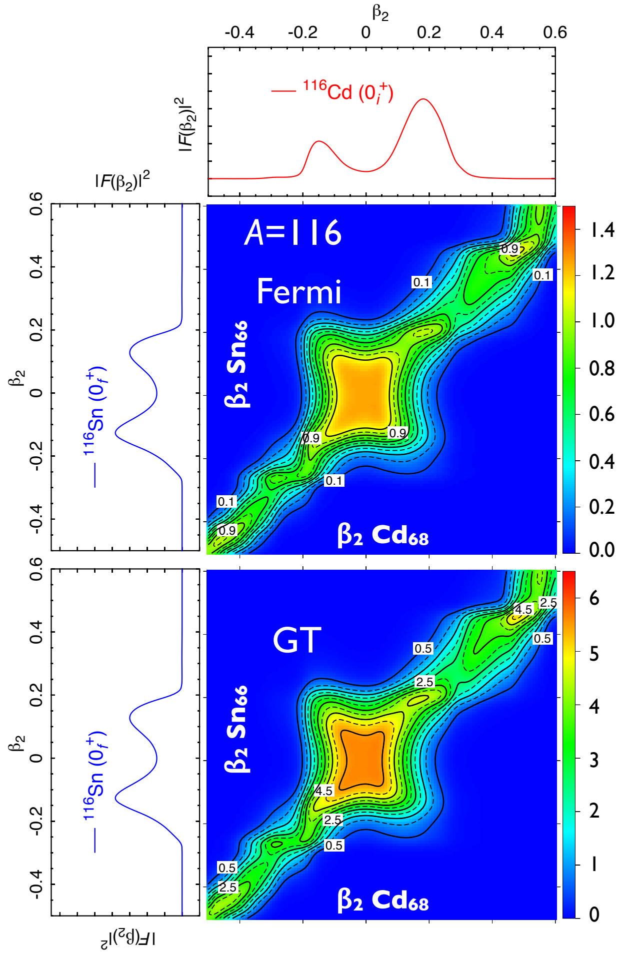

NME: $^{116}Cd \rightarrow ^{116}Sn$

A=116 (possible candidate for detection)

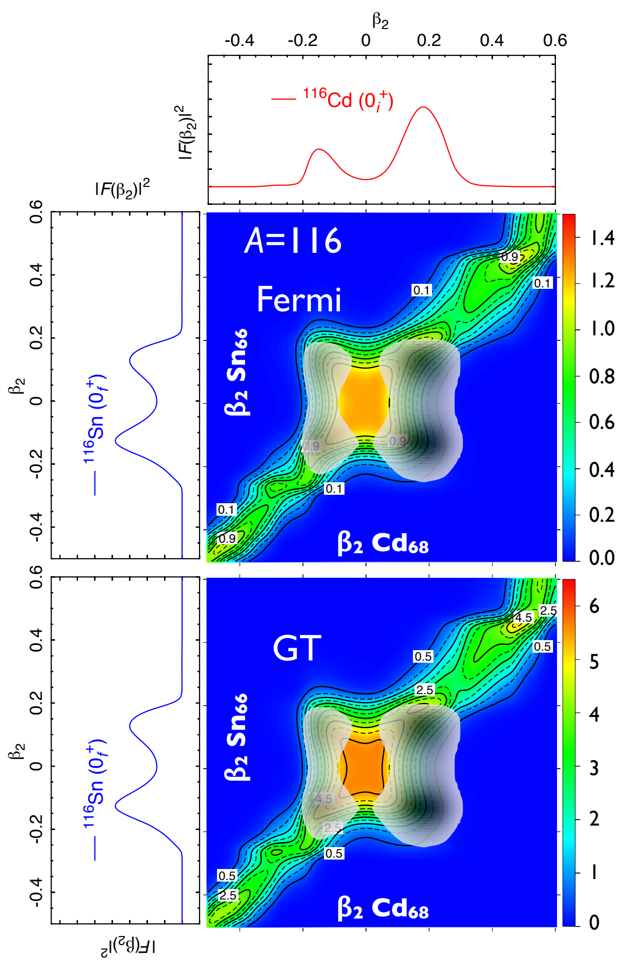

- Reduction of the NME with respect to the spherical value when shape mixing is included

NME: $^{116}Cd \rightarrow ^{116}Sn$

A=116 (possible candidate for detection)

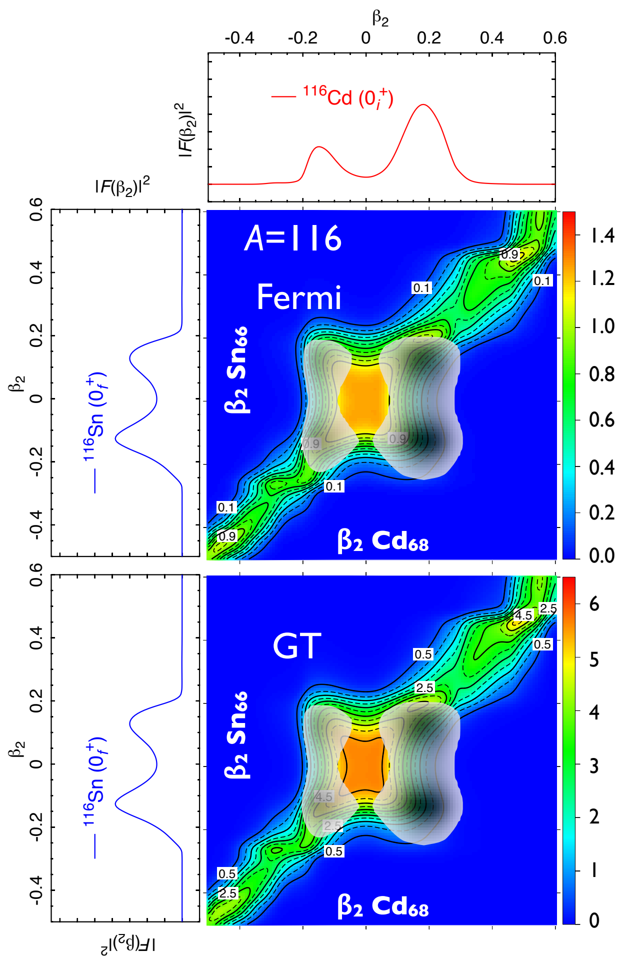

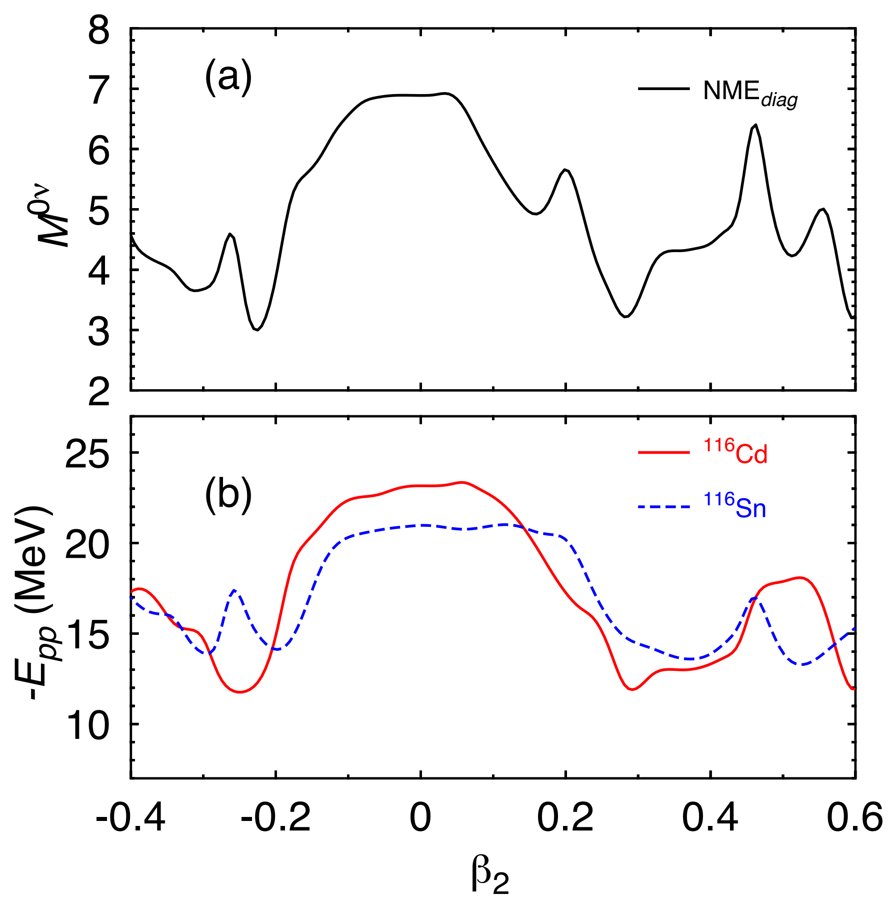

- Reduction of the NME with respect to the spherical value when shape mixing is included

- Larger pairing correlations in mother/ daughter nuclei produces larger NMEs.

NME: $^{116}Cd \rightarrow ^{116}Sn$

A=116 (possible candidate for detection)

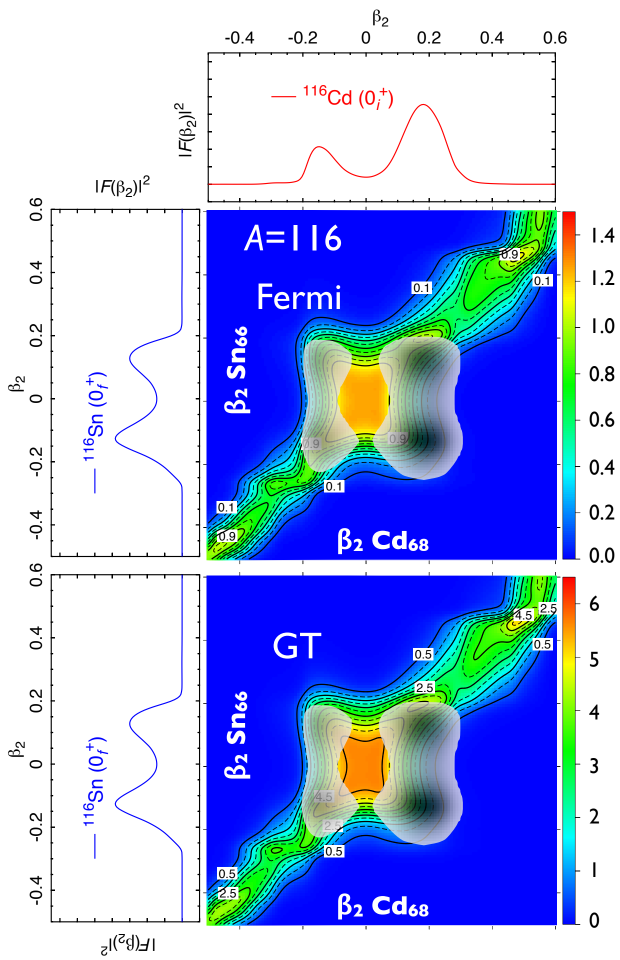

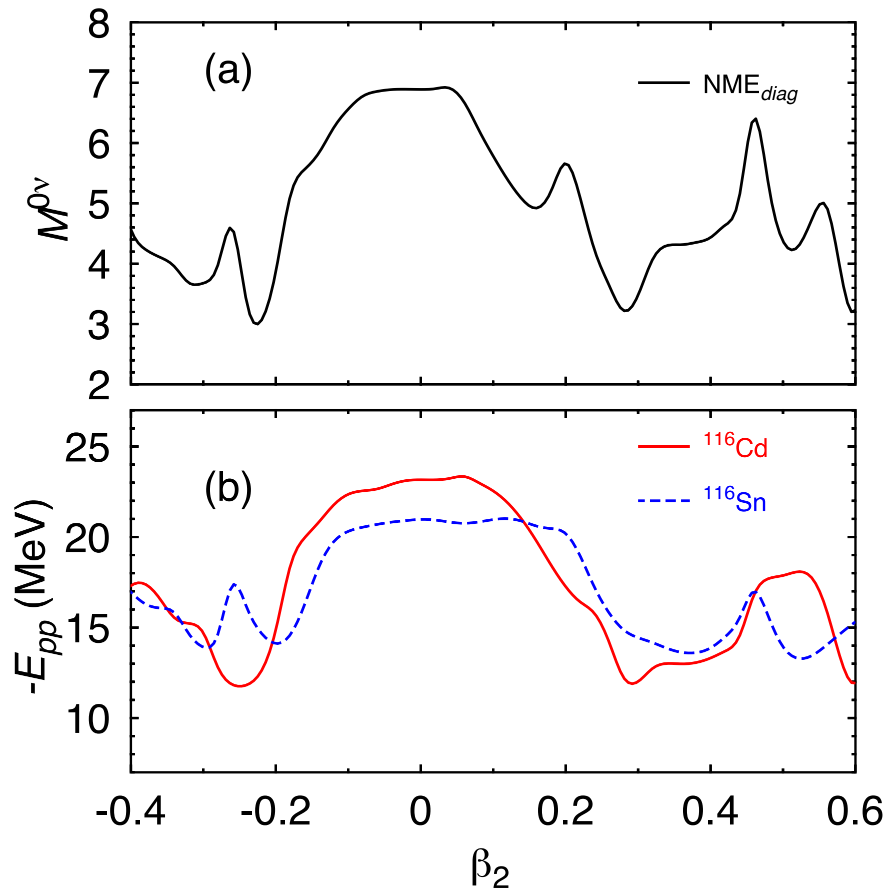

- Reduction of the NME with respect to the spherical value when shape mixing is included

- Larger pairing correlations in mother/daughter nuclei produces larger NMEs.

NME: ^{A}Cd→^{A}Sn Shell Effects

- GT component is always larger than Fermi.

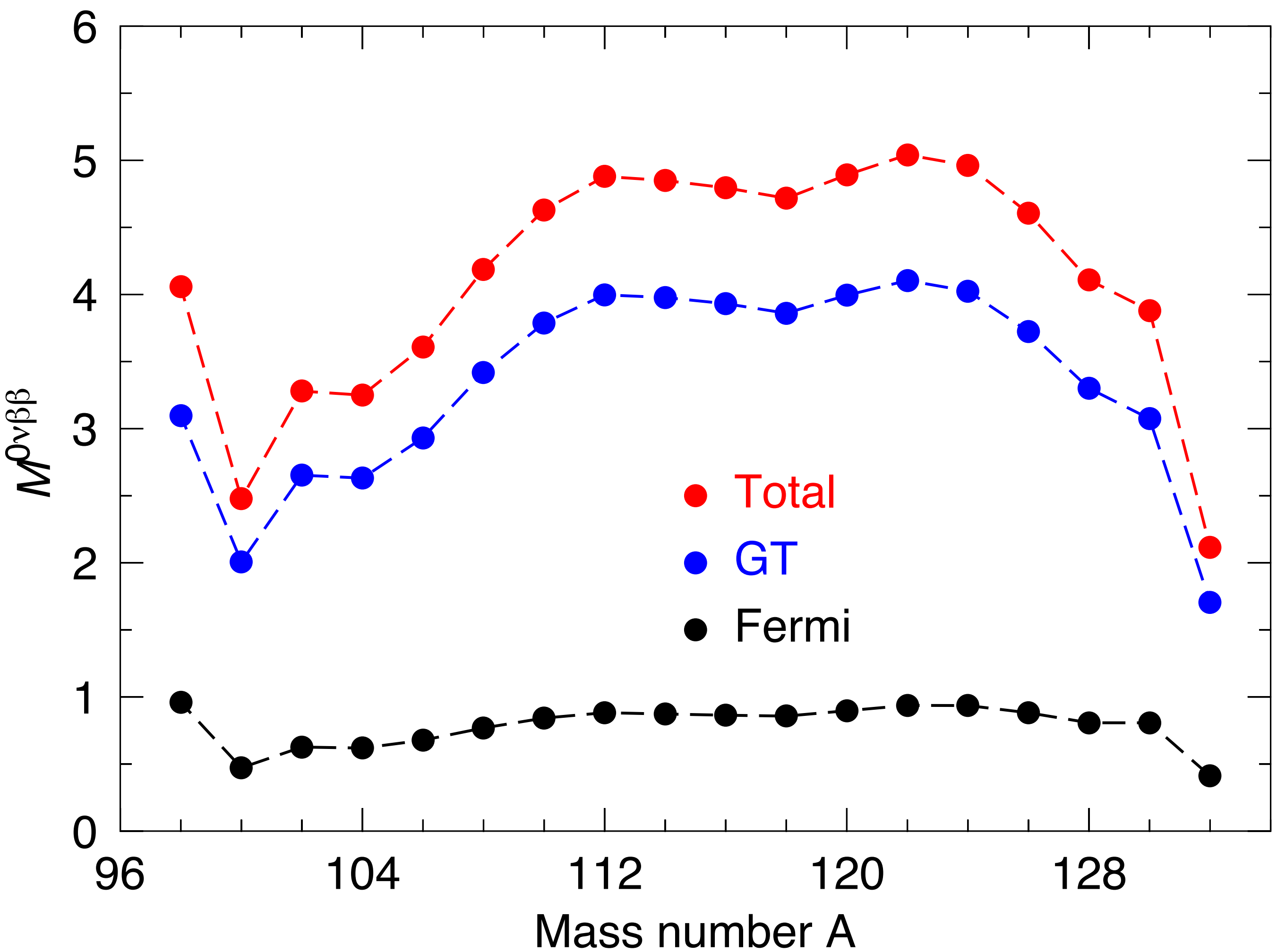

T.R.R., Martínez-Pinedo, PLB 719, 174 (2013)

NME: ^{A}Cd→^{A}Sn Shell Effects

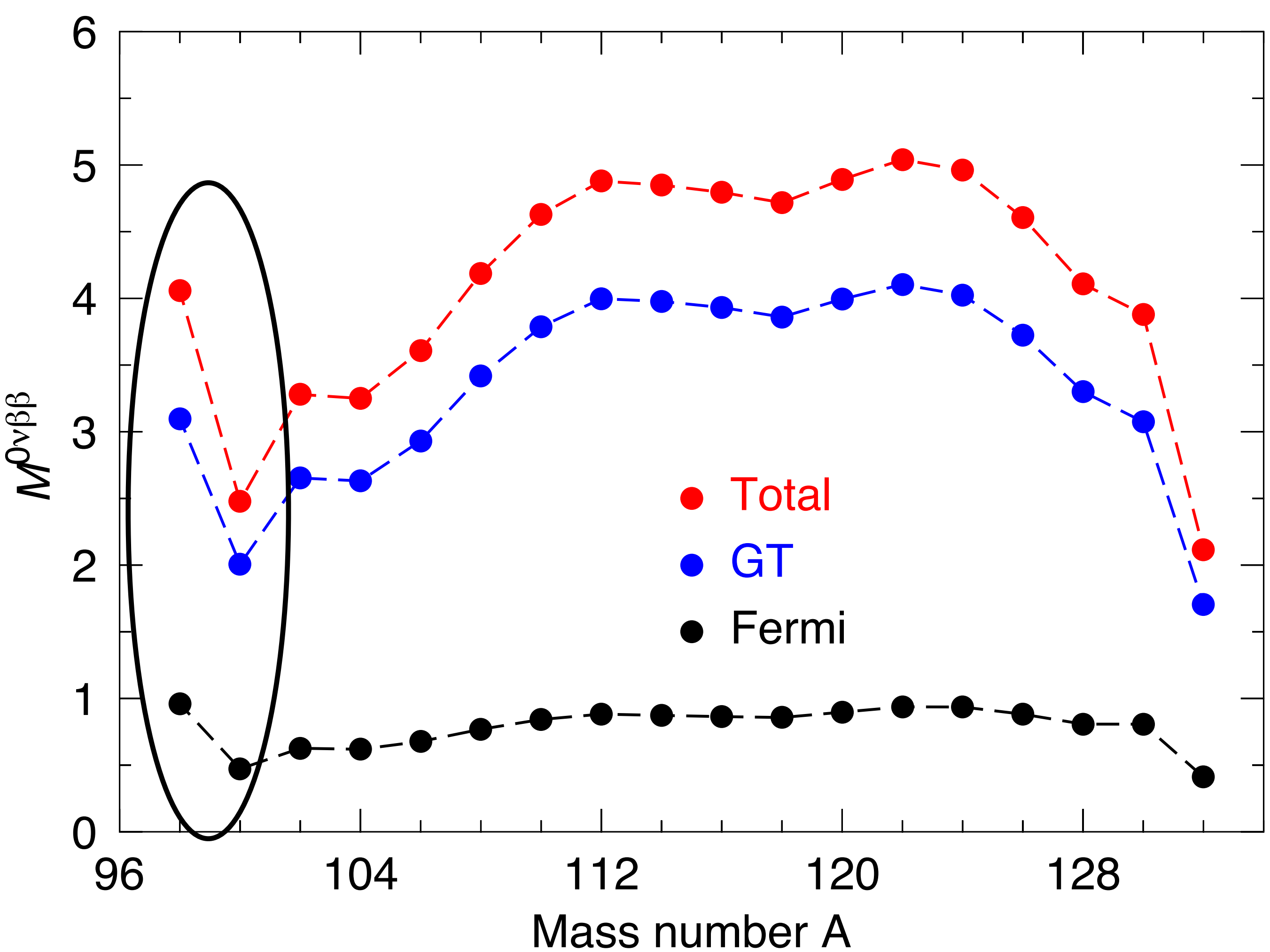

- GT component is always larger than Fermi.
- Large enhancement of the NME for the mirror decay *A*=98.

T.R.R., Martínez-Pinedo, PLB 719, 174 (2013)

NME: ^{A}Cd→^{A}Sn Shell Effects

UNIVERSIDAD AUTONOMA DE MADRID

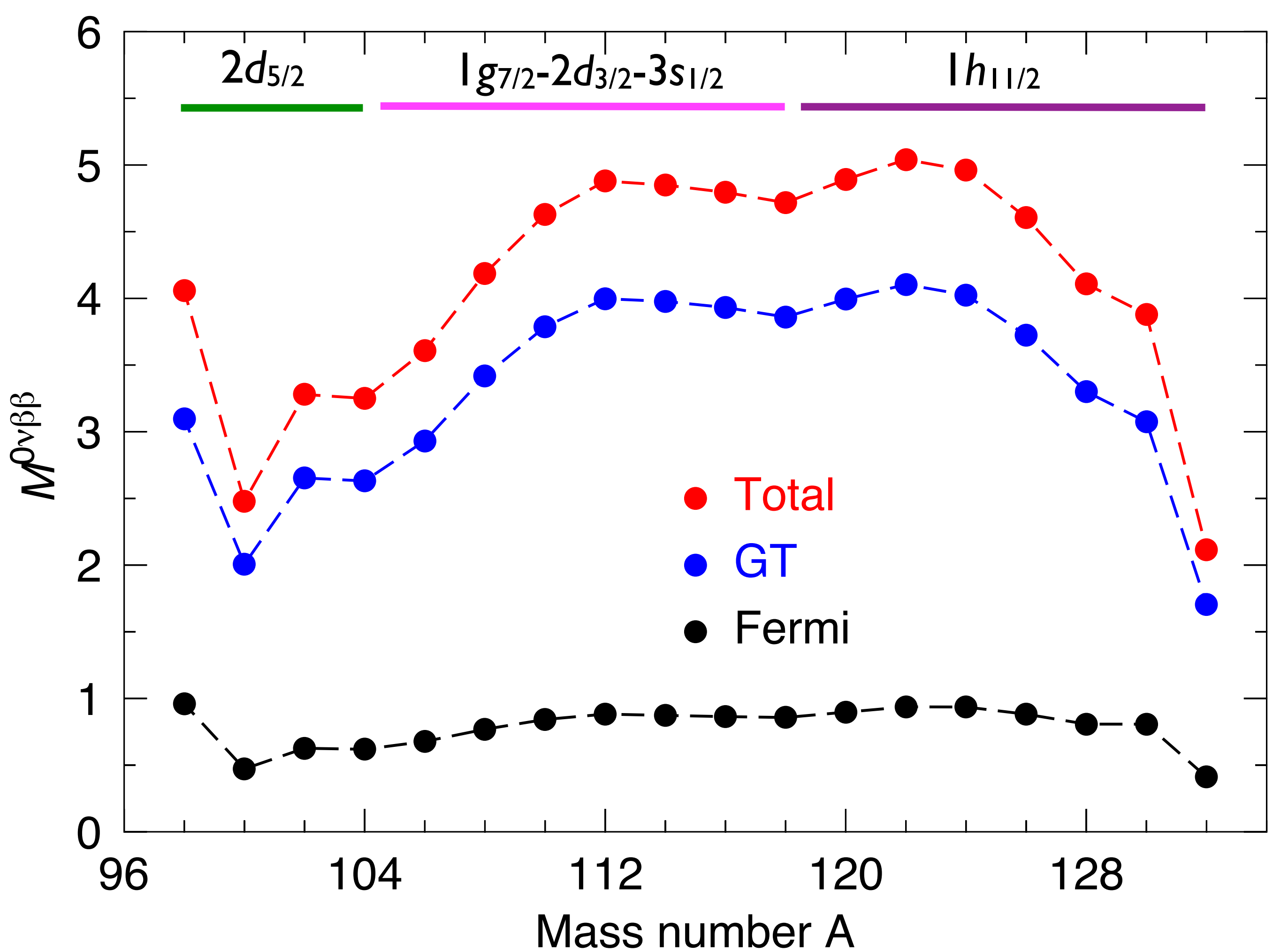

- GT component is always larger than Fermi.
- Large enhancement of the NME for the mirror decay A=98.
- Shell effects associated to the filling of neutrons in the corresponding sub-shells. Consistent with seniority model.

T.R.R., Martínez-Pinedo, PLB 719, 174 (2013)

NME: $^{A}Cd \rightarrow {}^{A}Sn$ Shell Effects

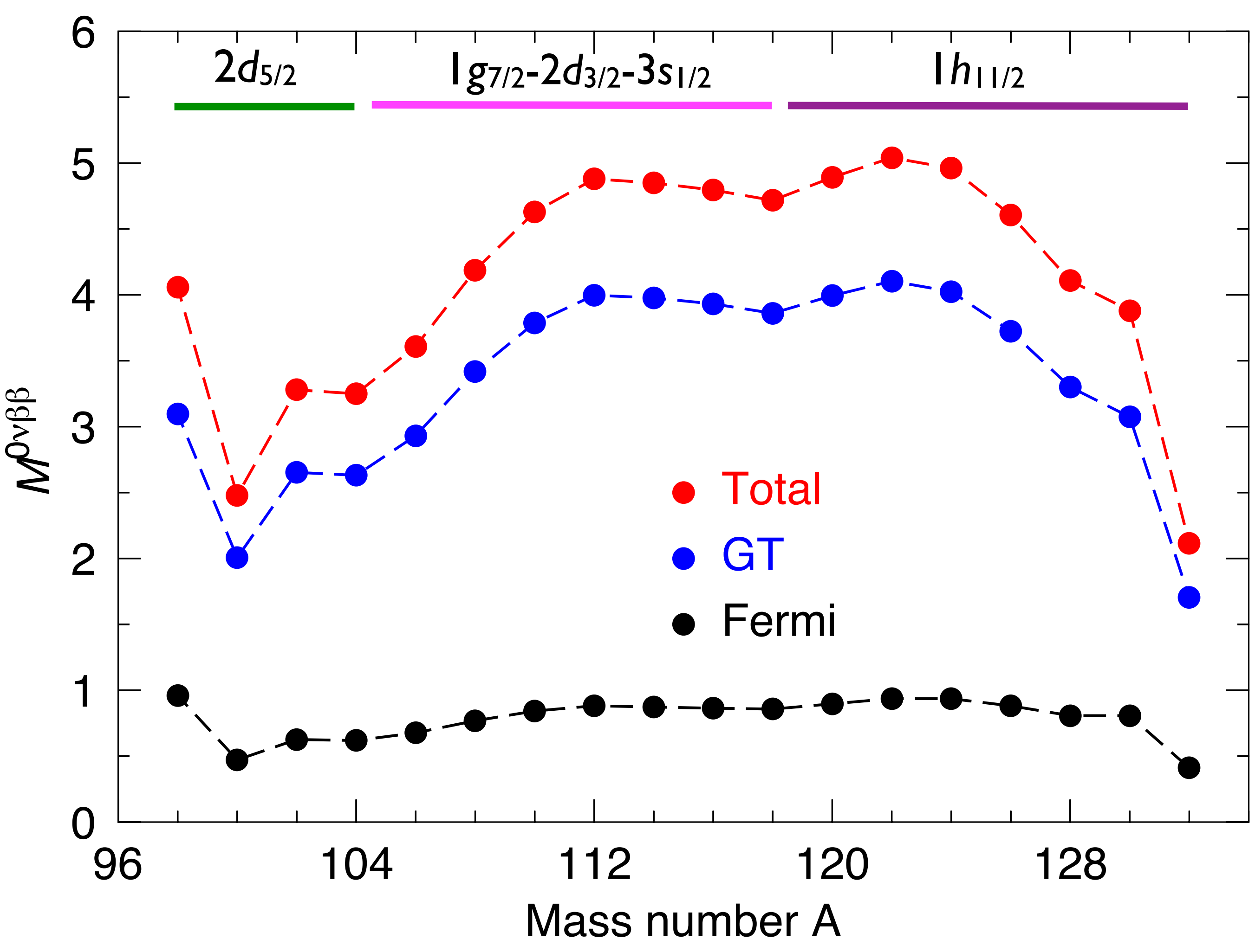

T.R.R., Martínez-Pinedo, PLB 719, 174 (2013)

- GT component is always larger than Fermi.
- Large enhancement of the NME for the mirror decay A=98.
- Shell effects associated to the filling of neutrons in the corresponding sub-shells. Consistent with seniority model.

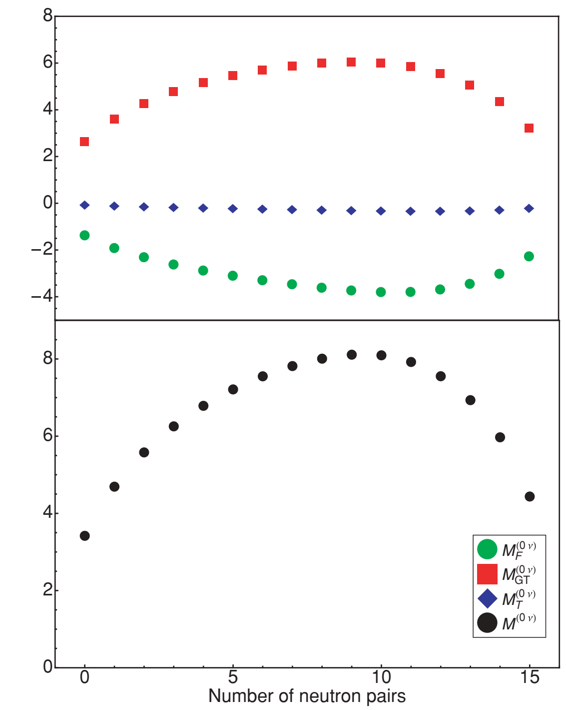

J. Barea and F. Iachello, Phys. Rev. C 79, 044301 (2009)

NME: $^{A}Cd \rightarrow {}^{A}Sn$

- Reduction of the NME with respect to the spherical value when shape mixing is included
- Larger reduction when the difference in deformation is larger

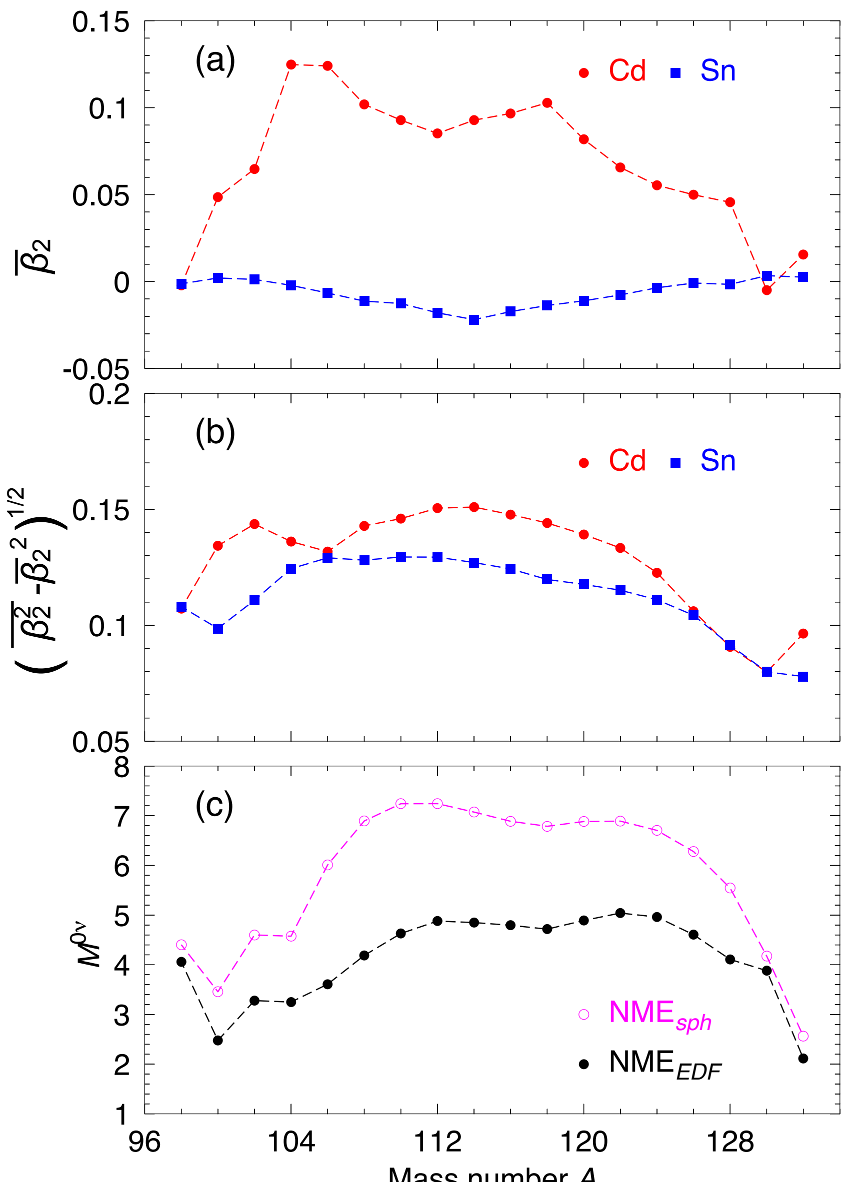

T.R.R., Martínez-Pinedo, PLB 719, 174 (2013)

NME: $^{A}Cd \rightarrow {}^{A}Sn$

- Reduction of the NME with respect to the spherical value when shape mixing is included
- Larger reduction when the difference in deformation is larger

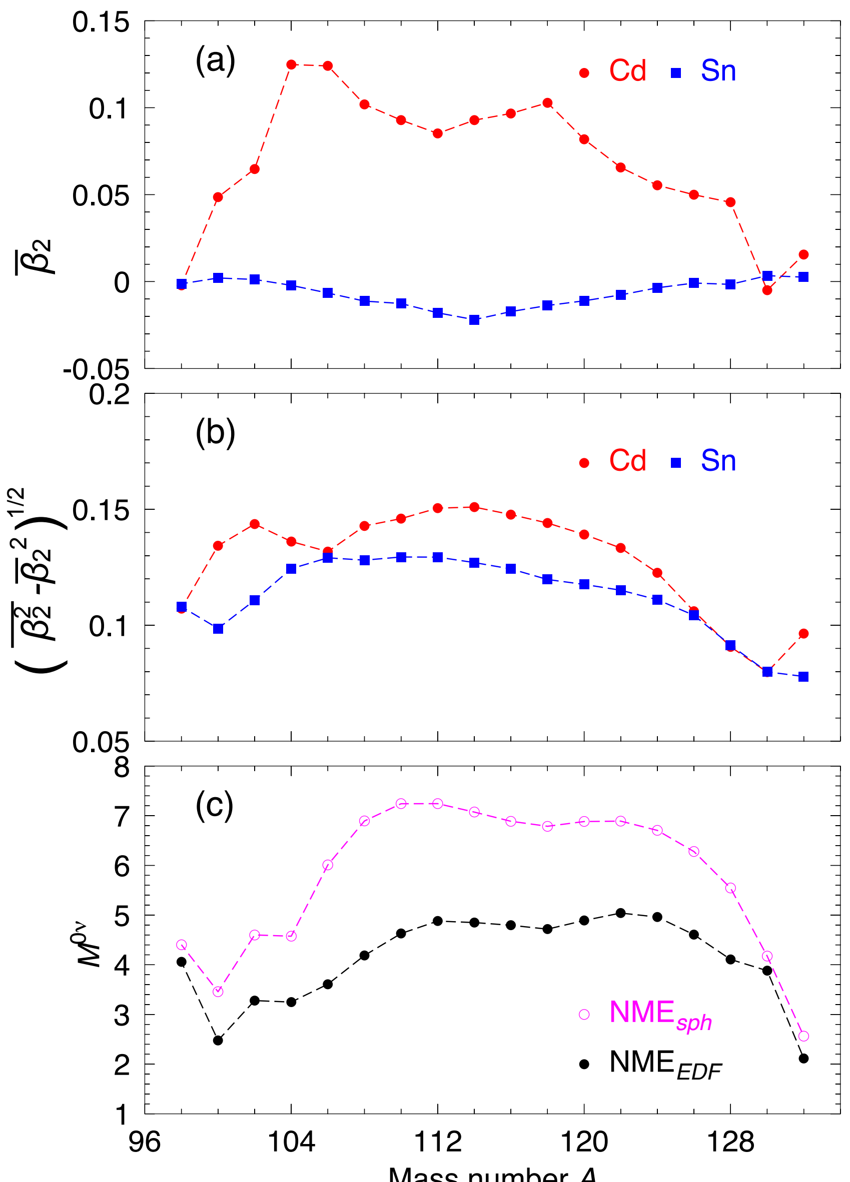

- Larger pairing correlations in mother/daughter nuclei produces larger NMEs.
- Closely related to shell effects

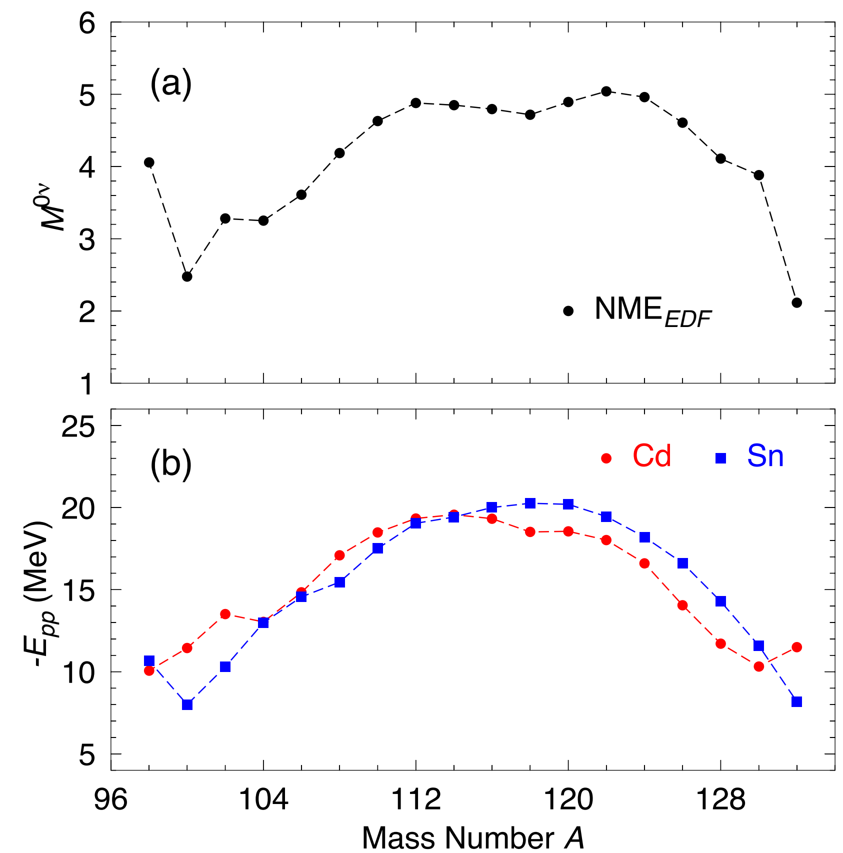

T.R.R., Martínez-Pinedo, PLB 719, 174 (2013)

NME: *pf*-shell

Where do the differences come from?

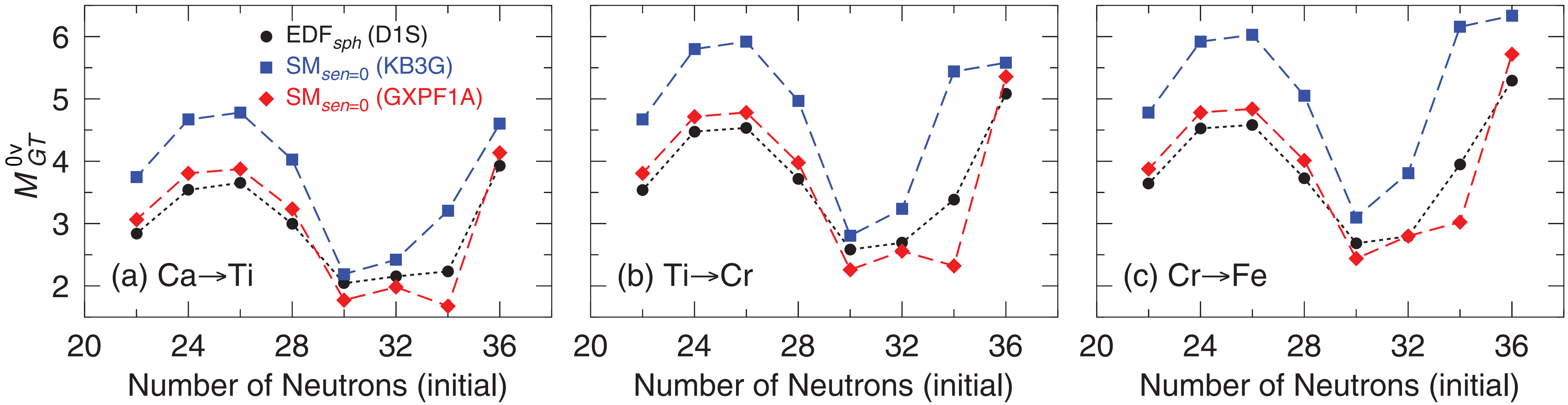

- Same pattern in spherical EDF, seniority 0 Shell Model, and Generalized Seniority model (overall scale?)

- What is the effect of including more **correlations**?

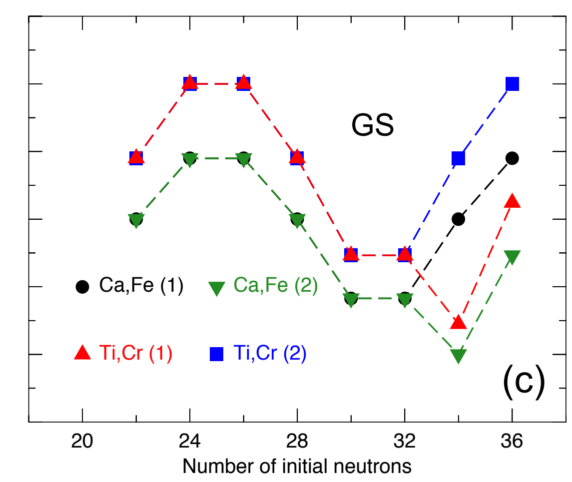

J. Menéndez, T. R. R., A. Poves, G. Martínez-Pinedo, PRC 90, 024311 (2014).

NME: *pf*-shell

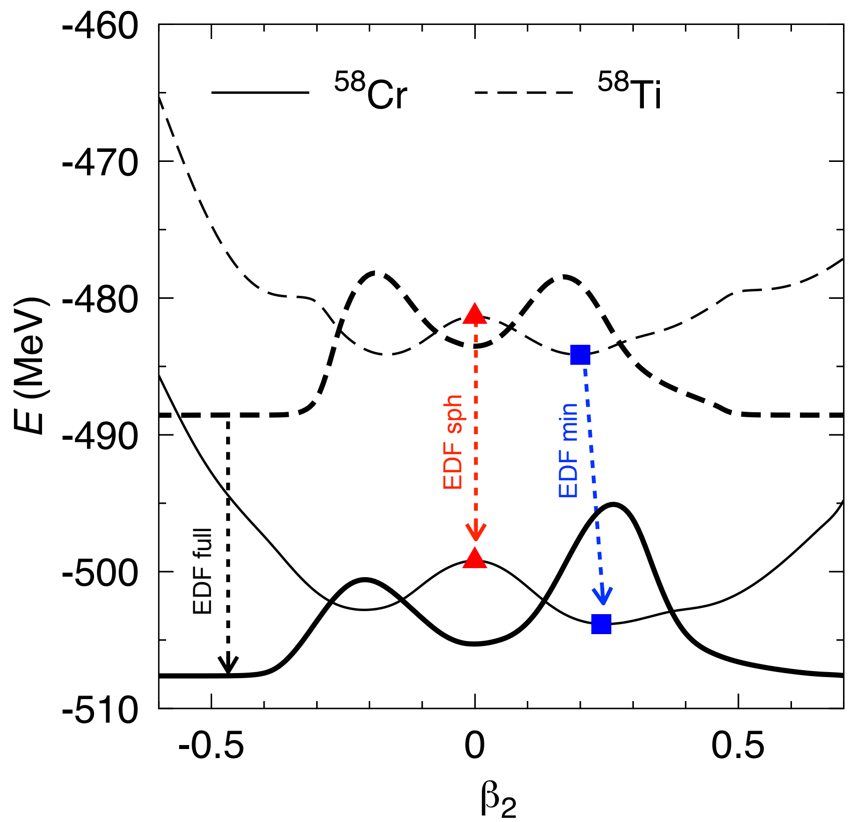

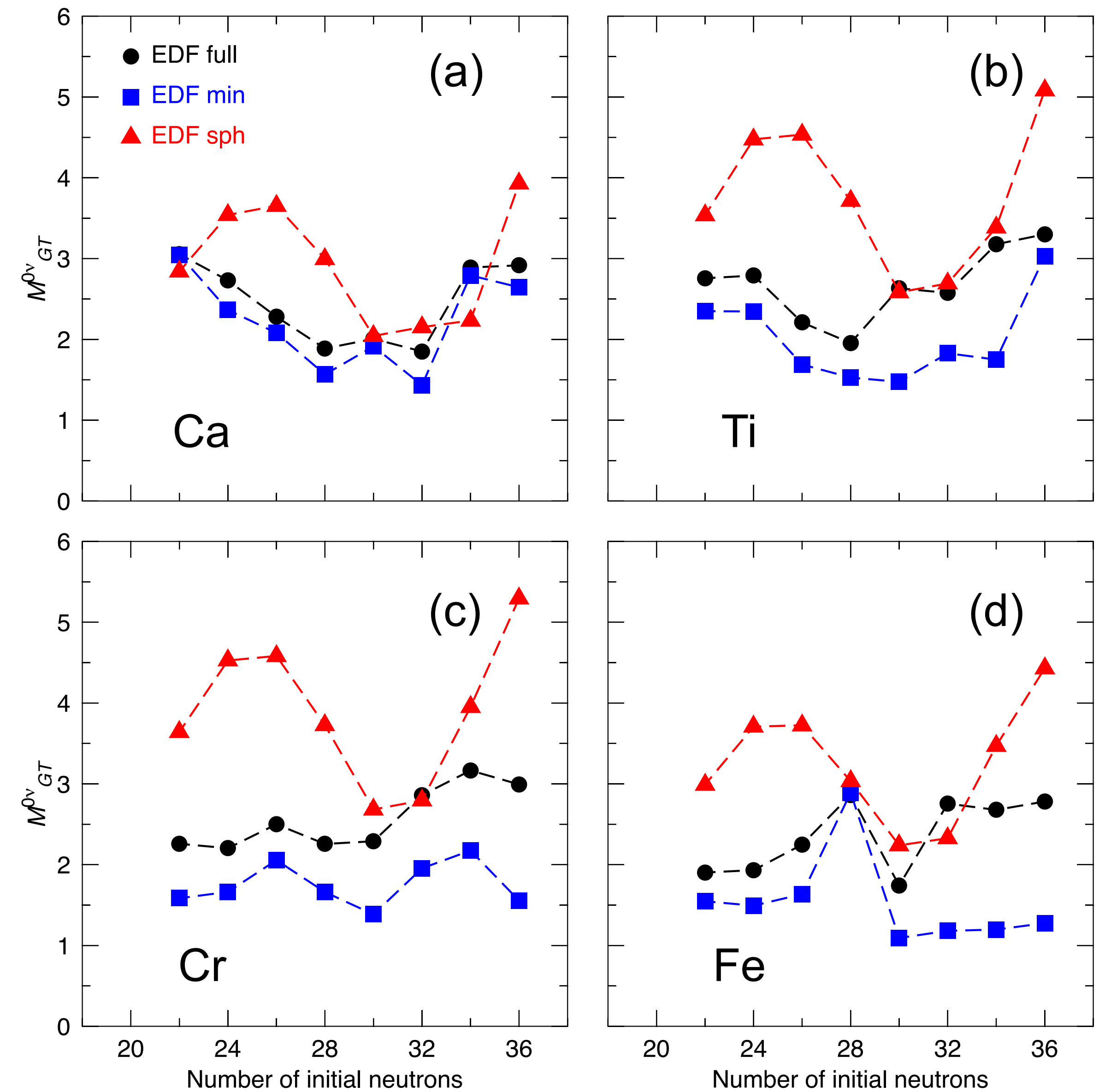

J. Menéndez, T. R. R., A. Poves, G. Martínez-Pinedo, PRC 90, 024311 (2014).

NME: *pf*-shell

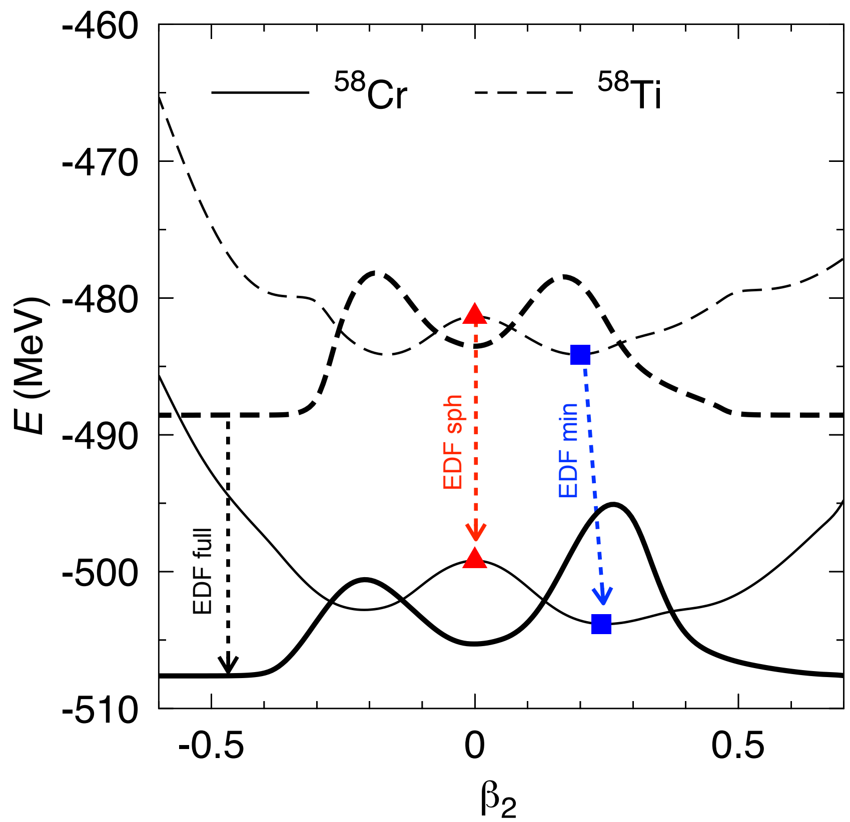

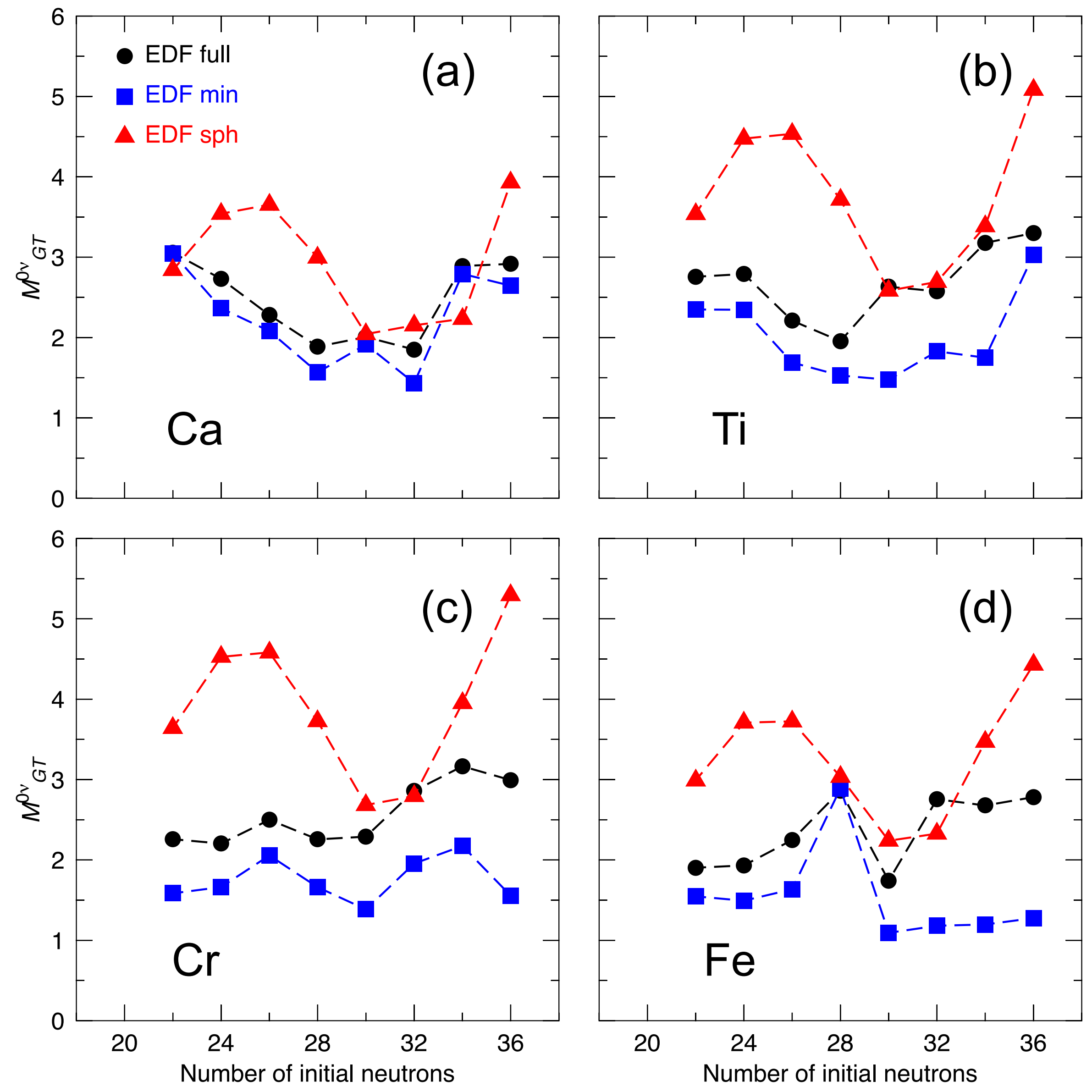

- NMEs are reduced with respect to the spherical value when correlations are included.

- The biggest reduction is produced by angular momentum restoration and configuration mixing produces an increase of the NME.

- Cross-check nuclei: ^{42}Ca, ^{50}Ca, ^{56}Fe

J. Menéndez, T. R. R., A. Poves, G. Martínez-Pinedo, PRC 90, 024311 (2014).

NME: *pf*-shell

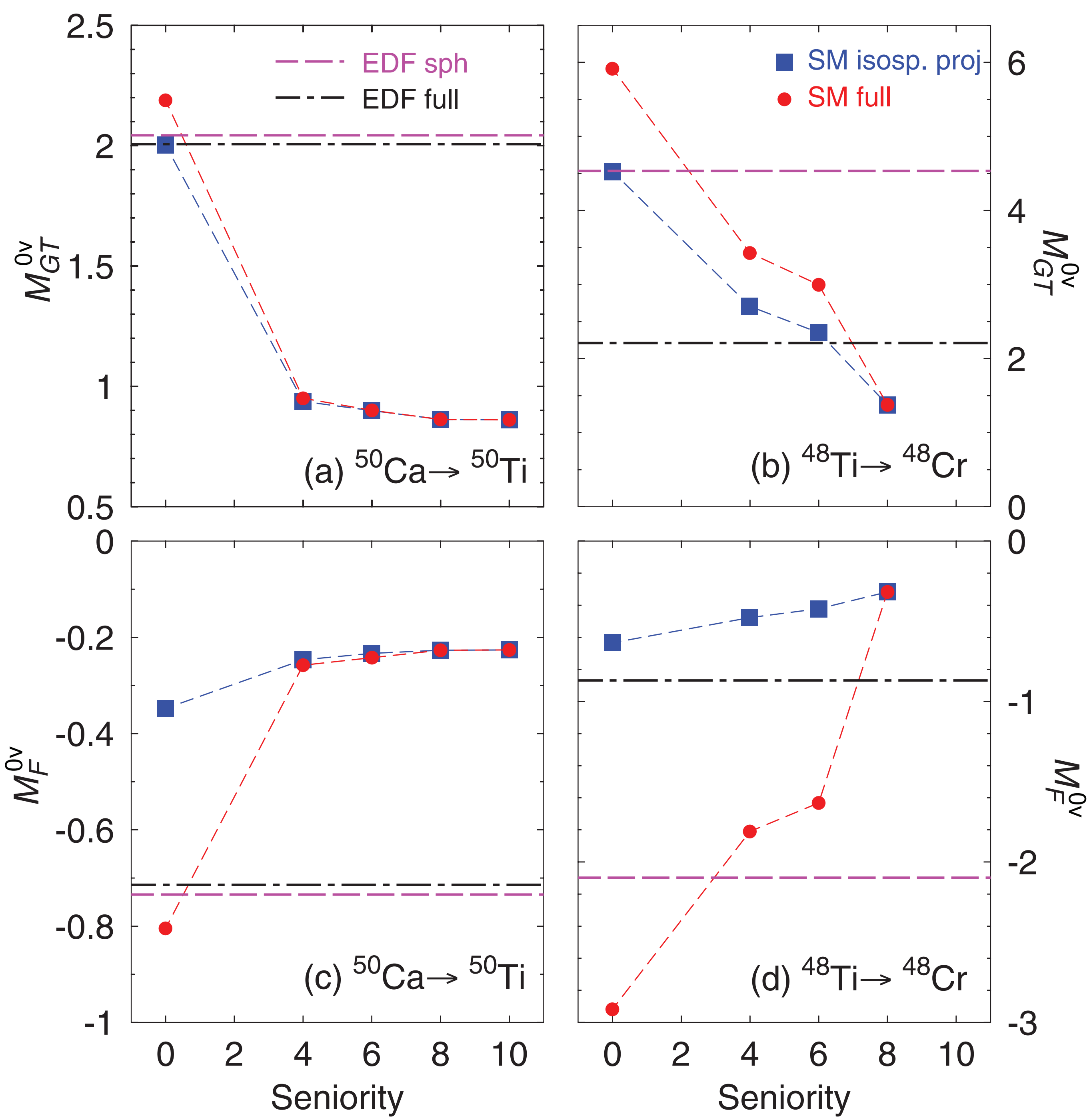

J. Menéndez, T. R. R., A. Poves, G. Martínez-Pinedo, PRC 90, 024311 (2014).

NME: *pf*-shell

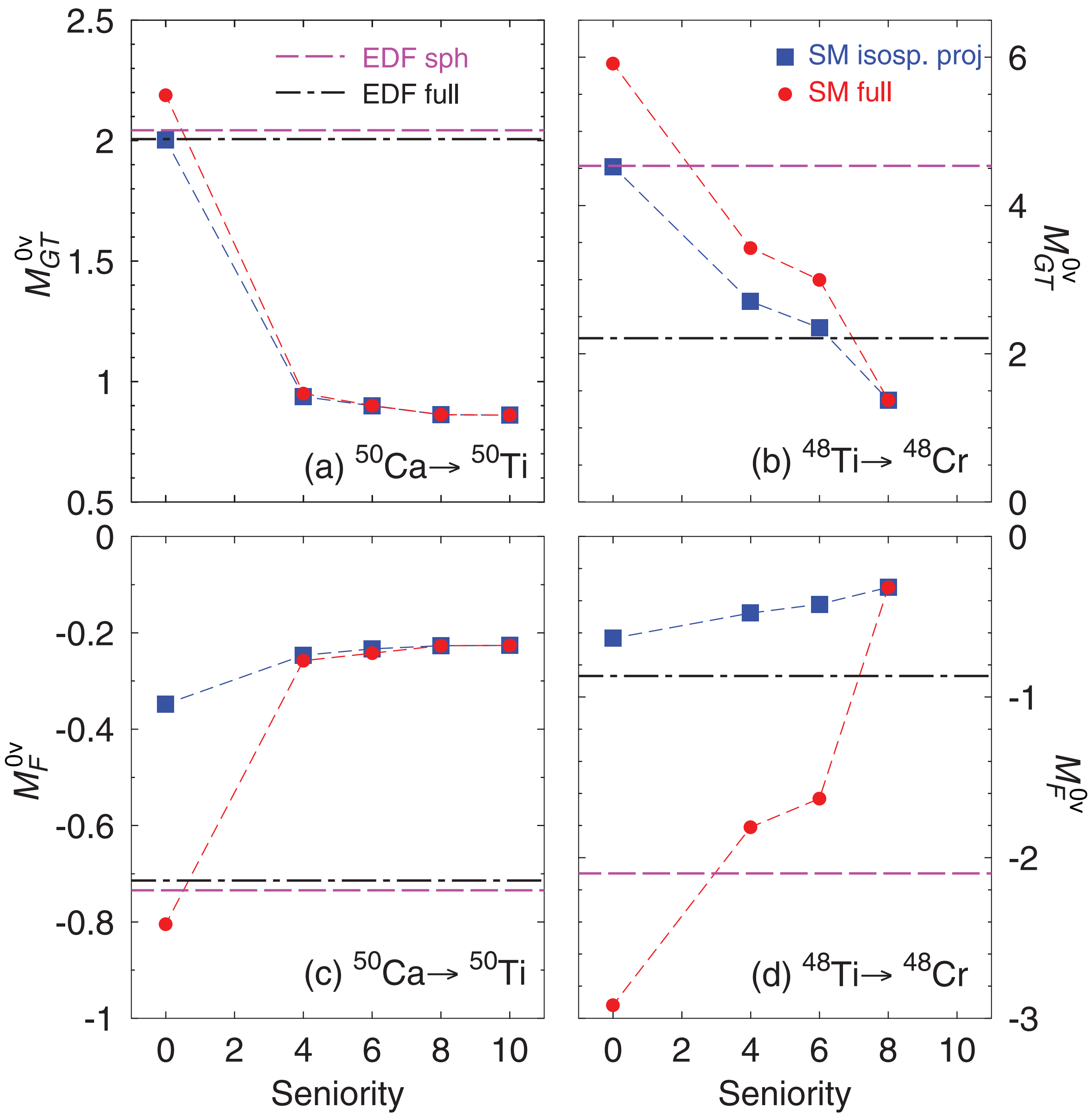

- The biggest reduction (in Shell model calculations) is produced by including higher seniority components in the nuclear wave functions.
- Isospin projection is relevant for the Fermi part of the NME and less important for the Gamow-Teller part.
- Isospin projection tends to reduce the NME.
- EDF does not include properly those higher seniority components, specially in spherical nuclei.
- p-n pairing effects could also be important in the reduction of the NME.

J. Menéndez, T. R. R., A. Poves, G. Martínez-Pinedo, PRC 90, 024311 (2014).

NME: *pf*-shell

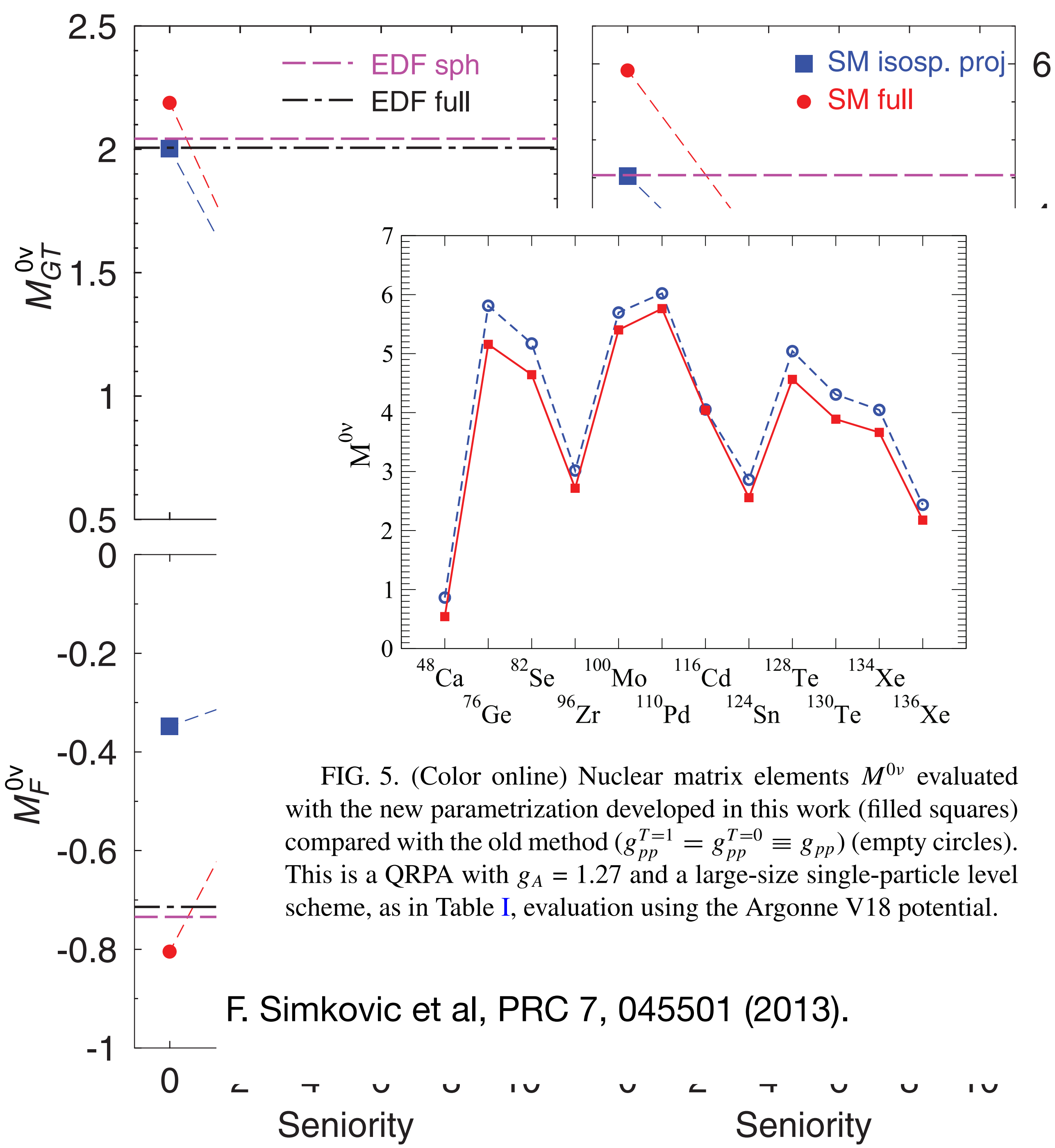

FIG. 5. (Color online) Nuclear matrix elements $M^{0\nu}$ evaluated with the new parametrization developed in this work (filled squares) compared with the old method ($g_{pp}^{T=1} = g_{pp}^{T=0} \equiv g_{pp}$) (empty circles). This is a QRPA with $g_A = 1.27$ and a large-size single-particle level scheme, as in Table I, evaluation using the Argonne V18 potential.

F. Simkovic et al, PRC 7, 045501 (2013).

- The biggest reduction (in Shell model calculations) is produced by including higher seniority components in the nuclear wave functions.
- Isospin projection is relevant for the Fermi part of the NME and less important for the Gamow-Teller part.
- Isospin projection tends to reduce the NME.
- EDF does not include properly those higher seniority components, specially in spherical nuclei.
- p-n pairing effects could also be important in the reduction of the NME.

J. Menéndez, T. R. R., A. Poves, G. Martínez-Pinedo, PRC 90, 024311 (2014).

NME: *pf*-shell

J. Menéndez, et al., PRC 93, 014305 (2016).

$$H_{\text{coll}} = H_M + g^{T=1} \sum_{n=-1}^{1} S_n^\dagger S_n + g^{T=0} \sum_{m=-1}^{1} P_m^\dagger P_m$$

$$+ g_{ph} \sum_{m,n=-1}^{1} : \mathcal{F}_{mn}^\dagger \mathcal{F}_{mn} : + \chi \sum_{\mu=-2}^{2} : Q_\mu^\dagger Q_\mu :$$

- Increase of the NME when isoscalar pairing is removed.
- Further increase when spin-isospin is also removed

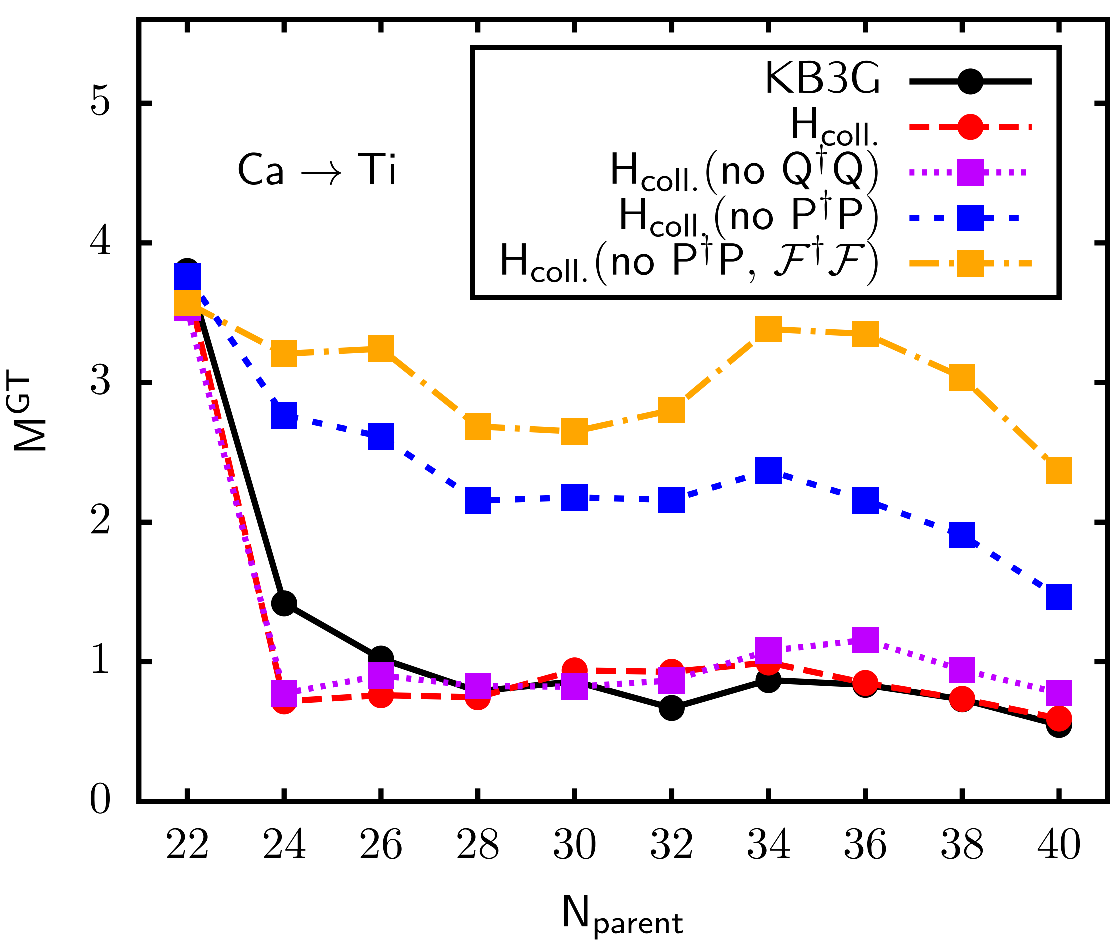

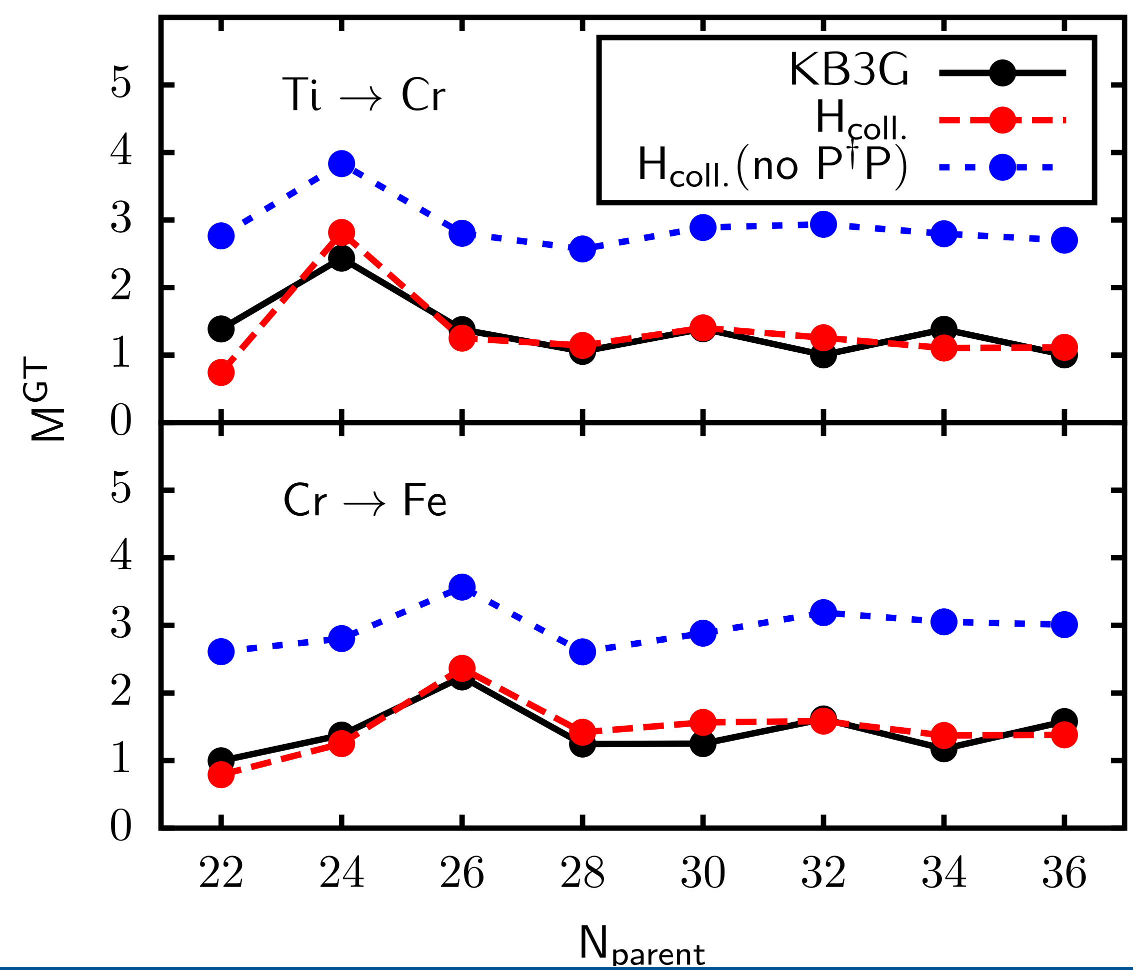

NME: *pf*-shell

$$H_{\rm coll} = H_M + g^{T=1}\sum_{n=-1}^{1} S_n^\dagger S_n + g^{T=0}\sum_{m=-1}^{1} P_m^\dagger P_m$$

$$+ g_{ph}\sum_{m,n=-1}^{1} :\mathcal{F}_{mn}^\dagger \mathcal{F}_{mn}: + \chi \sum_{\mu=-2}^{2} :Q_\mu^\dagger Q_\mu:$$

- GT operator is SU(4) invariant (neglecting the neutrino potential)
- GT operator can only connect states belonging to the same irreducible representation of SU(4)
- SU(4) is more broken when *T*=0 and spin-isospin terms are removed from the Hamiltonian⇒ the number of SU(4) irreps

  present both in the mother and daughter g.s. wave functions are larger⇒ larger NMEs

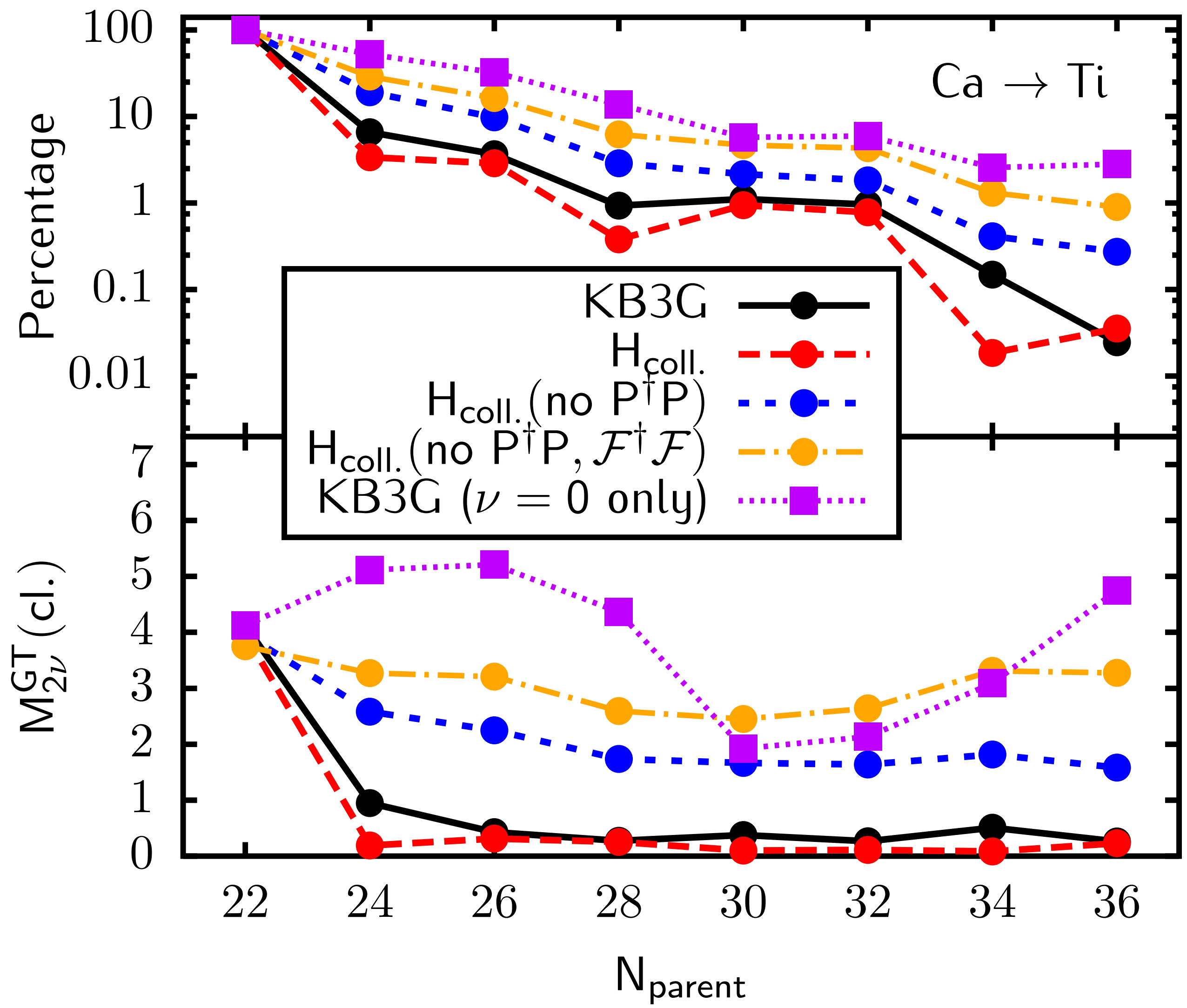

NME: *pf*-shell

$$H_{\rm coll} = H_M + g^{T=1} \sum_{n=-1}^{1} S_n^\dagger S_n + g^{T=0} \sum_{m=-1}^{1} P_m^\dagger P_m$$

$$+ g_{ph} \sum_{m,n=-1}^{1} : \mathcal{F}_{mn}^\dagger \mathcal{F}_{mn} : + \chi \sum_{\mu=-2}^{2} : Q_\mu^\dagger Q_\mu :$$

- SM/GCM comparison with **the same interaction.**

- 1D: only pn strength as a generator coordinate.
- 2D: pn strength and axial quadrupole deformation as generator coordinates.

EXACT vs. VARIATIONAL!!

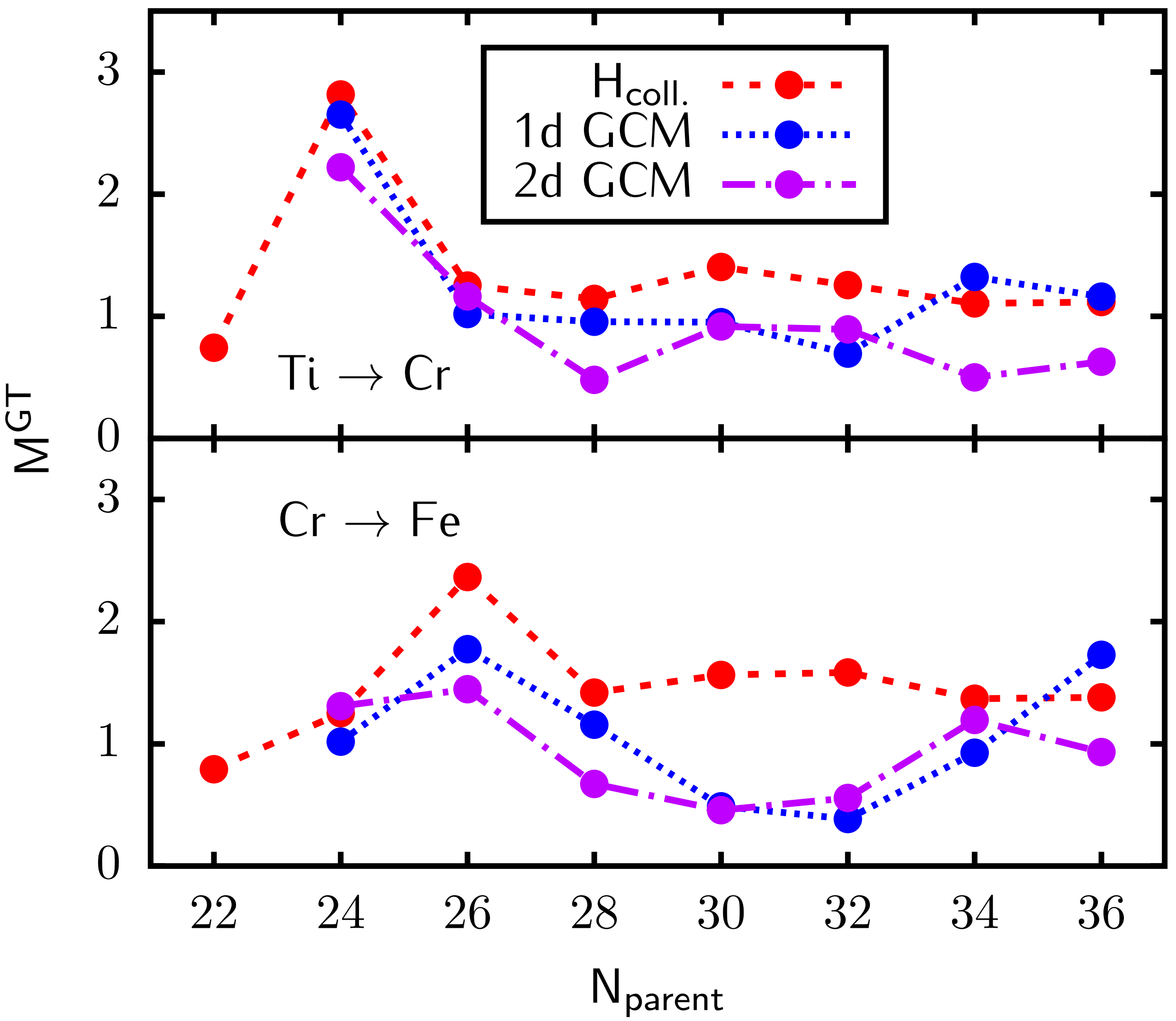

Occupation numbers

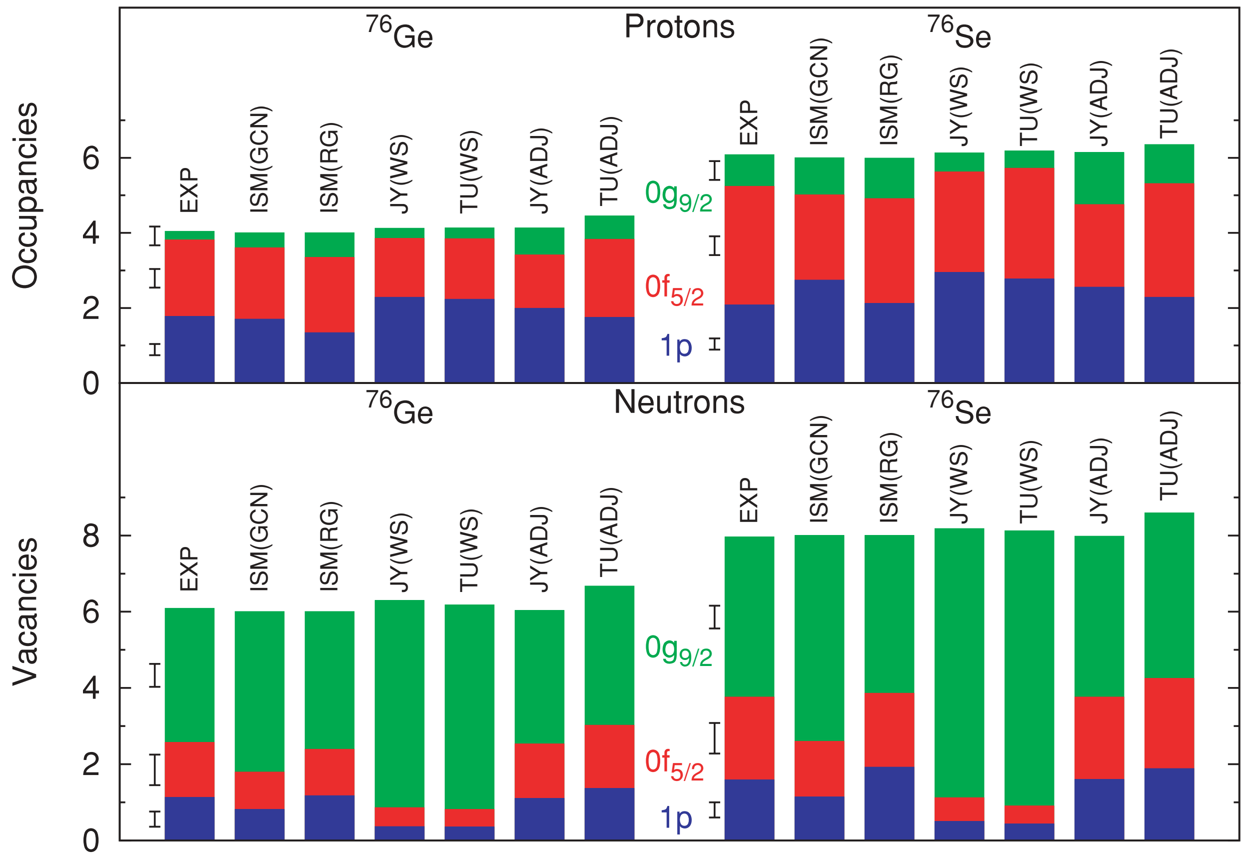

FIG. 1. (Color online) Comparison between experimental and theoretical occupation numbers for $A = 76$. Experimental values are from Refs. [1,2]. The ISM results correspond to the gcn28.50 (GCN) and rg (RG) interactions. The QRPA standard numbers, TU(WS) and JY(WS) give the occupancies at the BCS level. The QRPA occupancies with adjusted single particle energies are given at the BCS level in the case of JY(ADJ) and at QRPA level for TU(ADJ). JY and TU results from Refs. [5] and [6], respectively. The experimental error bars are also shown.

$M^{0\nu\beta\beta}$	GCN	WS	RG	ADJ-WS
ISM	2.81		3.26	
QRPA(JY)		5.36		4.11
QRPA(TU)		5.07–6.25		4.59–5.44

Fitting the underlying (WS) mean field to reproduce the “experimental” occupation numbers reduces the pnQRPA NMEs.

J. Menéndez et al., Phys. Rev. C 80, 048501 (2009)

Exp: J. Schiffer et al., Phys Rev. Lett. 100, 112501 (2008)

Occupation numbers

UNIVERSIDAD AUTONOMA DE MADRID

orbit	^{76}Ge ax	^{76}Ge triax	^{76}Ge exp	^{76}Se ax	^{76}Se triax	^{76}Se exp
$\nu 0f_{7/2}$	7.81	7.72	—	7.72	7.47	—
$\nu 1p$	5.38	4.88	4.87±0.20	4.74	4.30	4.41±0.20
$\nu 0f_{5/2}$	5.16	4.95	4.56±0.40	4.96	4.24	3.83±0.40
$\nu 0g_{9/2}$	4.65	4.84	6.48±0.30	3.92	4.10	5.80±0.30
$\nu 1d_{5/2}$	0.54	0.83	—	0.26	0.86	—
$\nu 0g_{7/2}$	0.16	0.24	—	0.19	0.31	—
$\nu 1d_{3/2}$	0.04	0.07	—	0.04	0.10	—
$\nu 2s_{1/2}$	0.03	0.09	—	0.02	0.12	—
$\pi 0f_{7/2}$	7.46	7.19	—	7.41	6.94	—
$\pi 1p$	2.11	2.17	1.77±0.15	3.29	2.69	2.08±0.15
$\pi 0f_{5/2}$	2.16	2.30	2.04±0.25	2.98	2.63	3.16±0.25
$\pi 0g_{9/2}$	0.17	0.19	0.23±0.25	0.21	1.16	0.84±0.25
$\pi 1d_{5/2}$	0.03	0.05	—	0.04	0.25	—
$\pi 0g_{7/2}$	0.06	0.09	—	0.08	0.15	—
$\pi 1d_{3/2}$	0.02	0.03	—	0.02	0.05	—
$\pi 2s_{1/2}$	0.01	0.01	—	0.01	0.03	—

T. R. R., J. Phys. G 44, 034002 (2017)

Summary

- Experimental data are already able to constrain very long lower limit half-lives (we cross fingers for a positive signal soon!).
- 0νββ preferred mechanism is the exchange of a light Majorana neutrino but some other mechanisms are being considered too.
- NMEs differ a factor of three between the different methods but we need to understand which are the pros/cons of each method to provide reliable numbers (precision vs. accuracy).
- Nuclear physics aspects like deformation, pairing, shell effects, etc., are understood similarly within different approaches.
- Systematic comparisons between ISM/EDF methods have been performed but… we need more!!

Open questions

- **Isospin mixing and restoration have to be done in the future. Why is it so difficult (perhaps impossible) with the current Gogny EDFs?**
- **Triaxiality has to be taken into account in *A*=76 and *A*=100 decays (at least).**
- **How relevant is the proper description of the spectra in $0\nu\beta\beta$ NMEs?**
- **Occupation numbers with EDF to define physically sound valence spaces.**
- **Odd-odd nuclei is still a major challenge for GCM calculations.**
- **Computational time?!?**

Proton-neutron pairing with Gogny EDF

In all of the Gogny codes, a factorization of the HFB-like wave function is assumed:

$$|\Phi\rangle = |\Phi\rangle_p \times |\Phi\rangle_n$$

Therefore, the HFB transformation is block-diagonal in isospin:

$$\beta_a^\dagger = \sum_b U_{ba} c_b^\dagger + V_{ba} c_b \rightarrow \quad U = \begin{pmatrix} U_{pp} & 0 \\ 0 & U_{nn} \end{pmatrix} \quad V = \begin{pmatrix} V_{pp} & 0 \\ 0 & V_{nn} \end{pmatrix}$$

and, consequently, the density matrix and pairing tensor are also block-diagonal in isospin:

$$\rho = \begin{pmatrix} \rho_{pp} & 0 \\ 0 & \rho_{nn} \end{pmatrix} \qquad \kappa = \begin{pmatrix} \kappa_{pp} & 0 \\ 0 & \kappa_{nn} \end{pmatrix}$$

Proton-neutron pairing with Gogny EDF

Given a two-body Hamiltonian: $\hat{H} = \sum_{ab} t_{ab} c_a^\dagger c_b + \frac{1}{4} \sum_{abcd} \bar{v}_{abcd} c_a^\dagger c_b^\dagger c_d c_c$

The HFB energy is given by: $E^{\mathrm{HFB}} = \mathrm{Tr}\left(t\rho\right) + \frac{1}{2}\mathrm{Tr}\left(\Gamma\rho\right) - \frac{1}{2}\mathrm{Tr}\left(\Delta\kappa^*\right)$

$$\Gamma_{ac} = \sum_{bd} \bar{v}_{abcd}\rho_{db} \rightarrow \text{HF field}$$

$$\Delta_{ab} = \frac{1}{2}\sum_{cd} \bar{v}_{abcd}\kappa_{cd} \rightarrow \text{Pairing field}$$

Which parts of the interaction are explored by these fields?

$$\bar{v}_{abcd} \rightarrow \left[\begin{array}{l} \bar{v}_{a_p b_p c_p d_p} \\ \bar{v}_{a_n b_n c_n d_n} \\ \bar{v}_{a_p b_n c_p d_n} \end{array}\right.$$

Proton-neutron pairing with Gogny EDF

Hartree-Fock field

$$\Gamma_{ac} \rightarrow \left[\begin{array}{l} \Gamma_{a_p c_p} = \sum_{bd} \bar{v}_{a_p b_p c_p d_p} \rho_{d_p b_p} + \bar{v}_{a_p b_n c_p d_n} \rho_{d_n b_n} \\ \Gamma_{a_n c_n} = \sum_{bd} \bar{v}_{a_n b_p c_n d_p} \rho_{d_p b_p} + \bar{v}_{a_n b_n c_n d_n} \rho_{d_n b_n} \\ \Gamma_{a_n c_p} = \sum_{bd} \bar{v}_{a_n b_p c_p d_n} \rho_{d_n b_p} \\ \Gamma_{a_p c_n} = \sum_{bd} \bar{v}_{a_p b_n c_n d_p} \rho_{d_p b_n} \end{array} \right.$$

Pairing field

$$\Delta_{ab} \rightarrow \left[\begin{array}{l} \Delta_{a_p b_p} = \frac{1}{2} \sum_{cd} \bar{v}_{a_p b_p c_p d_p} \kappa_{c_p d_p} \\ \Delta_{a_n b_n} = \frac{1}{2} \sum_{cd} \bar{v}_{a_n b_n c_n d_n} \kappa_{c_n d_n} \\ \Delta_{a_n b_p} = \frac{1}{2} \sum_{cd} \bar{v}_{a_n b_p c_n d_p} \kappa_{c_n d_p} + \bar{v}_{a_n b_p c_p d_n} \kappa_{c_p d_n} \\ \Delta_{a_p b_n} = \frac{1}{2} \sum_{cd} \bar{v}_{a_p b_n c_n d_p} \kappa_{c_n d_p} + \bar{v}_{a_p b_n c_p d_n} \kappa_{c_p d_n} \end{array} \right.$$

Proton-neutron pairing with Gogny EDF

Hartree-Fock field

$$\Gamma_{ac} \rightarrow \left[\begin{array}{l} \Gamma_{a_p c_p} = \sum_{bd} \bar{v}_{a_p b_p c_p d_p} \rho_{d_p b_p} + \bar{v}_{a_p b_n c_p d_n} \rho_{d_n b_n} \\ \Gamma_{a_n c_n} = \sum_{bd} \bar{v}_{a_n b_p c_n d_p} \rho_{d_p b_p} + \bar{v}_{a_n b_n c_n d_n} \rho_{d_n b_n} \\ \Gamma_{a_n c_p} = \sum_{bd} \bar{v}_{a_n b_p c_p d_n} \rho_{d_n b_p} \\ \Gamma_{a_p c_n} = \sum_{bd} \bar{v}_{a_p b_n c_n d_p} \rho_{d_p b_n} \end{array} \right.$$

Pairing field

$$\Delta_{ab} \rightarrow \left[\begin{array}{l} \Delta_{a_p b_p} = \frac{1}{2} \sum_{cd} \bar{v}_{a_p b_p c_p d_p} \kappa_{c_p d_p} \\ \Delta_{a_n b_n} = \frac{1}{2} \sum_{cd} \bar{v}_{a_n b_n c_n d_n} \kappa_{c_n d_n} \\ \Delta_{a_n b_p} = \frac{1}{2} \sum_{cd} \bar{v}_{a_n b_p c_n d_p} \kappa_{c_n d_p} + \bar{v}_{a_n b_p c_p d_n} \kappa_{c_p d_n} \\ \Delta_{a_p b_n} = \frac{1}{2} \sum_{cd} \bar{v}_{a_p b_n c_n d_p} \kappa_{c_n d_p} + \bar{v}_{a_p b_n c_p d_n} \kappa_{c_p d_n} \end{array} \right.$$

Proton-neutron pairing with Gogny EDF

Hartree-Fock field

$$\Gamma_{ac} \rightarrow \left[\begin{array}{l} \Gamma_{a_pc_p} = \sum_{bd} \boxed{\bar{v}_{a_pb_pc_pd_p}} \rho_{d_pb_p} + \boxed{\bar{v}_{a_pb_nc_pd_n}} \rho_{d_nb_n} \\ \Gamma_{a_nc_n} = \sum_{bd} \boxed{\bar{v}_{a_nb_pc_nd_p}} \rho_{d_pb_p} + \boxed{\bar{v}_{a_nb_nc_nd_n}} \rho_{d_nb_n} \\ \Gamma_{a_nc_p} = \sum_{bd} \bar{v}_{a_nb_pc_pd_n} \cancel{\rho_{d_nb_p}} \\ \Gamma_{a_pc_n} = \sum_{bd} \bar{v}_{a_pb_nc_nd_p} \cancel{\rho_{d_pb_n}} \end{array} \right.$$

pp/nn/pn are taken into account

Pairing field

$$\Delta_{ab} \rightarrow \left[\begin{array}{l} \Delta_{a_pb_p} = \frac{1}{2} \sum_{cd} \bar{v}_{a_pb_pc_pd_p} \kappa_{c_pd_p} \\ \Delta_{a_nb_n} = \frac{1}{2} \sum_{cd} \bar{v}_{a_nb_nc_nd_n} \kappa_{c_nd_n} \\ \Delta_{a_nb_p} = \frac{1}{2} \sum_{cd} \bar{v}_{a_nb_pc_nd_p} \kappa_{c_nd_p} + \bar{v}_{a_nb_pc_pd_n} \kappa_{c_pd_n} \\ \Delta_{a_pb_n} = \frac{1}{2} \sum_{cd} \bar{v}_{a_pb_nc_nd_p} \kappa_{c_nd_p} + \bar{v}_{a_pb_nc_pd_n} \kappa_{c_pd_n} \end{array} \right.$$

Proton-neutron pairing with Gogny EDF

Hartree-Fock field

$$\Gamma_{ac} \rightarrow \begin{cases} \Gamma_{a_p c_p} = \sum_{bd} \bar{v}_{a_p b_p c_p d_p} \rho_{d_p b_p} + \bar{v}_{a_p b_n c_p d_n} \rho_{d_n b_n} \\ \Gamma_{a_n c_n} = \sum_{bd} \bar{v}_{a_n b_p c_n d_p} \rho_{d_p b_p} + \bar{v}_{a_n b_n c_n d_n} \rho_{d_n b_n} \\ \Gamma_{a_n c_p} = \sum_{bd} \bar{v}_{a_n b_p c_p d_n} \cancel{\rho_{d_n b_p}} \\ \Gamma_{a_p c_n} = \sum_{bd} \bar{v}_{a_p b_n c_n d_p} \cancel{\rho_{d_p b_n}} \end{cases}$$

pp/nn/pn are taken into account

Pairing field

$$\Delta_{ab} \rightarrow \begin{cases} \Delta_{a_p b_p} = \frac{1}{2} \sum_{cd} \bar{v}_{a_p b_p c_p d_p} \kappa_{c_p d_p} \\ \Delta_{a_n b_n} = \frac{1}{2} \sum_{cd} \bar{v}_{a_n b_n c_n d_n} \kappa_{c_n d_n} \\ \Delta_{a_n b_p} = \frac{1}{2} \sum_{cd} \bar{v}_{a_n b_p c_n d_p} \cancel{\kappa_{c_n d_p}} + \bar{v}_{a_n b_p c_p d_n} \cancel{\kappa_{c_p d_n}} \\ \Delta_{a_p b_n} = \frac{1}{2} \sum_{cd} \bar{v}_{a_p b_n c_n d_p} \cancel{\kappa_{c_n d_p}} + \bar{v}_{a_p b_n c_p d_n} \cancel{\kappa_{c_p d_n}} \end{cases}$$

Proton-neutron pairing with Gogny EDF

Hartree-Fock field

$$\Gamma_{ac} \rightarrow \left[\begin{array}{l} \Gamma_{a_p c_p} = \sum_{bd} \bar{v}_{a_p b_p c_p d_p} \rho_{d_p b_p} + \bar{v}_{a_p b_n c_p d_n} \rho_{d_n b_n} \\ \Gamma_{a_n c_n} = \sum_{bd} \bar{v}_{a_n b_p c_n d_p} \rho_{d_p b_p} + \bar{v}_{a_n b_n c_n d_n} \rho_{d_n b_n} \\ \Gamma_{a_n c_p} = \sum_{bd} \bar{v}_{a_n b_p c_p d_n} \cancel{\rho_{d_n b_p}} \\ \Gamma_{a_p c_n} = \sum_{bd} \bar{v}_{a_p b_n c_n d_p} \cancel{\rho_{d_p b_n}} \end{array} \right.$$

pp/nn/pn are taken into account

Pairing field

$$\Delta_{ab} \rightarrow \left[\begin{array}{l} \Delta_{a_p b_p} = \frac{1}{2} \sum_{cd} \bar{v}_{a_p b_p c_p d_p} \kappa_{c_p d_p} \\ \Delta_{a_n b_n} = \frac{1}{2} \sum_{cd} \bar{v}_{a_n b_n c_n d_n} \kappa_{c_n d_n} \\ \Delta_{a_n b_p} = \frac{1}{2} \sum_{cd} \bar{v}_{a_n b_p c_n d_p} \cancel{\kappa_{c_n d_p}} + \bar{v}_{a_n b_p c_p d_n} \cancel{\kappa_{c_p d_n}} \\ \Delta_{a_p b_n} = \frac{1}{2} \sum_{cd} \bar{v}_{a_p b_n c_n d_p} \cancel{\kappa_{c_n d_p}} + \bar{v}_{a_p b_n c_p d_n} \cancel{\kappa_{c_p d_n}} \end{array} \right.$$

pp/nn only are taken into account

no pn pairing!!!

Proton-neutron pairing with Gogny EDF

Hartree-Fock field

$$\Gamma_{ac} \rightarrow \left[\begin{array}{l} \Gamma_{a_p c_p} = \sum_{bd} \boxed{\bar{v}_{a_p b_p c_p d_p}} \rho_{d_p b_p} + \boxed{\bar{v}_{a_p b_n c_p d_n}} \rho_{d_n b_n} \\ \Gamma_{a_n c_n} = \sum_{bd} \boxed{\bar{v}_{a_n b_p c_n d_p}} \rho_{d_p b_p} + \boxed{\bar{v}_{a_n b_n c_n d_n}} \rho_{d_n b_n} \end{array} \right.$$

pp/nn/pn are taken into account

We have to go beyond

$$|\Phi\rangle = |\Phi\rangle_n \times |\Phi\rangle_n$$

Pairing field

to include pn pairing.

pp/nn only are taken into account

no pn pairing!!!

$$\Delta_{ab} \rightarrow \left[\begin{array}{l} \Delta_{a_n b_n} = \frac{1}{2} \sum_{cd} \boxed{\bar{v}_{a_n b_n c_n d_n}} \kappa_{c_n d_n} \\ \Delta_{a_n b_p} = \frac{1}{2} \sum_{cd} \bar{v}_{a_n b_p c_n d_p} \cancel{\kappa_{c_n d_p}} + \bar{v}_{a_n b_p c_p d_n} \cancel{\kappa_{c_p d_n}} \\ \Delta_{a_p b_n} = \frac{1}{2} \sum_{cd} \bar{v}_{a_p b_n c_n d_p} \cancel{\kappa_{c_n d_p}} + \bar{v}_{a_p b_n c_p d_n} \cancel{\kappa_{c_p d_n}} \end{array} \right.$$

Proton-neutron pairing with Gogny EDF

On top of this, Gogny parametrizations are chosen to cancel out the pairing part coming from the density-dependent term when the HFB wave function is factorized.

$$\hat{V}^{DD}(\vec{r}_1, \vec{r}_2) = t_3(1 + x_0 P_\sigma)\delta(\vec{r}_1 - \vec{r}_2)\rho_H^\alpha\left(\frac{\vec{r}_1 + \vec{r}_2}{2}\right)$$ → density-dependent term

Proton-neutron pairing with Gogny EDF

On top of this, Gogny parametrizations are chosen to cancel out the pairing part coming from the density-dependent term when the HFB wave function is factorized.

$$\hat{V}^{DD}(\vec{r}_1,\vec{r}_2) = t_3(1+x_0P_\sigma)\delta(\vec{r}_1-\vec{r}_2)\rho_H^\alpha\left(\frac{\vec{r}_1+\vec{r}_2}{2}\right)$$ → density-dependent term

$$\bar{v}_{abcd}^{DD} = t_3 I_{abcd}^{DD}\left[S_{ac}S_{bd}\left(\delta_{\tau_a\tau_c}\delta_{\tau_b\tau_d} - x_0\delta_{\tau_a\tau_d}\delta_{\tau_b\tau_c}\right) + S_{ad}S_{bc}\left(x_0\delta_{\tau_a\tau_c}\delta_{\tau_b\tau_d} - \delta_{\tau_a\tau_d}\delta_{\tau_b\tau_c}\right)\right]$$ → two-body matrix elements

Proton-neutron pairing with Gogny EDF

On top of this, Gogny parametrizations are chosen to cancel out the pairing part coming from the density-dependent term when the HFB wave function is factorized.

$$\hat{V}^{DD}(\vec{r}_1,\vec{r}_2) = t_3(1+x_0P_\sigma)\delta(\vec{r}_1-\vec{r}_2)\rho_H^\alpha\left(\frac{\vec{r}_1+\vec{r}_2}{2}\right)$$ → density-dependent term

$$\bar{v}_{abcd}^{DD} = t_3 I_{abcd}^{DD}\left[S_{ac}S_{bd}\left(\delta_{\tau_a\tau_c}\delta_{\tau_b\tau_d} - x_0\delta_{\tau_a\tau_d}\delta_{\tau_b\tau_c}\right) + S_{ad}S_{bc}\left(x_0\delta_{\tau_a\tau_c}\delta_{\tau_b\tau_d} - \delta_{\tau_a\tau_d}\delta_{\tau_b\tau_c}\right)\right]$$ → two-body matrix elements

$$I_{abcd}^{DD} = \int \phi_a(\vec{r})\phi_b(\vec{r})\rho_H^\alpha(\vec{r})\phi_c(\vec{r})\phi_d(\vec{r})d^3\vec{r}$$

→ spatial integrals

Proton-neutron pairing with Gogny EDF

On top of this, Gogny parametrizations are chosen to cancel out the pairing part coming from the density-dependent term when the HFB wave function is factorized.

$$\hat{V}^{DD}(\vec{r}_1,\vec{r}_2) = t_3(1+x_0P_\sigma)\delta(\vec{r}_1-\vec{r}_2)\rho_H^\alpha\left(\frac{\vec{r}_1+\vec{r}_2}{2}\right)$$ → density-dependent term

$$\bar{v}_{abcd}^{DD} = t_3 I_{abcd}^{DD}\left[S_{ac}S_{bd}\left(\delta_{\tau_a\tau_c}\delta_{\tau_b\tau_d} - x_0\delta_{\tau_a\tau_d}\delta_{\tau_b\tau_c}\right) + S_{ad}S_{bc}\left(x_0\delta_{\tau_a\tau_c}\delta_{\tau_b\tau_d} - \delta_{\tau_a\tau_d}\delta_{\tau_b\tau_c}\right)\right]$$ → two-body matrix elements

→ To compute the HF field:

$$\tau_a = \tau_c \equiv \tau; \tau_b = \tau_d \equiv \tau'$$

$$\bar{v}_{abcd}^{DD} = t_3 I_{abcd}^{DD}\left[S_{ac}S_{bd}\left(1 - x_0\delta_{\tau\tau'}\right) + S_{ad}S_{bc}\left(x_0 - \delta_{\tau\tau'}\right)\right]$$

Proton-neutron pairing with Gogny EDF

On top of this, Gogny parametrizations are chosen to cancel out the pairing part coming from the density-dependent term when the HFB wave function is factorized.

$$\hat{V}^{DD}(\vec{r}_1,\vec{r}_2) = t_3(1+x_0P_\sigma)\delta(\vec{r}_1-\vec{r}_2)\rho_H^\alpha\left(\frac{\vec{r}_1+\vec{r}_2}{2}\right)$$ → density-dependent term

$$\bar{v}_{abcd}^{DD} = t_3 I_{abcd}^{DD}\left[S_{ac}S_{bd}\left(\delta_{\tau_a\tau_c}\delta_{\tau_b\tau_d} - x_0\delta_{\tau_a\tau_d}\delta_{\tau_b\tau_c}\right) + S_{ad}S_{bc}\left(x_0\delta_{\tau_a\tau_c}\delta_{\tau_b\tau_d} - \delta_{\tau_a\tau_d}\delta_{\tau_b\tau_c}\right)\right]$$ → two-body matrix elements

→ To compute the HF field:

$$\tau_a = \tau_c \equiv \tau; \tau_b = \tau_d \equiv \tau'$$

$$\bar{v}_{abcd}^{DD} = t_3 I_{abcd}^{DD}\left[S_{ac}S_{bd}\left(1 - x_0\delta_{\tau\tau'}\right) + S_{ad}S_{bc}\left(x_0 - \delta_{\tau\tau'}\right)\right]$$

→ To compute the pairing field:

$$\tau_a = \tau_b \equiv \tau; \tau_c = \tau_d \equiv \tau'$$

$$\bar{v}_{abcd}^{DD} = t_3 I_{abcd}^{DD}\left[S_{ac}S_{bd}\left(1 - x_0\right) + S_{ad}S_{bc}\left(x_0 - 1\right)\right]\delta_{\tau\tau'}$$

Proton-neutron pairing with Gogny EDF

On top of this, Gogny parametrizations are chosen to cancel out the pairing part coming from the density-dependent term when the HFB wave function is factorized.

$$\hat{V}^{DD}(\vec{r}_1,\vec{r}_2) = t_3(1+x_0P_\sigma)\delta(\vec{r}_1-\vec{r}_2)\rho_H^\alpha\left(\frac{\vec{r}_1+\vec{r}_2}{2}\right)$$ → density-dependent term

$$\bar{v}_{abcd}^{DD} = t_3 I_{abcd}^{DD}\left[S_{ac}S_{bd}\left(\delta_{\tau_a\tau_c}\delta_{\tau_b\tau_d} - x_0\delta_{\tau_a\tau_d}\delta_{\tau_b\tau_c}\right) + S_{ad}S_{bc}\left(x_0\delta_{\tau_a\tau_c}\delta_{\tau_b\tau_d} - \delta_{\tau_a\tau_d}\delta_{\tau_b\tau_c}\right)\right]$$ → two-body matrix elements

→ To compute the HF field:

$$\tau_a = \tau_c \equiv \tau; \tau_b = \tau_d \equiv \tau'$$

$$\bar{v}_{abcd}^{DD} = t_3 I_{abcd}^{DD}\left[S_{ac}S_{bd}\left(1 - x_0\delta_{\tau\tau'}\right) + S_{ad}S_{bc}\left(x_0 - \delta_{\tau\tau'}\right)\right]$$

→ To compute the pairing field:

$$\tau_a = \tau_b \equiv \tau; \tau_c = \tau_d \equiv \tau'$$

$$\cancel{\bar{v}_{abcd}^{DD} = t_3 I_{abcd}^{DD}\left[S_{ac}S_{bd}\left(1 - x_0\right) + S_{ad}S_{bc}\left(x_0 - 1\right)\right]\delta_{\tau\tau'}}$$ → in all parametrizations $x_0 = 1$

Proton-neutron pairing with Gogny EDF

On top of this, Gogny parametrizations are chosen to cancel out the pairing part coming from the density-dependent term when the HFB wave function is factorized.

$$\hat{V}^{DD}(\vec{r}_1,\vec{r}_2) = t_3(1+x_0P_\sigma)\delta(\vec{r}_1-\vec{r}_2)\rho_H^\alpha\left(\frac{\vec{r}_1+\vec{r}_2}{2}\right)$$ → density-dependent term

$$\bar{v}^{DD}_{abcd} = t_3 I^{DD}_{abcd}\left[S_{ac}S_{bd}\left(\delta_{\tau_a\tau_c}\delta_{\tau_b\tau_d} - x_0\delta_{\tau_a\tau_d}\delta_{\tau_b\tau_c}\right) + S_{ad}S_{bc}\left(x_0\delta_{\tau_a\tau_c}\delta_{\tau_b\tau_d} - \delta_{\tau_a\tau_d}\delta_{\tau_b\tau_c}\right)\right]$$ → two-body matrix elements

→ To compute the HF field:

$$\tau_a = \tau_c \equiv \tau; \tau_b = \tau_d \equiv \tau'$$

$$\bar{v}^{DD}_{abcd} = t_3 I^{DD}_{abcd}\left[S_{ac}S_{bd}\left(1 - x_0\delta_{\tau\tau'}\right) + S_{ad}S_{bc}\left(x_0 - \delta_{\tau\tau'}\right)\right]$$

→ To compute the pairing field:

$$\boxed{\tau_a = \tau_b \equiv \tau; \tau_c = \tau_d \equiv \tau'}$$ → it does not hold in the general case!!

$$\cancel{\bar{v}^{DD}_{abcd} = t_3 I^{DD}_{abcd}\left[S_{ac}S_{bd}\left(1 - x_0\right) + S_{ad}S_{bc}\left(x_0 - 1\right)\right]\delta_{\tau\tau'}}$$ → in all parametrizations $x_0 = 1$